



OAK RIDGE NATIONAL LABORATORY

Operated by
UNION CARBIDE NUCLEAR COMPANY
Division of Union Carbide Corporation



Post Office Box X
Oak Ridge, Tennessee

EXTERNAL DISTRIBUTION
AUTHORIZED

ORNL
CENTRAL FILES NUMBER
61-6-28

DATE: June 15, 1961
SUBJECT: Status Report on Oxidation
Analyses for the EGCR
TO: Listed Distribution
FROM: M. H. Fontana

G CPR - DEPT 242
COORDINATION
SECTION

AUG 23 '61

ANSWER REQ'D
IN.....DAYS

ANS. BY	NO ANS.

Abstract

This report summarizes the work done to date by ORNL, Allis-Chalmers, and Kaiser Engineers on the EGCR graphite combustion problem that may follow from the maximum credible accident, that is, the rapid loss of pressure from the primary reactor coolant system. The solution to date is to protect the fuel support sleeves with a siliconized silicon-carbide coating and to allow the moderator surfaces to oxidize. The moderator surfaces have available only 6.5% of the total core flow which places an upper limit on the rate of oxidation. The rate of heat removal through the sleeve to the main coolant flow is sufficient to cause a decrease in temperature throughout the reactor and subsequent quenching of the oxidation. This method depends only on continued coolant flow from one blower. Problems attendant with this and other schemes of controlling the fire are discussed.

ACTION NOTATION

pls route
JUN 22 1961
WFS
[Handwritten signatures and initials]
149-7

"Distribution Limited to Recipients Indicated"

NOTICE

This document contains information of a preliminary nature and was prepared primarily for internal use at the Oak Ridge National Laboratory. It is subject to revision or correction and therefore does not represent a final report. The information is not to be abstracted, reprinted or otherwise given public dissemination without the approval of the ORNL patent branch, Legal and Information Control Department.

Facsimile Price \$ 9.60
Microfilm Price \$ 3.77
Available from the
Office of Technical Services
Department of Commerce
Washington 25, D. C.

108 Mc. 416

Table of Contents

<u>Section</u>		<u>Page</u>
I	Introduction	3
II	Principles of Oxidation Analysis	5
III	The Experimental Program	14
	Tests with Solid Graphite Plug	23
	Tests with Solid Nonreactive Plug	28
	Tests with Coated Graphite Sleeve	33
IV	Oxidation Rate Equations	40
V	Graphite Oxidation Analysis in the EGCR	48
VI	Proposed Methods for Controlling Combustion in the EGCR	65
VII	Discussion of the Coated Sleeves and Attendant Problems	71
VIII	Conclusions and Recommendations	75
	Nomenclature	77
Appendix A	Determination of Reaction Rates from Experimental Data	79
Appendix B	Original Allis-Chalmers Graphite Oxidation Calculation Model	87
Appendix C	IBM 7090 Graphite Oxidation Calculation Model	110
	References	117

I. Introduction

The Experimental Gas-Cooled Reactor (EGCR) is a pressurized, helium-cooled, graphite-moderated reactor in which seven fuel rods per element are suspended in graphite support sleeves which are stacked six high in each of 232 coolant channels. In safety analyses of the plant, credible accidents are postulated, and their effects, particularly on the release of fission products to the surroundings, are studied. The worst accident that is credible is called the maximum credible accident (MCA). In the EGCR, the MCA is taken to be a rupture of the main coolant system, either a pipe rupture or a nozzle blowout, such that the size of the hole does not exceed the area of one pipe.¹ This accident further presumes that at least one main coolant blower and heat-removal system remain operative for several days after the accident.

If this accident were to occur, air would enter the system. The graphite, being at temperatures of approximately 510 to 1075°F, could ignite and cause a runaway combustion. If the heat of oxidation from this fire is not removed, the containment vessel pressure would exceed the design pressure of the containment shell. Thus the possibility of this ignition's occurring must be determined, and action must be taken to control the fire if it occurs.

Unfortunately, graphite is a variable substance with an unusual variation in reaction rate. Also, the temperatures in the EGCR graphite are such that it is not immediately obvious that a fire will or will not occur; to determine this requires a more sophisticated analysis than is usually done in "worst case" hazards calculations. Preliminary calculations have been done by American Car and Foundry² (now Allis-Chalmers) and Prados.³ The results of these studies were not acceptable to the project because of the lack of knowledge of the rate equations to be used and the fact that relatively small (100°F) changes in temperature could change the result.

It became apparent that further knowledge of the oxidation kinetics of graphite was required, and a three-pronged attack on the problem was begun. This included an experimental program, the development of a more refined analytical model of graphite oxidation in an EGCR core channel, and an extensive literature search of graphite reaction rates.

The experimental program currently under way at Hanford has two parts: 1) a basic research program aimed at determining the effects of different variables to be described later and 2) an applied program in which tests are run in a prototype burning rig in which the conditions of one of the EGCR channels are approximated. These experimental programs were set up primarily to back up an analytical model for graphite combustion that could be applied to the EGCR.

The analytical model developed largely by A-C has been set up by both A-C - on the Bendix G-15 - and by Oak Ridge, on the IBM 7090. Although validation of the model and the rate equations used is not yet complete, it is believed that the model is basically correct and would require only slight changes in input to describe the EGCR conditions with reasonable accuracy.

At this time it appears that coating the graphite sleeves with silicon carbide will be effective in controlling the graphite combustion. It is impractical to coat the moderator channels, and, if this accident should occur, these surfaces will oxidize. The heat of oxidation, however, will be transferred from the annulus region to the coolant flowing at a high rate in the central channel. Under worst possible conditions the oxidation in the annulus region would be starved by the low annular flow which is prescribed by the designer to be 6.5% of the total flow entering a channel. Actually, the oxidation probably will not reach rates at which this effect is important, and it is expected that the temperatures throughout the core will reach a maximum before starvation effects become of great significance assuming one blower remains operative.

This report presents a simple exposition of the oxidation process in sufficient detail to build a background necessary to understand the following discussions: descriptions of the calculational models, description of the Hanford experimental programs, summaries of the calculations, thinking that led to the choice of the coated sleeves as the method for controlling the oxidation, the attendant operational problems that must be solved, and further work that must be accomplished as backup for this concept when presented for operational approval from the AEC.

II. Principles of Oxidation Analysis

Graphite is a relatively nonreactive material. Two of the products of chemical reaction are its oxides CO and CO₂ which are gaseous. Since no protective oxide film is formed on graphite, oxidation will occur indefinitely. Presently we are interested in runaway combustion which is the condition when heat cannot be removed at as fast a rate as it is generated, thus resulting in an uncontrolled increase in temperature.

The reaction rate constant of graphite follows the Arrhenius equation:

$$k = a e^{-c/RT} \quad (1)$$

where a is the frequency factor, c is the activation energy, R is the universal gas constant, and T is the graphite temperature. The heat removal, q , from the reaction zone to a flowing gas in the absence of thermal radiation, is:

$$q/A = h (T_{\text{graphite surface}} - T_{\text{air}}) \quad (2)$$

where the heat transfer coefficient h depends on the gas properties as follows:⁴

$$h = \frac{0.023 k}{D_{eq}} \left(\frac{W D_{eq}}{S_f \mu} \right)^{0.8} \left(\frac{C_p \mu}{k} \right)^{0.4} \quad (3)$$

The ratios $(k/\mu^{0.8})$ and $(C_p \mu/k)^{0.4}$ are relatively insensitive to temperature, so the heat transfer coefficient is primarily dependent on the eight-tenths power of the flow rate.

At a given flow rate, the heat removal is linearly dependent on the temperature difference between the graphite surface and the air stream at that point. The heat generation rate, however, depends on the exponential $e^{-c/RT}$. These relationships are shown in Fig. 1.

For a given graphite, the heat generation rate is shown on curve c. The heat removal rate at a given flow rate, W, is shown on curve a which crosses the heat generation curve at two points, d and e. The lower point, e, represents a stable point, that is, a slight perturbation in temperature would result in the temperature returning to T_1 . Point d, however, is an unstable point. It can be seen that if the temperature is decreased, the heat removal exceeds the heat generation and the temperature will decrease to point e. If the temperature is increased slightly, however, the heat generation exceeds the heat removal, causing the temperature to increase until the reaction is limited by the transport of reactants by diffusion and convection to the graphite surface from the bulk gas stream. This is called a runaway combustion. The effect of heat removal is obviously important. For instance, if the heat removal is too slow, as shown by curve b in Fig. 1, the heat generation always would exceed the heat removal, and the temperature would increase. The effect of different reaction rates obviously is important, as can be shown by curve f in Fig. 1. Whereas curves b and c would result in a runaway, the same heat removal curve, b, is sufficient at temperatures below T_3 to prevent runaway when the reaction rate is as shown by curve f.

The heat release due to oxidation as a function of temperature depends on the rate of oxidation. The rate of oxidation in graphite

UNCLASSIFIED
ORNL-LR-DWG 59133

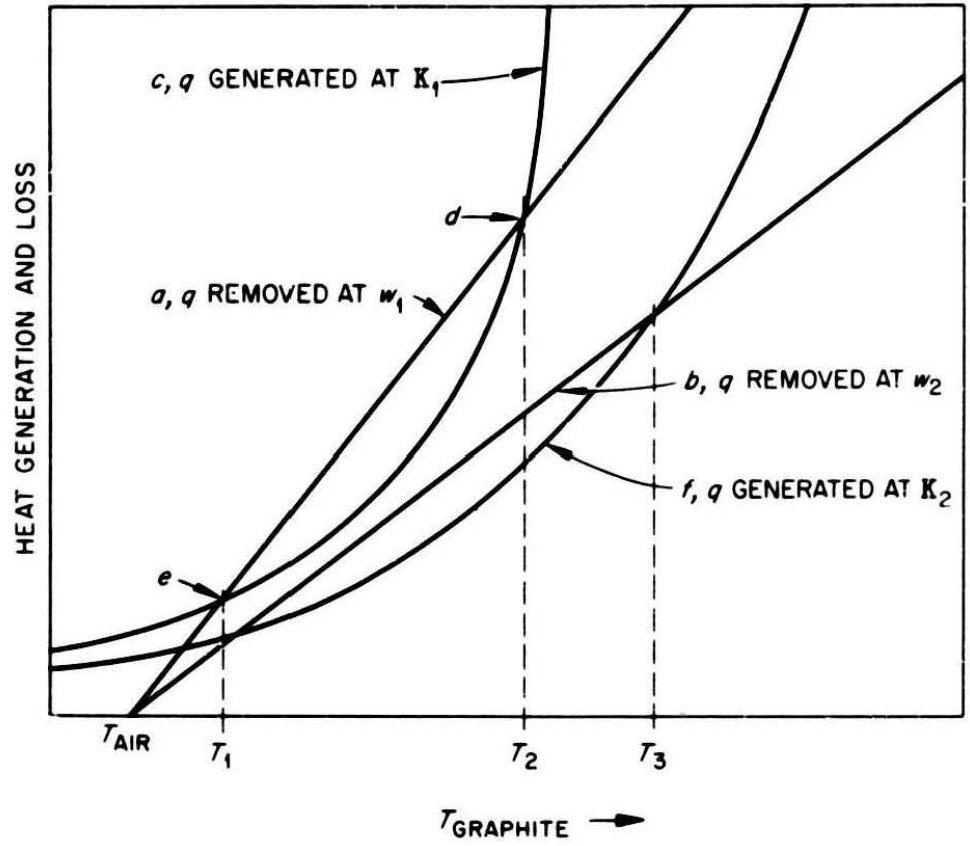


Fig. 4. Relation Between Heat Generation and Heat Removal.

is complicated by the fact that graphite is a porous material, and the effect of surface-to-volume ratio can be crucial. Reaction rates obtained from small-scale laboratory tests must be applied to larger scale models, such as the EGCR, which require rate equations for use in calculations. Depending on the temperature, this scaling up of data can be in significant error if either a simple fraction of total weight lost per hour or if a simple surface-to-volume scaling is used. It appears that the concept of diffusional control of oxidation can be used for the scaling. To understand this concept, some preliminary comments on the kinetics of graphite oxidation are in order.

Since graphite is a porous material, the reactant, in this case oxygen, can diffuse into the graphite to a considerable depth to reach active sites where it can react with the carbon. The reaction can be classified into three zones identified by Walker:⁵ I, II, and III. These are schematically shown in Fig. 2.

In zone I at low temperatures the reaction proceeds at a relatively slow rate compared to the rate of diffusion of oxygen in the pores, so that the reaction proceeds at a constant rate throughout the volume of the solid. In this case, the rate of reaction is controlled by the chemical kinetics. In zone II, at somewhat higher temperatures, the reaction proceeds at a rate faster than the rate at which the reactants can proceed through the pores to the reaction sites, and the rate of oxidation decreases exponentially from a maximum value at the surface to zero at some distance within the graphite. As the temperature increases further, the rate of chemical reaction becomes significant compared with the rate of mass transfer of oxygen to the external surface. In zone IIIa both solid-phase diffusion and gas-phase mass transfer resistance limit the flow of reactants to the active sites within the graphite. In zone III at high temperatures the rate is essentially a surface reaction with the rate of reaction being controlled by diffusion of products across the boundary layer and therefore by the coolant velocity. This approaches the equilibrium

UNCLASSIFIED
ORNL-LR-DWG 59134

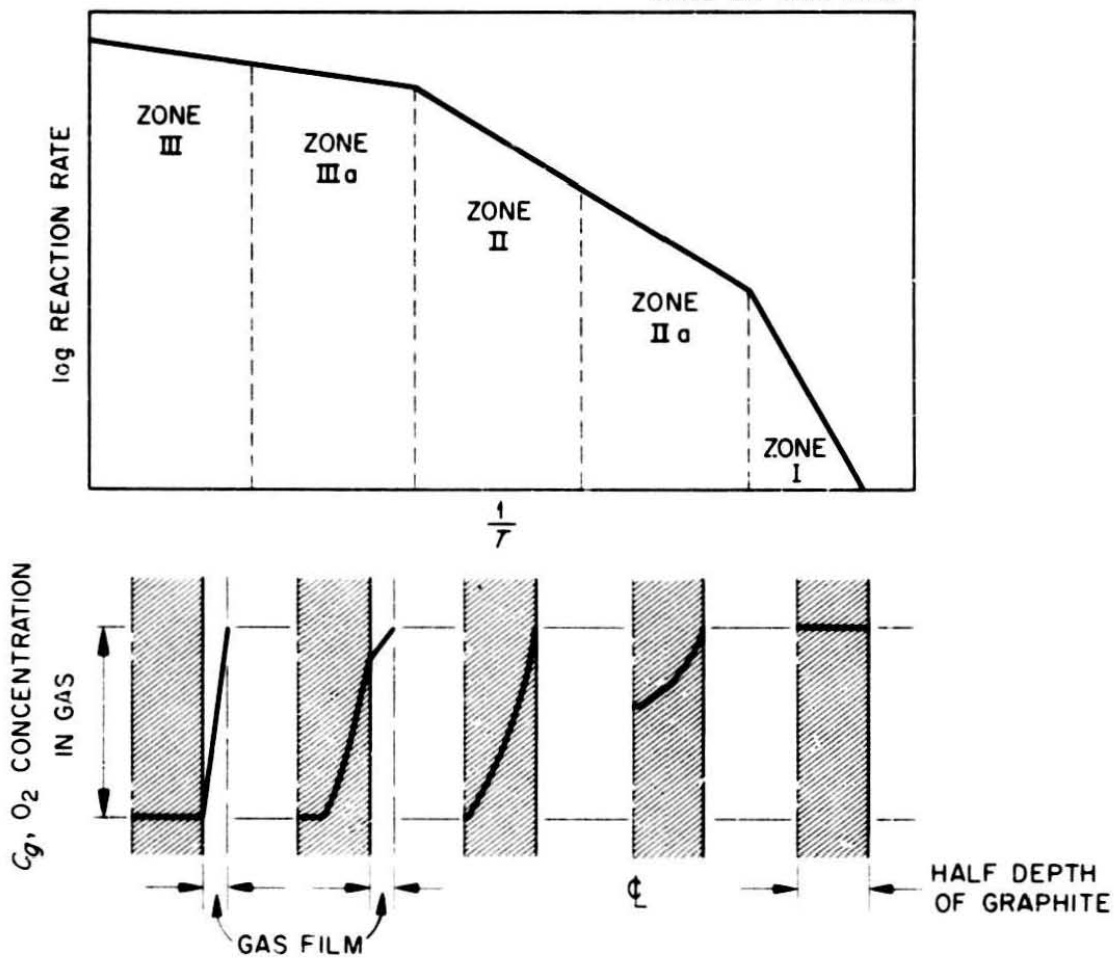
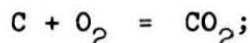


Fig. 2. Schematic of Reaction Rate Zones and Oxygen Concentration as a Function of Temperature⁵.

flame conditions which are of no concern in the EGCR, since, if these rates are reached, the situation is out of control.

It is expected that the conditions in the EGCR will approach those of zone II. This effect is treated in the rate equations by the method of "depth of diffusion", as outlined by P. J. Robinson.⁶ For purposes of calculation, it is assumed that 1) the oxygen diffuses according to Fick's law into the graphite under isothermal conditions; 2) the reaction rate depends on the concentration of oxygen at the element of volume under consideration; 3) the moles of products equal the moles of reactant gas, that is, the reaction is:



and 4) the rate of change of reactant concentration with time is so small at any location within the pores that steady-state conditions exist.

Application of the laws of conservation of mass to a small-volume element of graphite under the conditions specified above leads to the governing differential equations for this process at any point within the graphite.*

$$\nabla^2 C = \frac{k_v}{D_p} C \quad (5)$$

where

C = O₂ concentration in graphite pores, moles/volume of gas

k_v = "volume rate constant," moles O₂ reacting/("active"*** vol of sample)(time)(mole of O₂/volume of gas)

* This development follows closely that given in the appendix of ref. 7.

*** The concept of "active" volumes is described in refs. 6 and 7 and is related to experimentally determined rate constants.

D_p = effective diffusivity of oxygen in pores of sample,
length²/time

This equation must be solved subject to the condition that at the external surface of the graphite sample:

$$C = C_o$$

where

C_o = O₂ concentration at the outer sample surface

It is convenient to let:

$$L = \sqrt{D_p/k_v} \quad (6)$$

The parameter, L, has the dimension of length and is determined by the relative rates of diffusion and chemical reaction. It takes on a special significance in situations where L, the so-called "depth of diffusion", is small relative to the sample dimensions. In such cases, the mathematical problem reduces to that of unidirectional diffusion-reaction in an infinite slab where Eq. (5) becomes:

$$\frac{d^2C}{dx^2} = \frac{C}{L^2} \quad (7)$$

The boundary conditions are:

$$C = C_o \quad \text{at } x = 0$$

$$C = 0 \quad \text{at } x = \infty$$

The solution is:

$$C = C_o e^{-x/L} \quad (8)$$

The reaction rate in an infinitesimal section, dx in thickness, normal to the sample surface, would be $k_v CSdx$ where S is the external surface area of the sample. Hence the total reaction rate, Q, in moles of oxygen reacting per unit time for the entire sample would be:

$$Q = \int_0^{\infty} k_v C_o e^{-x/L} S dx \quad (9)$$

If it is assumed that temperature (and hence k_v) remains constant over the range of integration, one obtains:

$$Q = k_v C_o SL \quad (10)$$

that is, the rate of reaction is equal to that which would have been observed had the oxygen concentration remained constant at C_o for a depth L into the sample and had been zero elsewhere. If there were no diffusional resistance to oxygen penetration into the sample, the concentration C_o would exist uniformly through the pores, and the "diffusion-free" reaction rate would be given by:

$$Q^* = k_v C_o V \quad (11)$$

where V is the total sample volume. Hence, for the special case where L is much smaller than the smallest dimension of the sample, the ration, η , of the true reaction rate to the diffusion-free rate is:

$$\eta = \frac{Q}{Q^*} = \frac{k_v C_o SL}{k_v C_o V} = \frac{SL}{V} \quad (12)$$

The relationship for η for solid slabs and solid long cylinders is given by Prados⁷ as follows.

For a slab:

$$\eta = \frac{\tanh(b/L)}{(b/L)} \quad (13)$$

where b is the half-thickness of the slab. It should be noted that as $(b/L) \rightarrow 0$, $\eta \rightarrow 1$, as would be expected for cases where diffusion is rapid relative to reaction. Also, as $(b/L) \rightarrow \infty$, $\eta \rightarrow 1/(b/L) = SL/V$, as expected for cases where diffusion is slow relative to reaction.

For a long solid cylinder of radius b :

$$\eta = \frac{2}{(b/L)} \frac{I_1(b/L)}{I_0(b/L)} \quad (14)$$

For small values of (b/L) , $\eta \rightarrow 1$. For the case of large (b/L) , $\eta \rightarrow 2/(b/L) = SL/V$.

Similar expressions for a sphere and hollow cylinder are given by Robinson.⁶

An approximate relation for η which appears to hold well for most solids of reasonable shape is:

$$\eta = \frac{1}{\phi} \tanh \phi \quad (15)$$

where

$$\phi = V/SL$$

This equation is exact for a large slab and gives close agreement for spheres and solid and hollow cylinders, as shown by Robinson.⁶

Prados⁷ gives a method of reducing reaction rate data to the active mass basis which is given in Appendix A.

The actual EGCR geometry and conditions are too complex to be described accurately by the development in Appendix A. A digital computer program will be described in section V. The information in Appendix A has been included to check the depth-of-diffusion concept which is fundamental to further analysis. There are other factors which affect the reaction rate of graphite which will be discussed in conjunction with descriptions of the experimental programs given in section III.

III. The Experimental Program

An experimental program is under way at Hanford which consists of two approaches: 1) a basic program to determine the effects on the combustion of graphite of variables that cannot be duplicated on a large-scale test and 2) a prototype program in which a channel of the EGCR is duplicated in full scale in the radial dimensions and is 6 ft long. The graphite-air oxidation studies may be outlined as follows:

I. Laboratory Experiments

A. Rate Determination

1. Effect of

a. manufacturing variables

(1) density

(2) purity

(3) coke and pitch source

b. temperature

c. flow rates

d. gamma field

e. irradiation damage

f. surface-to-volume ratio

g. oxygen partial pressure

h. prior oxidation

i. water vapor

B. Combustion Experiment (laboratory scale)

1. Test validity of theoretical model in prediction of ignition conditions

a. air or oxygen flow

b. graphite temperature

c. graphite of varied reactivities

2. Test inhibitors

II. Prototype Experiments

- A. Experiments to Test Validity of Model (these experiments have been and will continue to be done in mock-up of the EGCR)
 - 1. Graphite temperature, 1100°F
 - 2. Air inlet temperature, 80 to 550°F
 - 3. Various air flows
- B. Experiment Designed to Simulate More Closely EGCR Accident Conditions
 - 1. Programmed heat decay
 - 2. Fuel element geometry
 - d. Duplication of temperature and flow in desired region
- C. Evaluation of Inhibitors under Runaway Conditions

The effect of manufacturing variables is secondary in EGCR applications because tests have been run with EGCR moderator graphite.

The effect of temperature depends greatly on the activation energy, E_a , in the Arrhenius equation. This value can vary, but Dahl of Hanford⁸ feels that 50 kcal/g-mole is a reasonable number. Further discussions on rate equations will be given in section IV.

The role played by the gas flow was discussed in section III. The experimental program has not produced any evidence to dispute the analyses as previously given.

The effect of gamma field is currently being studied in a continuous weight-monitoring rig at Hanford. It has been suggested that the definite accelerating effect of gamma radiation on the oxidation rate of graphite is due to formation of ozone, which in turn has a higher reaction rate with graphite. Although there are some effects of the volume of gas upstream from the reacting sample undergoing radiation, the greatest contribution is thought to be due to the formation of ozone in the gas existing in the pores. It is expected that the gamma effect is similar to adding a constant to the rate over a range of temperatures. Thus, at low temperatures the effect

would be more significant than at higher temperatures. This would show up as a change in the activation energy. At the present time, however, the only thing that has been done is to multiply the frequency factor by a factor of 1.7. Although it is recognized that this is not strictly correct, it is expected to be conservative.

The effect of stored energy due to radiation damage is not expected to have a great effect on the reaction rates at the temperatures existing in the EGCR. The apparent reduction in specific heat of the graphite, however, could affect the rates of temperature rise in the transients following the accident. Also, radiation damage could have an effect through the mechanism of opening of surface sites and increasing the porosity.

The effect of surface-to-volume ratio becomes extremely important in the temperature ranges in which diffusion control becomes important. This was described in some detail in section II.

Some controversy exists as to the effect of oxygen partial pressure. Many workers have reported a first-order dependency, that is, the reaction rate is directly proportional to the concentration of oxygen in the ambient gas, but there have been some cases of zero-order dependency. The Hanford experimenters were originally prone to accept the zero-order dependency as applied to the EGCR analysis, but recent data⁹ show that the order is about 0.5 at temperatures below about 500°C and increasing to about first order above this temperature. This can be explained by noting that at the lower temperatures the chemical step, probably the desorption of products from active sites, is the controlling step so that various concentrations of oxygen will nearly always supply sufficient reactants. At higher temperatures, however, diffusion control becomes important, and the rate would depend on oxygen concentration. In the EGCR analysis, to be described in section IV, a first-order dependency is used.

The existence of prior oxidation affects the reaction rate. Figure 3 shows that the rate is lower at the first 1 to 2% burnoff, and then it

UNCLASSIFIED
ORNL-LR-DWC. 50289

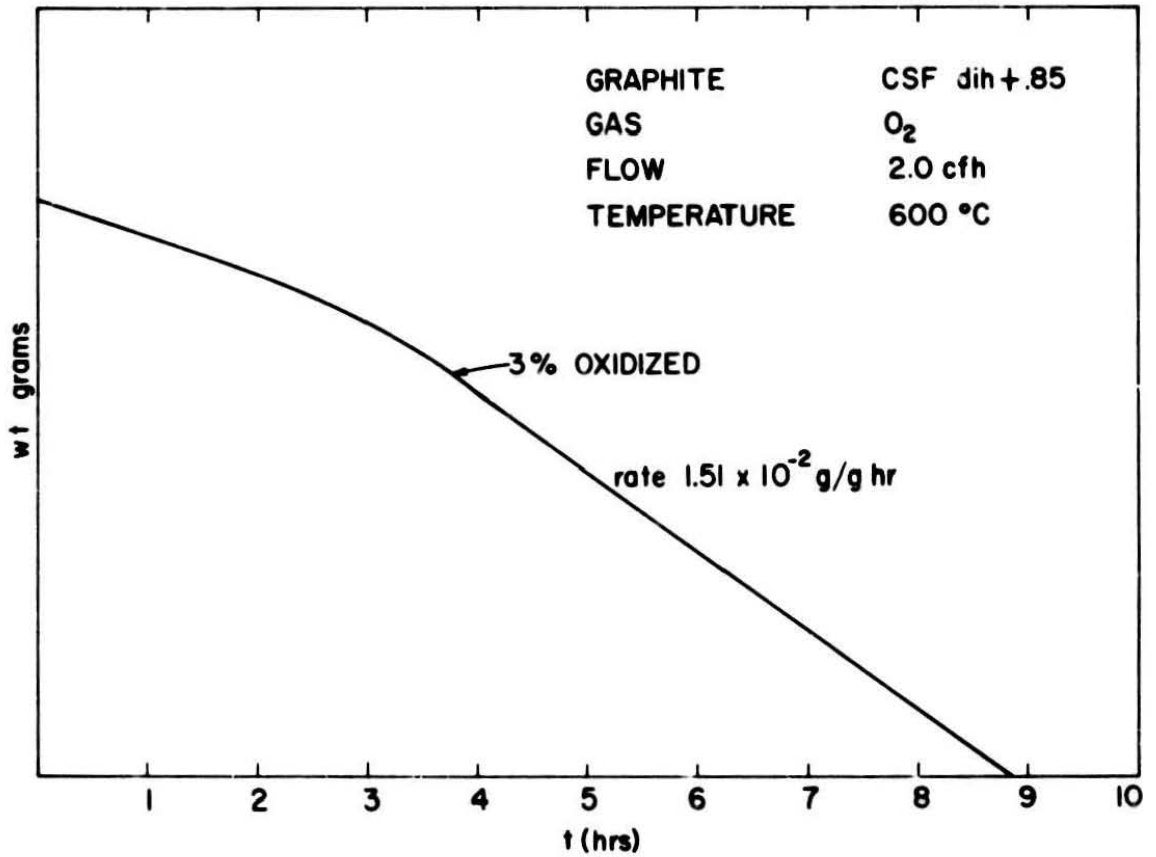


Fig.3. Graphite Sample Weight vs Time During Oxidation Rate Test.

increases to a steady value at higher burnoffs. This is felt to be due to the unplugging of pores on or near the surface of the graphite, caused by initial oxidation, allowing more active sites to become available to the reactants. Dahl and deHalas feel that the higher rate, which can be two or three times higher than the initial rate, will be applicable to the EGCR in case of an accident; impurities in the gas stream under operating conditions over a period of time will react with graphite sufficiently to put it in the region of the higher rates.

Water vapor can be very tightly adsorbed on graphite,¹⁰ as shown in Table I, and has a very great catalyzing effect, probably of several

TABLE I

Retention of Untreated Water on Graphite during
Heat Treatment in Vacuo¹¹

<u>Heat Treatment</u>		<u>Fraction Retained</u>
<u>°C</u>	<u>Minutes</u>	
300	25	74.3
400	10	65.5
500	20	37.0
600	35	16.7
700	5	16.1
800	20	9.0
900	10	6.8
1000	15	4.4
1100	25	1.5
1200	15	0.5

orders of magnitude. Not much work has been expended on this subject at Hanford. The EGCR is expected to have about 0.01% water in the gas stream under operating conditions. No attempt will be made to control the water concentration rigidly in the burning rig, the feeling being that the graphite would adsorb moisture in air previous to assembly of the rig, and enough would remain adsorbed even during the preliminary temperature elevation to 1100°F. Also, the inlet air is expected to have moisture comparable to that in the containment vessel prior to rupture of the main coolant system. Since the greatest change in reaction rates is expected between perfectly "dry" graphite and that containing trace amounts of moisture - any greater amounts having a smaller effect - it is felt that the rig would not need tight moisture control to approximate the EGCR.

Whereas the basic program will be used to discover fundamentals of the graphite-air reaction, the prototype burning rig will be used not only to validate rate equations used in the computer analysis of the EGCR burning problem but also will attempt to duplicate the EGCR channel as closely as possible. The flow diagram of the prototype burning rig is shown in Fig. 4. The burning region is enclosed in a stainless steel pipe containing six 1-ft-long axial graphite sections mocking up the EGCR annulus. The fuel sleeves in the early tests were simulated by a 5-in.-o.d. graphite plug nested within annular graphite pieces of 5 1/4-in.-i.d. and approximately 8.5 in.-o.d., corresponding to the moderator. Gamma heating is simulated by four calrods in the moderator. In the early tests four calrods simulated gamma heating in the central plug. In later tests actual EGCR sleeves were used with the fuel elements being simulated by seven 3/4-in.-o.d. steel rods inserted through the center of the sleeves. Further tests will be performed with a globar through the centers of the sleeves to mock up the radiant heat load due to the levelization of the temperature structure in the fuel pellets.

UNCLASSIFIED
ORNL-LR-DWG 59135

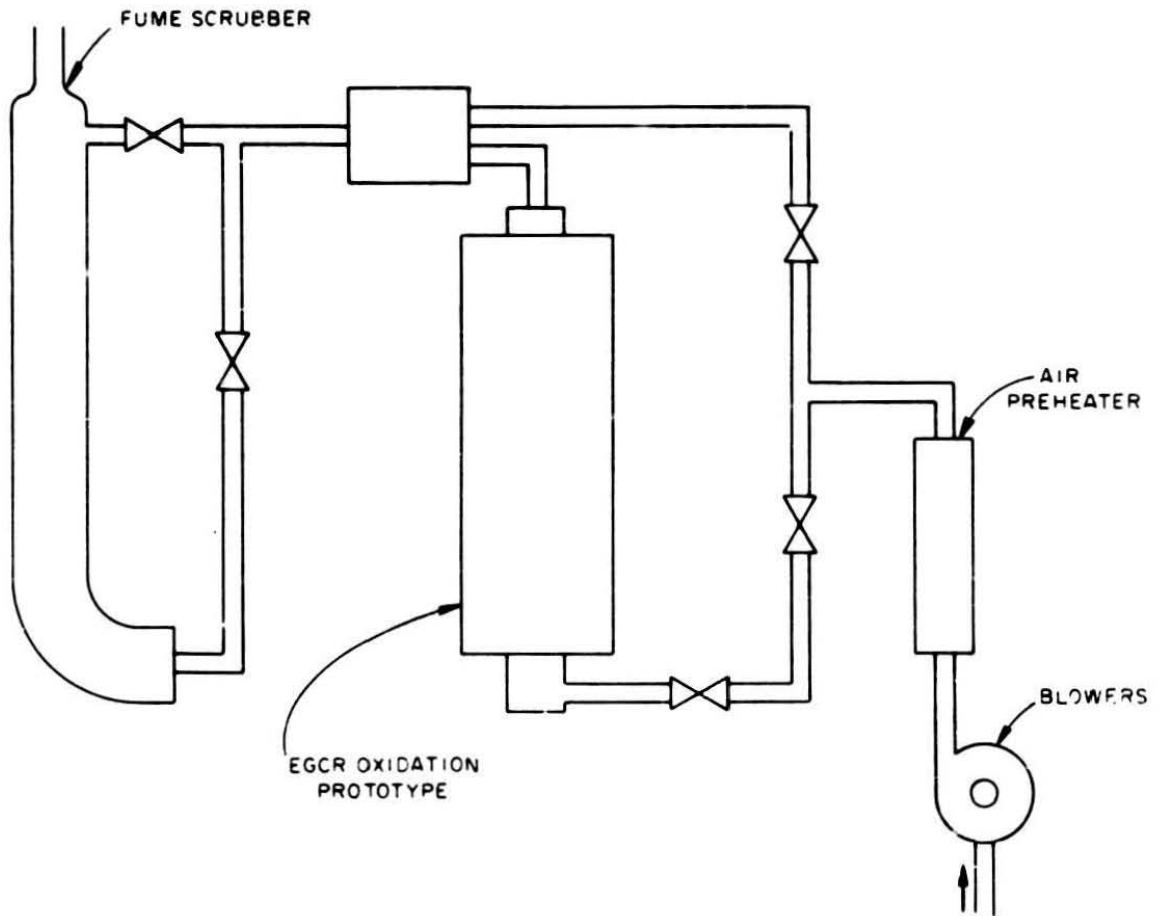


Fig. 4. Engineering Scale Prototype Unit.

Eighteen thermocouples capable of measuring up to approximately 1000°C are placed on 1-ft axial spacings, as shown in Fig. 5. On each axial plane one thermocouple measures the gas stream temperature, one placed 1/32 in. in from the surfaces measures the moderator temperature, and one placed 1/32 in. from the plug surface measures the simulated sleeve temperature.

The graphite is brought to temperature by means of the calrods with a slight drift of argon past the graphite. When the desired temperature is reached, the heat power is reduced to that required to maintain adiabatic conditions. Meanwhile, air can be moved by the blower through a preheater and exhausted up the bypass. Oxidation is initiated by valving this preheated air through the graphite assembly. The rig is so designed that the air can pass through a scrubber column before discharge to the air if noxious inhibiting agents such as chlorine are being tested. The capability exists of diluents being introduced into the air upstream of the graphite to simulate the effects of air mixed with helium and to check the effects of oxygen depletion and CO and CO₂ production in the gas stream. It is not possible to recycle the gas because of the temperature limitations on the blower. The system is constructed of stainless steel to withstand the high temperatures involved, but due to its susceptibility to chlorine corrosion, extensive chlorine suppression tests should be performed near the end of the program.

At the present time, the air preheater can heat the inlet air to approximately 800°F. Most of the tests to date have been operated with 80°F. Since the heat generation rate is dependent on the exponential of the graphite temperature and the heat removal is linearly dependent on the temperature difference between the graphite and the air temperature at a point, and since at lower flow rates the temperature of the air rises quite quickly during its transit along the channel, it is expected that the effect of air inlet temperature is very small compared to other effects. Also, it is believed that these effects of variant inlet temperatures can be evaluated analytically.

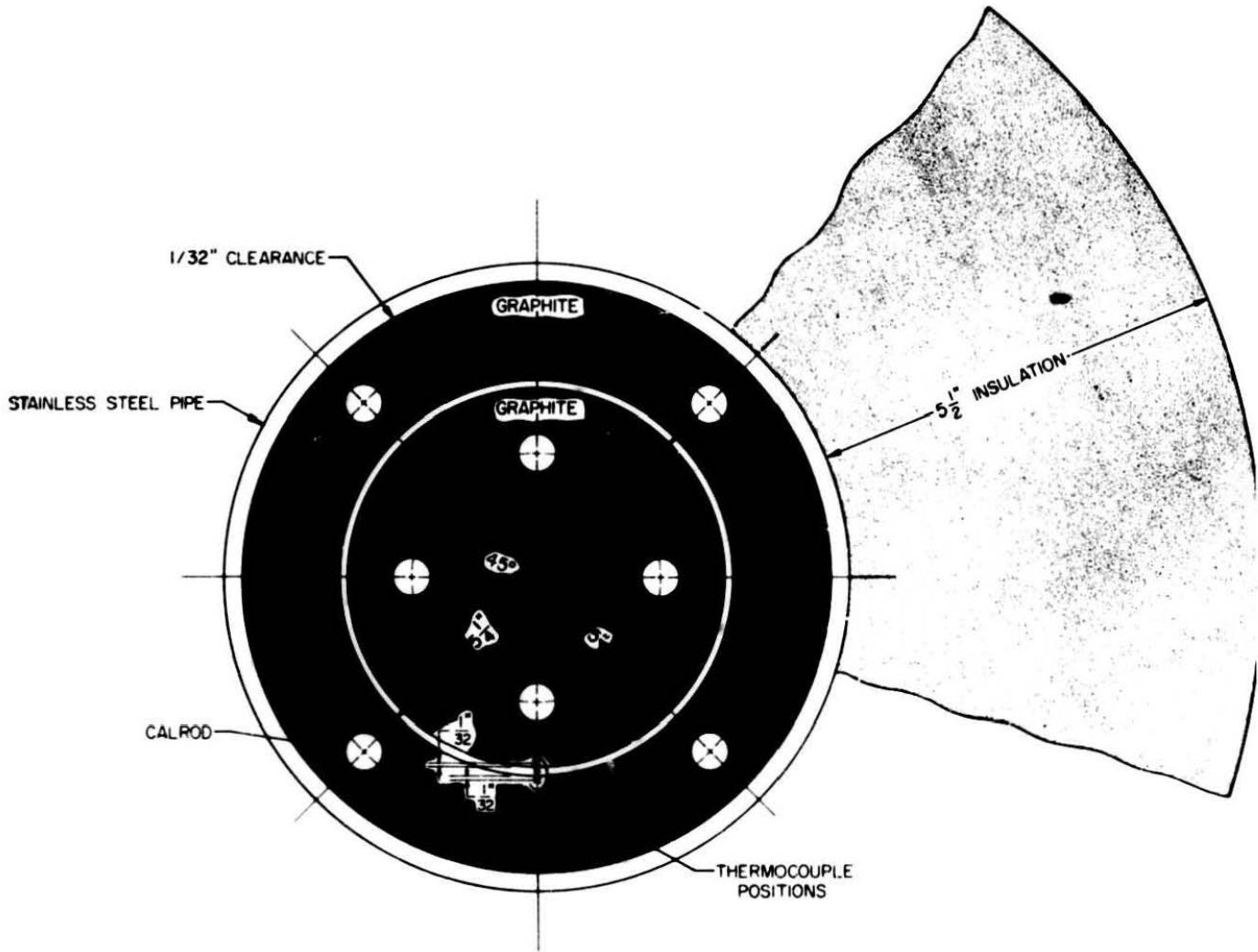


FIG. 5. CROSS SECTION OF PROTOTYPE UNIT

Blowers of 225 lb/hr are available, and they are sufficient to simulate any condition expected in the EGCR. The rig is capable of executing any programmed heat input and is currently being reworked to allow testing of the coated sleeves with a globar heater simulating the fuel elements located in the center.

The full-scale burning rig is intended to perform two functions: 1) approximate the EGCR as closely as possible and 2) provide a test bed to check the analytical models developed for the computer programs to be discussed in section V. This last phase is necessary because of the inability to simulate directly in the burning rig the effects of γ irradiation, prior irradiation of the graphite, the true transients after the loss-of-pressure accident (which never truly can be analyzed either), and the effects of the shorter length of the channel.

Up to the present time, three classes of tests have been performed on the burning rig. In the first series, a solid graphite plug, internally heated, was used to simulate the fuel sleeve. The test simulated the annulus region on the EGCR. In the second series, a steel pipe was placed over the central graphite slug to simulate a perfectly nonreactive sleeve. The third series, now in progress, includes tests of coated sleeves of varying quality, with and without internal globar heating.

Tests with Solid Graphite Plug

The experiments using the solid graphite central plug are described in ref. 10, and the results are shown in Figs. 6, 7, and 8. The principal mode of heat removal in these tests was by the gas flowing in the annulus. Graphite in the tests was Speer nuclear grade 2 with density of 1.68 and diH purity ranging between 0.256 and 0.312. Oxidation experiments showed the reactivity of this graphite to be 2.8 times that of CSF and approximately the same as EGCR moderator graphite.

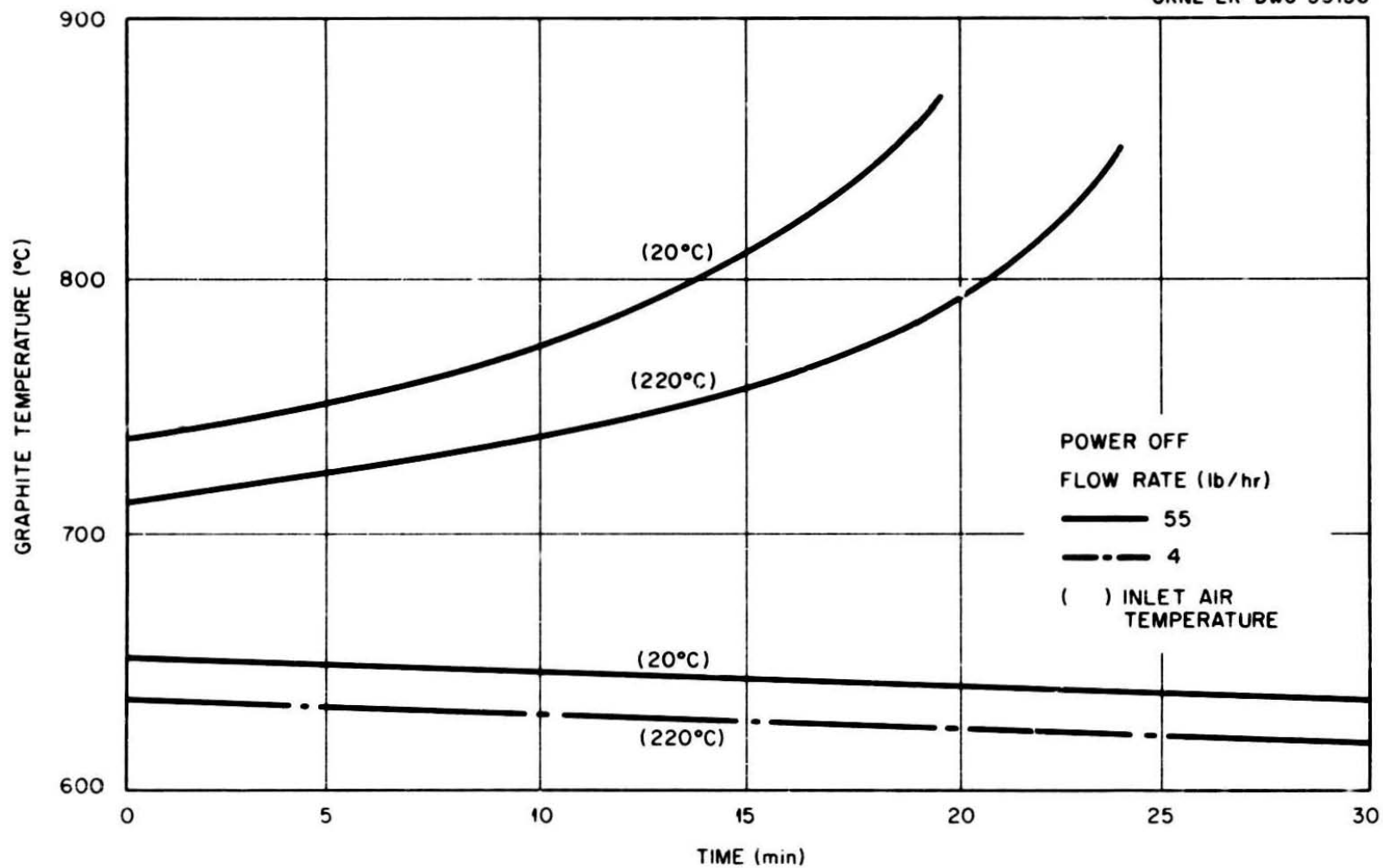


Fig. 6. Graphite Temperature vs Time for Experiment 1 (from Ref 10)

UNCLASSIFIED
ORNL-LR-DWG 59137

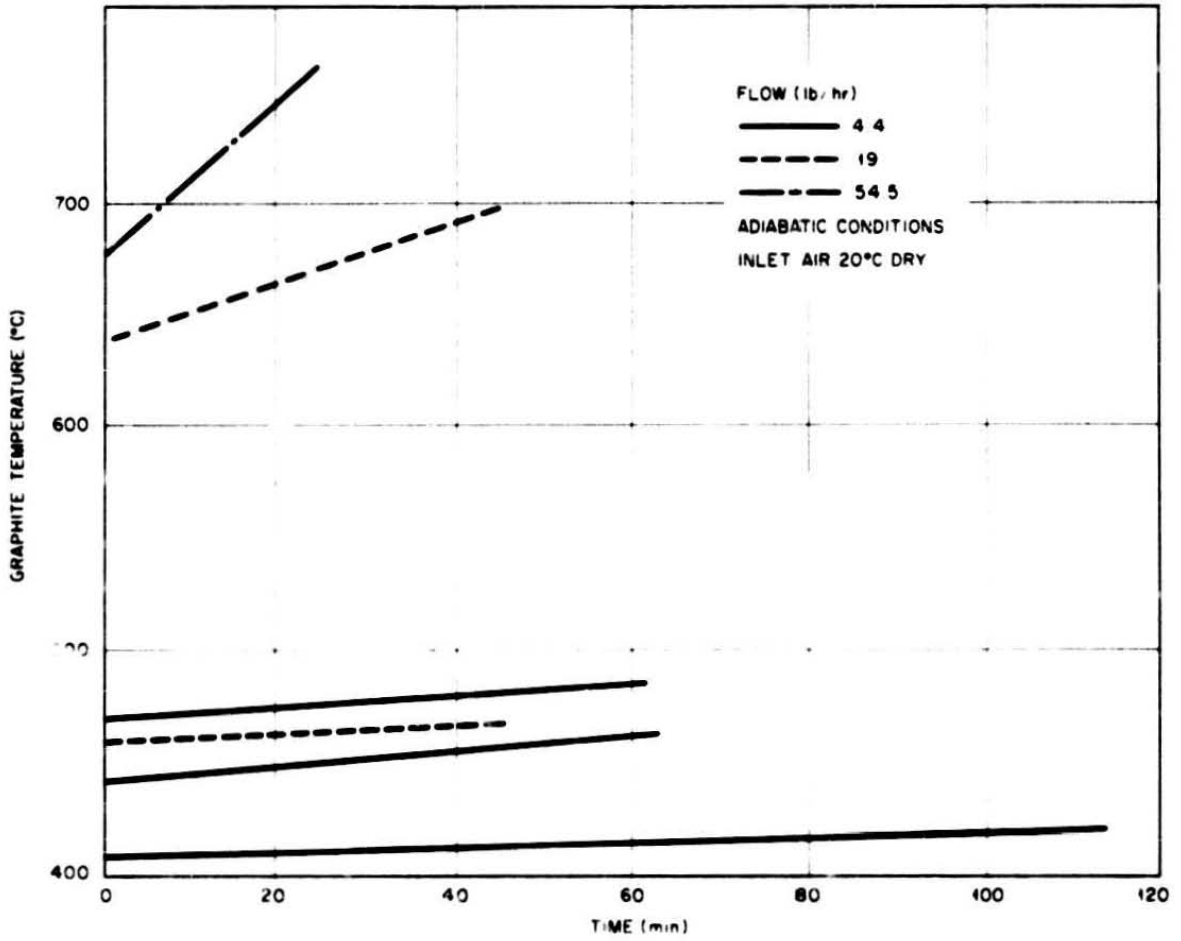


Fig. 7. Graphite Temperature vs Time for Experiment 2 (from Ref 10).

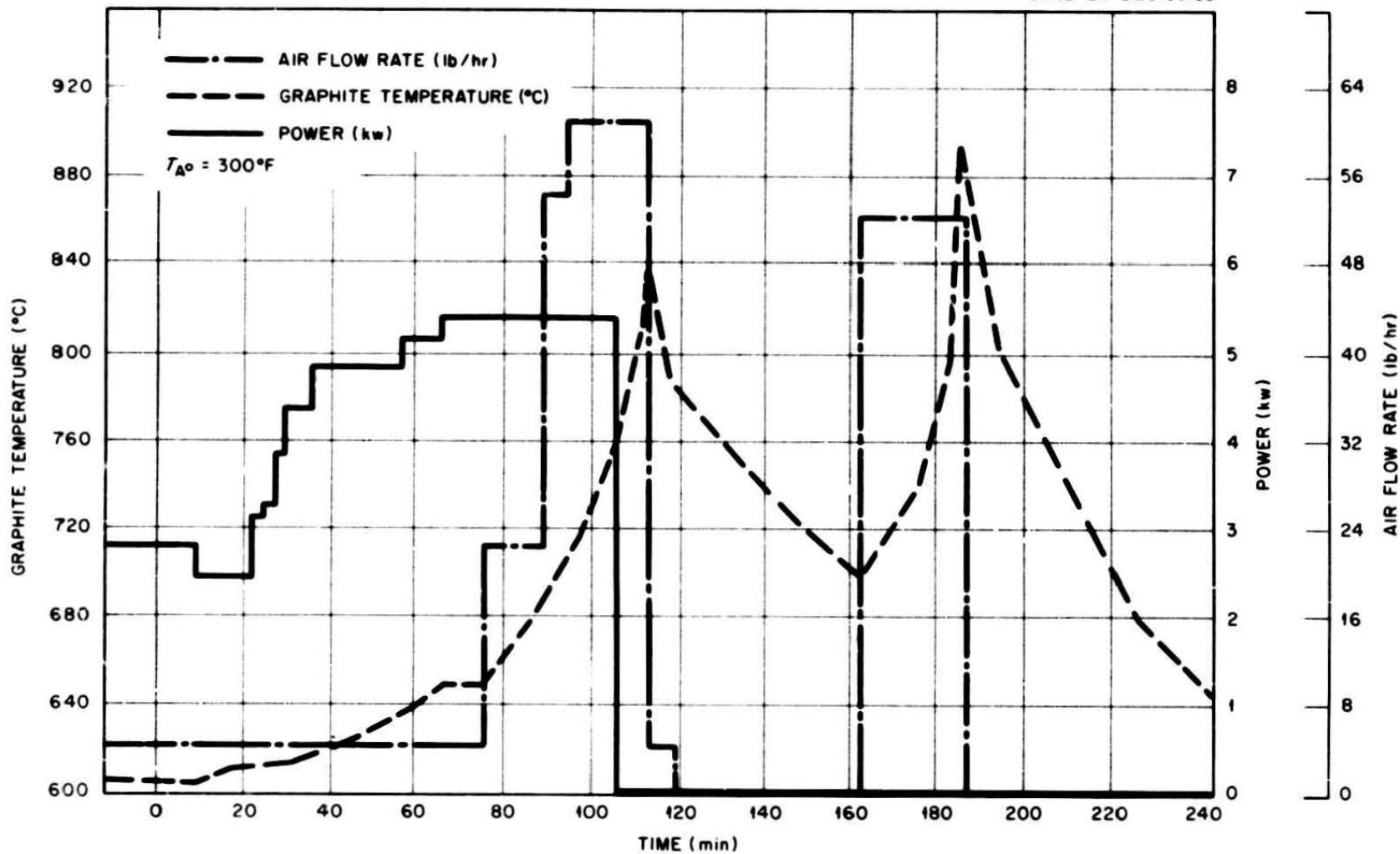


Fig. 8. Conditions for Experiment 3 (from Ref 10).

In the first set of experiments the graphite was raised to a desired temperature, then the power to the heaters was cut off, and air was introduced. Under these conditions there was considerable radial heat loss causing a less severe test than would be encountered in an accident. However, as may be seen in Fig. 6, runaway did take place under these conditions above 710°C with flow as high as 40 lb/hr. During these particular tests, a longitudinal temperature gradient of at least 200°C existed between the center of the column and the inlet - a distance of 3 ft. Increased flow served only to enhance oxidation, generate additional heat, and speed the course of the runaway.

The next basic type of experiment was designed to simulate more nearly a channel in an infinite lattice array with adiabatic conditions. In these runs the graphite was again raised to temperature, then the power to the heaters in the central fuel sleeve only was cut off. The power in the outer bank of the heaters was adjusted to keep the surface of the moderator at the same temperature as the fuel sleeve. Thus heat from adjacent channels was simulated, and radial heat loss was essentially nullified.* As shown in Fig. 7, the temperatures of the moderator and fuel sleeve did not decrease when the graphite temperature exceeded 400°C , with flow ranging between 4 lb/hr and 19 lb/hr of dry air at inlet temperatures of between 20 and 210°C . Runaway could be considered to have taken place under these conditions. When a severe runaway had been established, a 10-fold increase in air flow served only to speed the course of the runaway rather than arrest it. Additional data on the graphite temperature response as a function of air flow and heater power are shown in Fig. 8.

* It was later discovered that this is an ultraconservative procedure in that the heat capacity of the moderator was practically nullified. Luckily, in most of the runs the temperature of the moderator was in excess of that of the plug, and this effect was not needed.

Tests with Solid Nonreactive Plug

In the second series of tests, a nonreactive sleeve was simulated by placing a 4-in. dia. 40 stainless steel pipe over the central graphite column. These experiments are described in ref. 12. The experimental procedure was to bring the graphite to the desired initial temperature with no gas flow, then shut off power to the inner bank heaters, introduce the air flow, and hold constant power to the outer bank heaters. As in the first series of experiments, the only mode of heat removal was by the air passing through the annulus; therefore, the results are not indicative of the EGCR because with coated sleeves the bulk of the heat removal will be by the large flow passing through the center of the sleeve around the fuel elements.

Figure 9 is an identification of the thermocouples which will be referred to by number in the following figures. Figure 10 shows the static power vs temperature plot, that is, the power required to maintain the given temperatures with no heat of oxidation. Figure 11 show that, when the initial temperatures are approximately 600°C or less with flow rates of approximately 4 lb/hr and with 2.1 kw heater power, temperatures throughout the rig eventually decrease with time. The estimated annular flow rate with one blower operating on air at atmospheric pressure is 25.2 lb/hr. Hence, this test is of value in that it shows that with considerably lower flow rates in the annulus than would exist in the EGCR and attendant lower cooling, the temperatures do not rise. The effect of the lower flow rates is significant in that no evidence of starving exists, that is, as the system approaches equilibrium, the upstream temperatures do not exceed those farther along the channel. Under these conditions, the rate of burning is controlled by the temperature, not the oxygen supply, and the effect of increased flow would be to increase the cooling and hence the rate of temperature decrease. As can be seen in Fig. 10, a power rate of 2.1 kw would maintain a static temperature of approximately 550°C. However, the low gas flow rate used in this test was sufficient to reduce the temperatures at all channel stations.

UNCLASSIFIED
ORNL-LR-DWG 59139

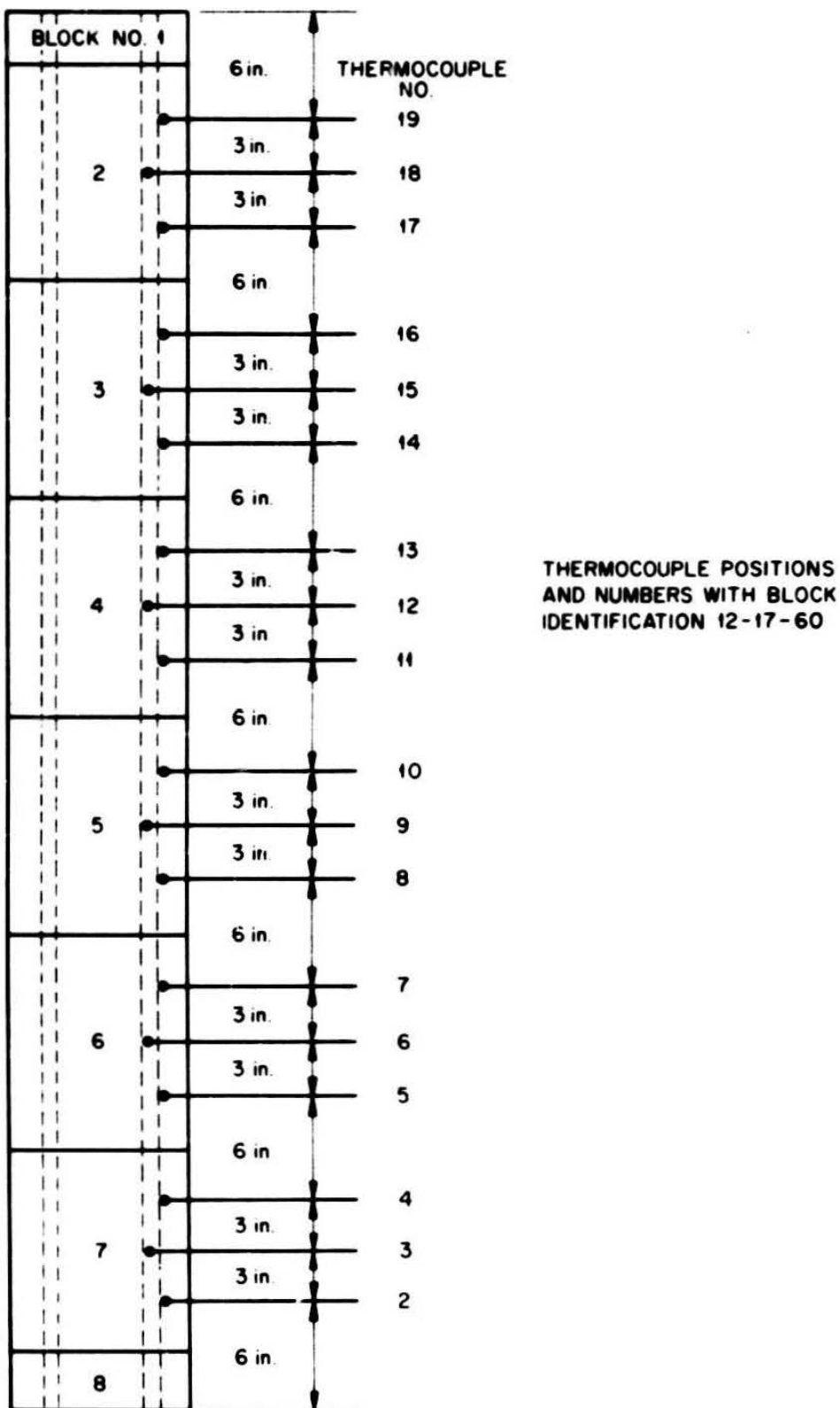


Fig. 9. EGCR Graphite Column - Experiment 2.

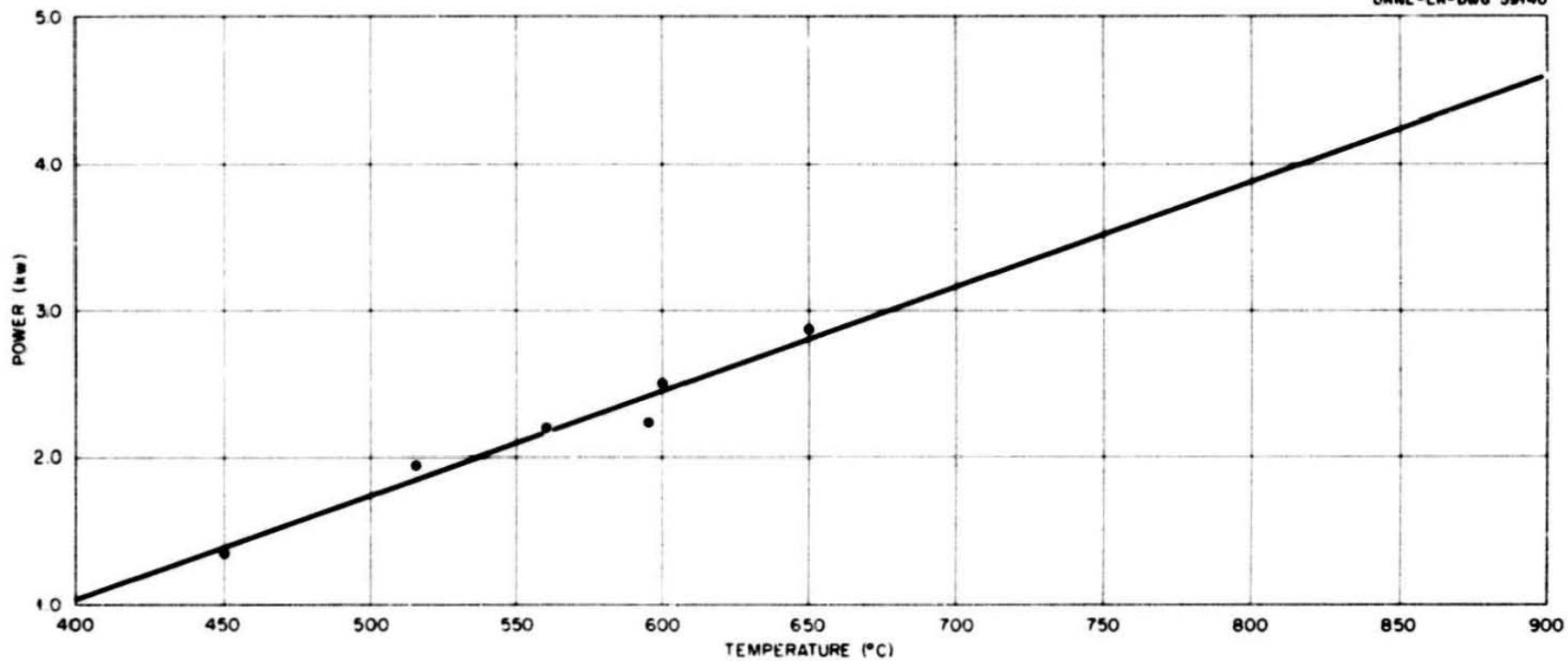


Fig. 10. Static Power vs Temperature for Experiment 2.

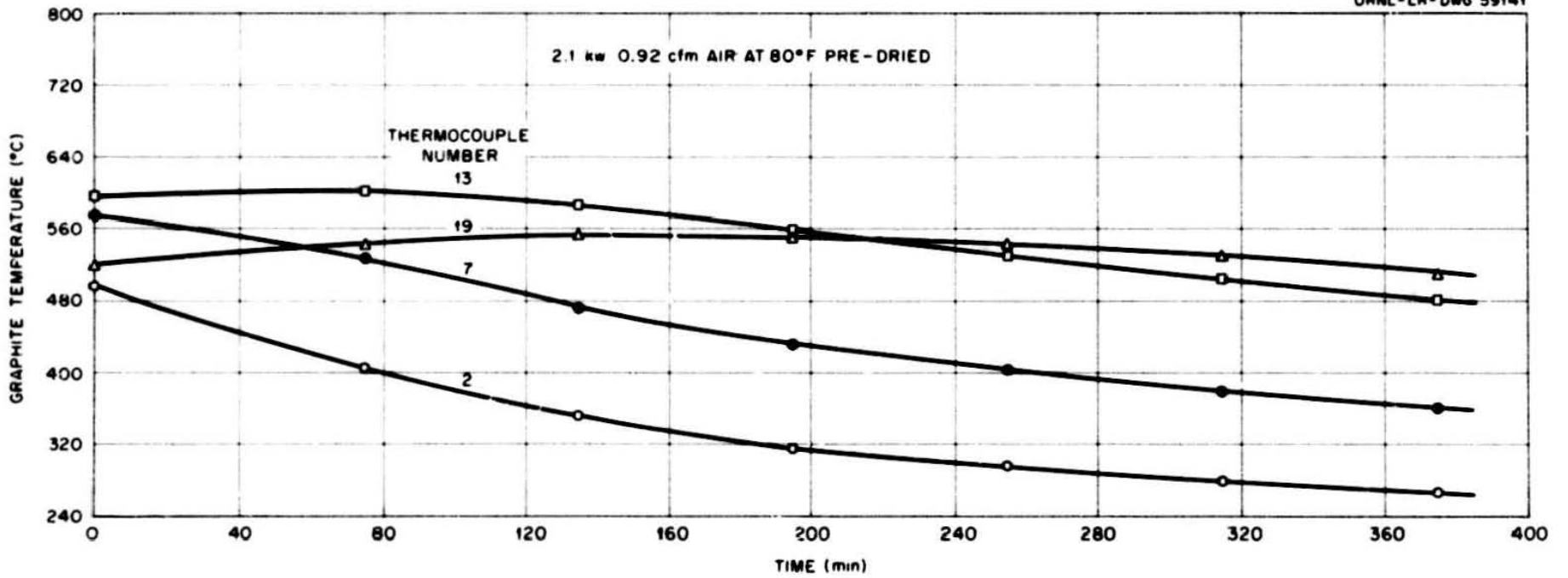


Fig. 11. Graphite Temperature vs. Time, Test No. 1. of Experiment 2.

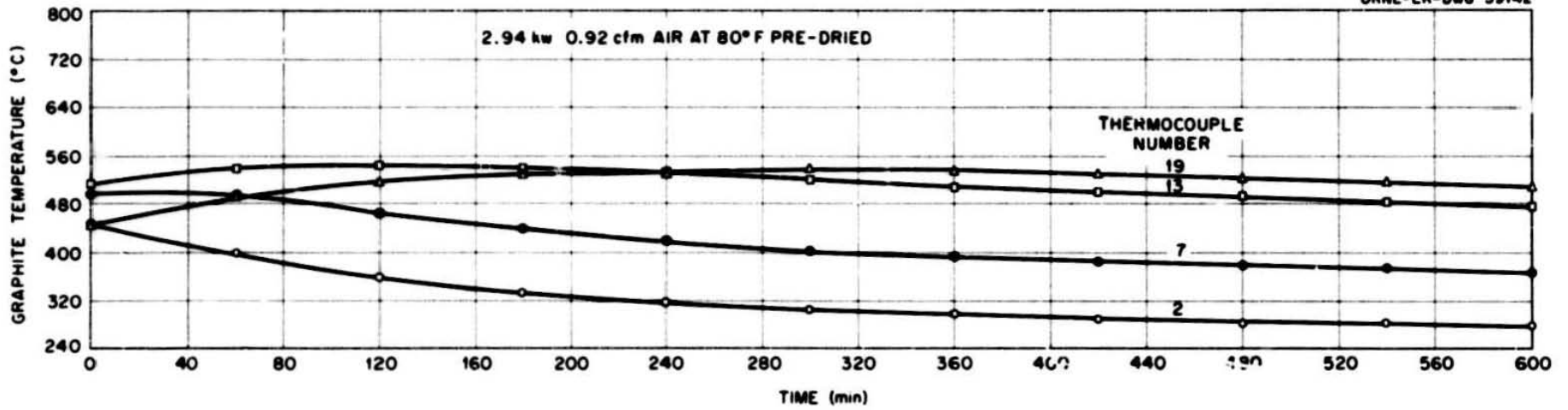


Fig.12. Graphite Temperature vs. Time, Test No. 2. of Experiment 2.

Figure 12 shows the same phenomenon as Fig. 11 but for a heater power of 2.94 kw. At 120 min after the initiation of the tests, the maximum temperature of 540°C is reached, after which all temperatures except that of station 19 decrease, although the heater power is sufficient to maintain a static temperature of 600°C. Station 19 reaches its maximum 320 min after the start of the tests.

Figure 13 shows a slow rise in temperature starting with a temperature of 640°C. At 200 min when the temperature of station 7 has risen to that of station 13 farther up the channel, the rate of rise of the temperature of station 13 increases. This is apparently due to reduced cooling at station 13 which results in greater oxidation.

The results of a similar experiment with slightly different initial conditions are shown in Fig. 14. This test was allowed to continue for 420 min before the heater power was turned off. The most significant feature of these data occurs at around 360 min when the rate of rise of station 7 increases at a time when the rate of rise of stations 13 and 19 is beginning to taper off. Inasmuch as the cooling effect of the gas would act in an opposite fashion, this test clearly indicates that the downstream channel locations were starved for oxygen.

Tests with Coated Graphite Sleeve

The third series of experiments are those testing actual EGCR coated sleeves. Preliminary results of tests on poorly coated sleeves are reported in ref. 13. These tests were of a preliminary nature and were used to get a rough estimate of the efficacy of the coated sleeves in controlling graphite oxidation. Sleeves having known defects such as bare areas, cracks, and excessive porosity that were available at ORNL were sent to Hanford for testing, the philosophy being that if these sleeves raised the runaway ignition temperature a significant amount, then the sleeves of quality high enough for use in the EGCR could easily prevent runaway combustion.

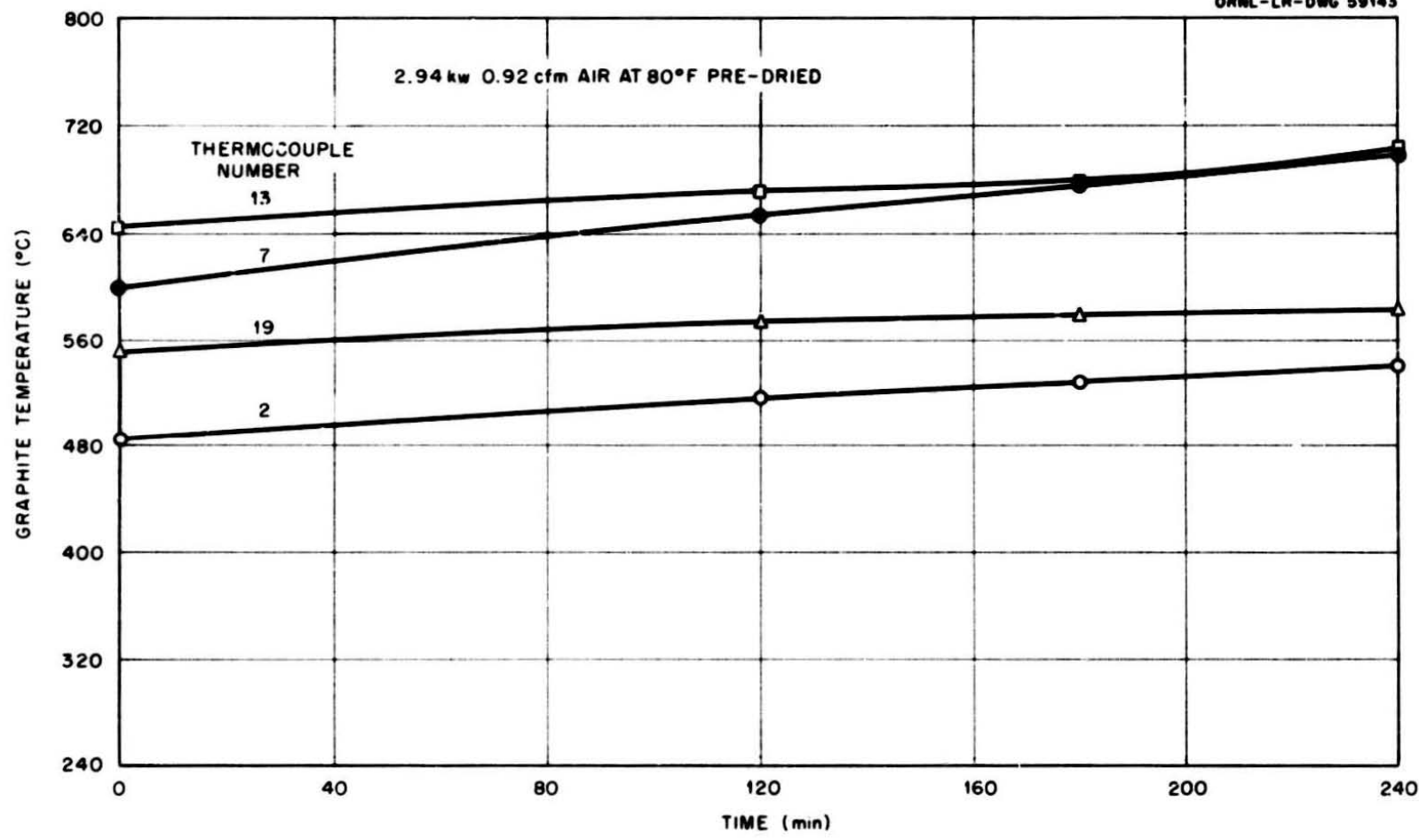


Fig. 13. Graphite Temperature vs. Time, Test No. 4, Experiment 2.

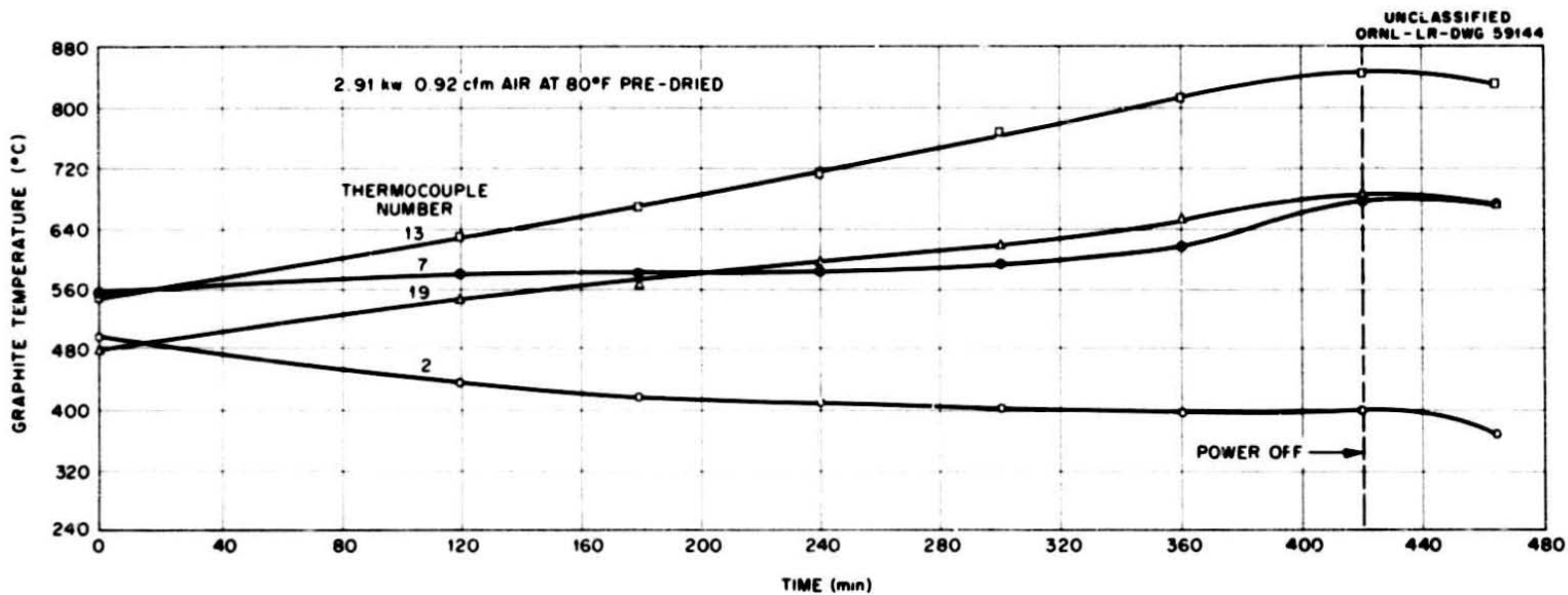


Fig. 14. Graphite Temperature vs. Time, Test No. 7. of Experiment 2.

A full-scale radial channel mockup which included EGCR moderator graphite, SiC-coated fuel sleeves, and dummy fuel elements was used in this experiment. Inlet air flow was 186 lb/hr which is the flow in the lowest power channel in the EGCR when the channels were orificed for constant maximum fuel element clad temperature. (After these tests were run, it was determined that the channels should be orificed for constant outlet temperature. This would decrease the temperature of the graphite in the hottest channel but would increase the temperature in the lower power channels.) Percentage of the flow directed through the fuel sleeve was 93.5 and 6.5 through the annulus between the moderator and the sleeve. Inlet air was not preheated or predried. Sufficient power was maintained to the heaters in the moderator to offset radial heat losses at the beginning of each run and was maintained during most runs. Graphite and sleeve temperatures were monitored at 30 positions along the length of the column.

Self-sustained combustion occurred during two of the nine runs (Nos. 3 and 9). Test 3 began with midplane temperatures of both the sleeve and moderator about 700°C. Temperatures at the ends of the column ranged from 600 to 625°C. Immediately after the air flow was begun temperatures in the center of the column rose rapidly and within 40 min reached 1100°C. At this point air flow was shut off and the test concluded. It is believed that because of a failure in one of the sleeves the damage to moderator block 4 (see Fig. 15) was caused at this time. Test 9 was begun with the temperature in the lower blocks around 350°C, the center about 500°C, and the top about 900°C.

When air flow was introduced, the temperature of the top blocks rose to 1040°C in 1 hr while the lower end cooled to 200°C. At this point air flow was cut from 186 to 47 lb/hr and the top blocks cooled to about 950°C while temperatures in the center and lower sections fell 100 to 300°C in an hour. The top section of the column was the only part to be exposed to severe oxidizing conditions. This exposure



Fig. 15. Damage to Moderator Block No. 4.

lasted 2 1/2 hr. During intervening runs initial temperatures ranged from 650 to 550°C. Rapid cooling took place in each case.

Three sleeves were used, one with a National Carbon Company coating on graphite manufactured by National Carbon, another an American Lava Corporation coating on a Great Lakes Carbon Company graphite, and the third a Norton Company coating on graphite of unknown origin. Pretest inspection of the sleeves showed large uncoated areas on the inside surfaces, bare graphite ends, and cracks in the coatings. Simulated reactor accident conditions caused severe oxidation to take place at the uncoated surfaces and particularly at unprotected sleeve ends. These tests show that unless the sleeve ends are properly coated, a sequence of events can occur which will seriously increase the combustion hazard during a reactor incident. 1) If any two adjoining sleeves do not properly fit together, the resulting gap will have an abundant oxygen supply from the inner channel which will cause the graphite to oxidize. 2) The oxidation widens the gap and the rate of oxygen flow through the gap increases. It will thus oxidize rapidly, especially when the rate of reaction is controlled by the coolant velocity. 3) The increase in oxygen flow increases the rate of oxidation in the gap, causing further widening of the gap. Soon a large hole will open up which greatly increases the oxygen supply in the annulus. Furthermore, as oxidation progresses, the coating is undercut and spalls off. The exposed bare graphite accelerates the rate of growth of the hole. Such a hole is shown in Fig. 16. The air jetting through the hole has a severe effect on the moderator. Holes completely through the 1 1/2-in.-thick moderator blocks were produced allowing air to escape into the static zone on the outer surface of the block. It should be noted that during this test the initial graphite temperature was 700°C and rose to 1100°C.

Even with these poorly coated sleeves, the runaway ignition temperature was raised to 675°C.¹⁴ Runaway did not occur at temperatures below 665°C. However, on the basis of these tests, it was decided to

UNCLASSIFIED
PHOTO 54425

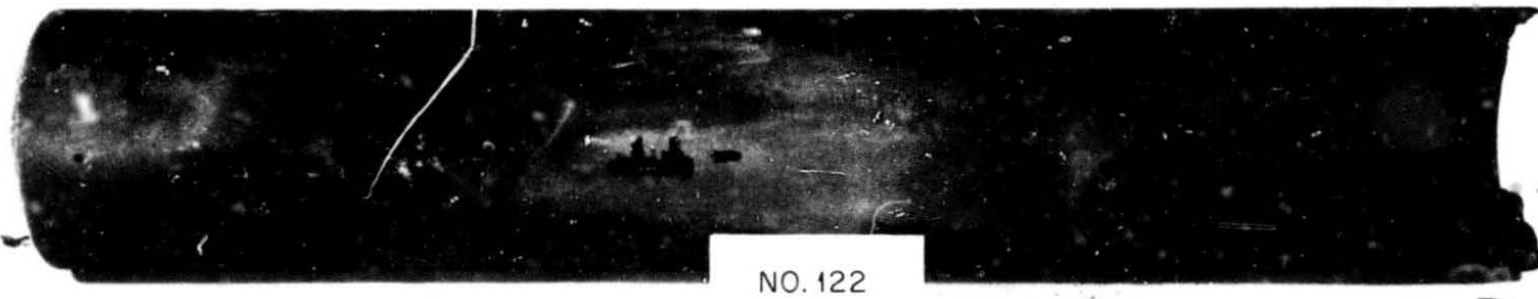


Fig. 16. Damage to a Coated Sleeve.

coat the ends of the sleeves. It had been originally planned to leave the ends of the sleeves uncoated to allow easier machining and mating of the adjacent sleeve surfaces. Investigation showed that grinding and polishing the ends of the sleeves to a fit tight enough to maintain leakage below an acceptable level would actually cost less than breaking away the coating on the ends of the sleeves and machining as originally planned.

The burning rig will soon test good-quality coated sleeves and sleeves with no coatings at all, with the fuel elements simulated by a globar which will be programmed to give the same radiant heat load to the inner surface of the sleeve as expected in the EGCR.

IV. Oxidation Rate Equations

The development of rate equations to be used in determining the heat release due to graphite oxidation in the analyses has been one of the fundamental problems confronting the graphite oxidation program for the EGCR. Initial work performed by Allis-Chalmers² used Kosiba's data¹⁵ for irradiated graphite and used surface-to-volume ratio scaling for use in the EGCR geometry. This was in significant error in two ways. 1) The activation energy of the equations as determined by the low-temperature points was such that at extrapolations to higher temperatures unirradiated data crossed over to yield higher reaction rates than the irradiated data. This is shown by the X points in Fig. 17. 2) Use of the surface-to-volume ratio assumes that the reaction proceeds both on the surfaces of the experimental sample and the graphite in the reactor. As explained quite thoroughly in section II, the oxidation of graphite is not just surface reaction, but proceeds into the graphite to significant depths.

Realization of these shortcomings led to the Hanford experimental work described in section III and the work done by Prados.⁷ This work

UNCLASSIFIED
ORNL-LR-DWG 51520

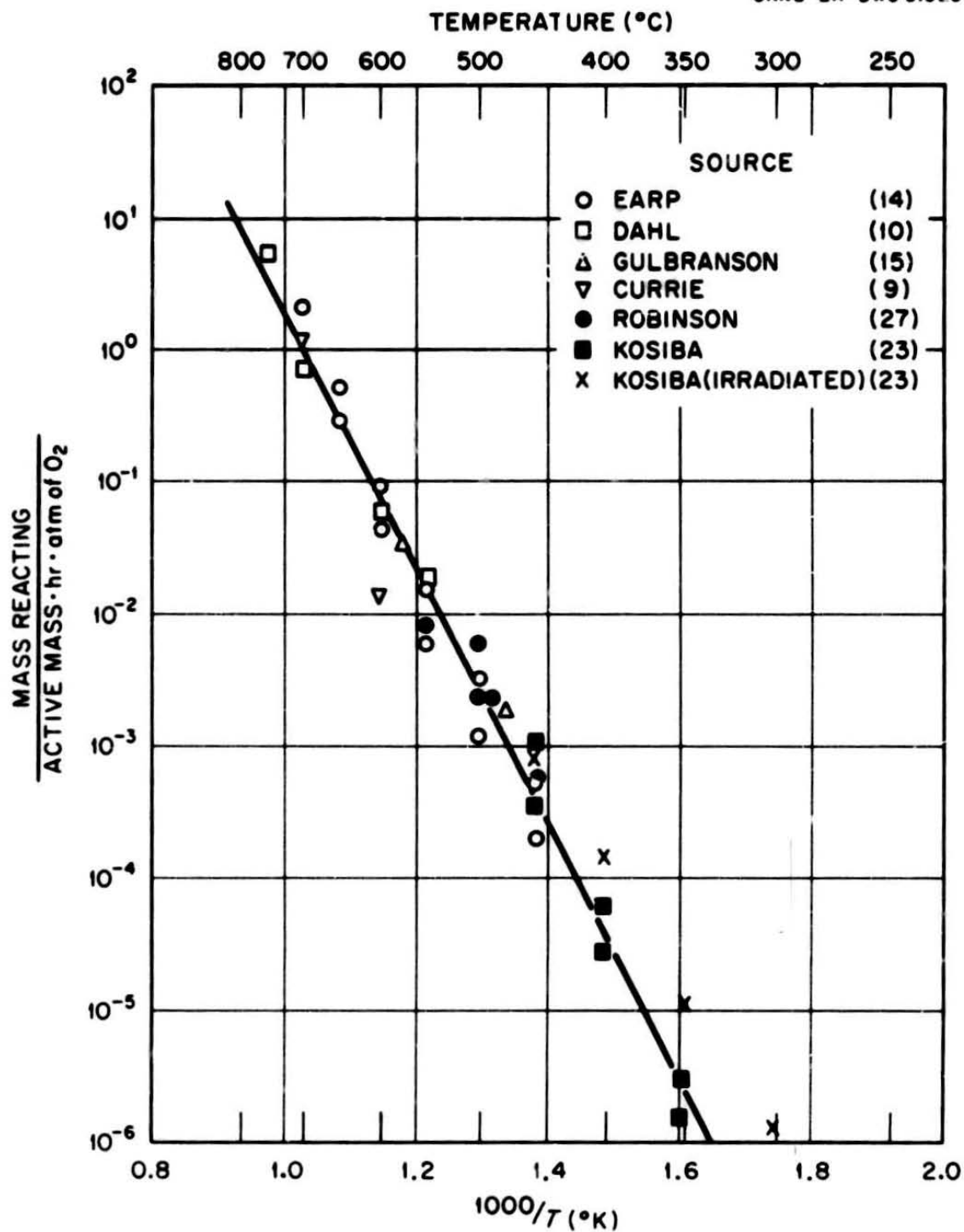


Fig.17. Graphite Oxidation Rate as a Function of Temperature

consists of a critical analysis of data on high-purity (reactor-grade) graphite from six different sources. Prados points out that attempts to describe the rate of the graphite-oxygen reaction quantitatively are complicated by a number of factors of which the following are the most serious: 1) The dependence of the reaction rate on oxygen on partial pressure (reaction order) is in some doubt. 2) The primary reaction product may be either CO, CO₂, or both. Both products enter into secondary reactions, and it is difficult to determine which, indeed, is the primary product under any given set of conditions. 3) Since graphite is porous, reaction may occur on internal pore surfaces as well as at the external surface. Hence, diffusion of oxygen and product gases within the pore structure may play an important role in determining the over-all rate of reaction. At higher temperatures, gas-phase diffusion of reactants to the external surface may also be a rate-determining mechanism. 4) The graphite-oxygen reaction is strongly catalyzed by traces of inorganic impurities. The quantitative effect of these impurities is difficult to determine since impurity content may vary within a given sample of graphite. Variations in graphite crystal orientation may also produce variations in oxidation rates. 5) Oxidation rates may be markedly accelerated by neutron and gamma radiation. 6) Rates may be retarded by the presence of certain halogen-containing substances in the gas phase.

Prados proceeded to reduce the data by means of the depth-of-diffusion concept and assumption of oxygen first-order dependency to a consistent basis of fraction of active mass reacting per unit time, active mass being the mass given by the volume generated by the product of the surface area and the pseudodepth of diffusion. This is described in more detail in Appendix A, and the results of this work are shown in Fig. 17. The rate equation describing the least squares fit of the data is:

$$k = 7.24 \times 10^9 \exp(-22100/T) \quad (16)$$

where M has units of weight fraction oxidized per hour per atmosphere of O_2 , and T is in $^{\circ}K$.

The activation energy obtained from the above expression is 44.0 kcal/g atom. This is within the range of values reported from individual investigations but is somewhat below the average (about 50 kcal/g atom). Points for unirradiated, high-purity graphite agree with each other within a factor of 6 or less. It is felt that the major cause for such a discrepancy lies in variations among the graphite specimens investigated of such factors as impurity content, crystal orientation, pore size distribution, etc.

Using this rate equation, the depth of oxidation was found as a function of temperature and is shown in Fig. 18.

The heat release equations used in the analysis of the reactor hazard were estimated on the assumption that graphite is oxidized completely to CO_2 to a depth given by the depth of diffusion L where L as defined in Eq. (6) may also be expressed as:

$$L = \sqrt{MD_p / (M RT)} \quad (17)$$

The heat release per unit surface area of graphite is:

$$q/S = P_o \Delta H \frac{P}{M} ML \quad (18)$$

where P_o is the partial pressure of O_2 and ΔH is the heat of reaction in BTU/lb. mole.

When combined, Eqs. (17), (18), and (16) yield for air at one atmosphere:

$$q = (S)(7.53 \times 10^7)(T/1660)^{0.25} \exp(-19,900/T) \quad (19)$$

where q is the heat release in $P+u/hr$, S is the macroscopic surface area of the graphite in ft^2 , and T is the temperature in $^{\circ}R$. The $(T/1660)^{0.25}$ term was included in this manner for convenience because in the temperature range of interest (around $1100^{\circ}F$), this term is close to one and is relatively insensitive to temperature compared to the exponential term.

UNCLASSIFIED
ORNL-LR-DWG 51523

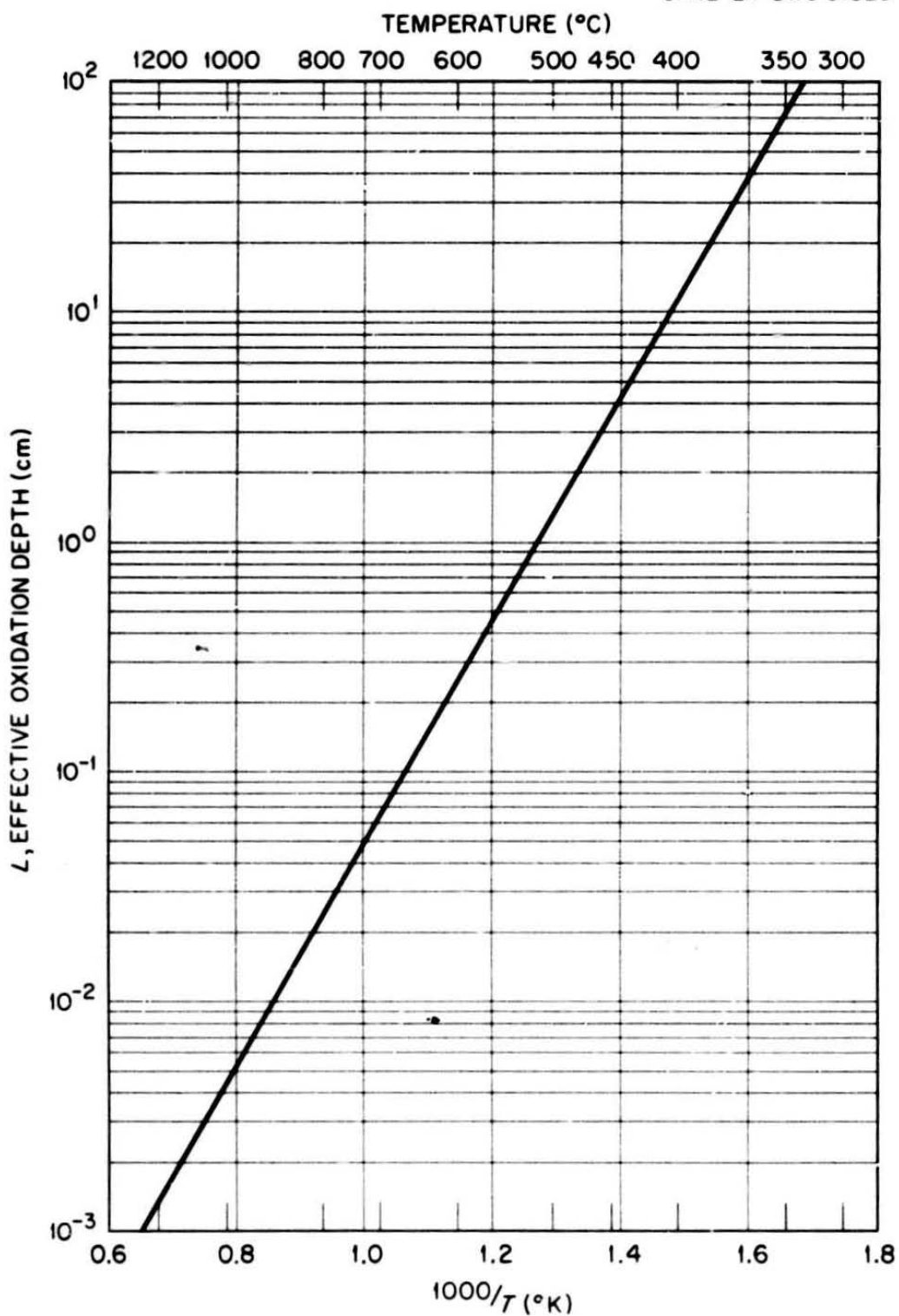


Fig.18. Effective Oxidation Depth L , vs Temperature (for $\epsilon = 0.24$).

The above heat release equation includes the depth-of-diffusion term. When the depth of diffusion, L , exceeds the dimensions of the piece undergoing oxidation, Eq. (19) is no longer strictly correct, and the diffusion-free equation is used in which L in Eq. (18) is replaced by the dimension of the piece.

Equation (18) also does not include factors for the γ irradiation effect and prior neutron irradiation. It is expected that the γ effect becomes less significant at higher temperatures (above 500-600°C), but it perhaps is justifiable in the interest of conservatism to include a factor in the analysis.

Hanford has also done experimental work on EGCR graphite and CSF graphite and has reported rate equations. A rate for EGCR graphite was reported¹⁶ to be:

$$k = 1.0 \times 10^{11} \exp(-25,000/T) \quad (20)$$

where k is the fraction of active mass oxidizing per hour per atmosphere of air, and T is temperature in °K. The actual data are shown in Fig. 19.¹⁷ Comparison of Eq. (20) with Fig. 19 shows that the equation does not fit the experimental curves. This is so because of the following reasons.¹⁸ The recommended equation is based on an activation energy of 50 kcal/mole and an increase in the frequency factor by 1.7X to allow for rate enhancement by γ irradiation. Hanford has recommended 50 kcal/mole as the activation energy on the basis of data from a series of kinetic experiments conducted on CSF graphite. Since many more experiments were conducted on this graphite than have been run on EGCR graphite to date, they feel much more confident of the data. Experimental error produces a range of ± 4 kcal/mole, and since the apparent activation energy of EGCR graphite (47 kcal/mole) falls within this range, it was deemed valid to use the established value of 50. Assuming constant activation energy, frequency factors were calculated for each observed rate and averaged (see Table II).

UNCLASSIFIED
ORNL-LR-DWG 59445

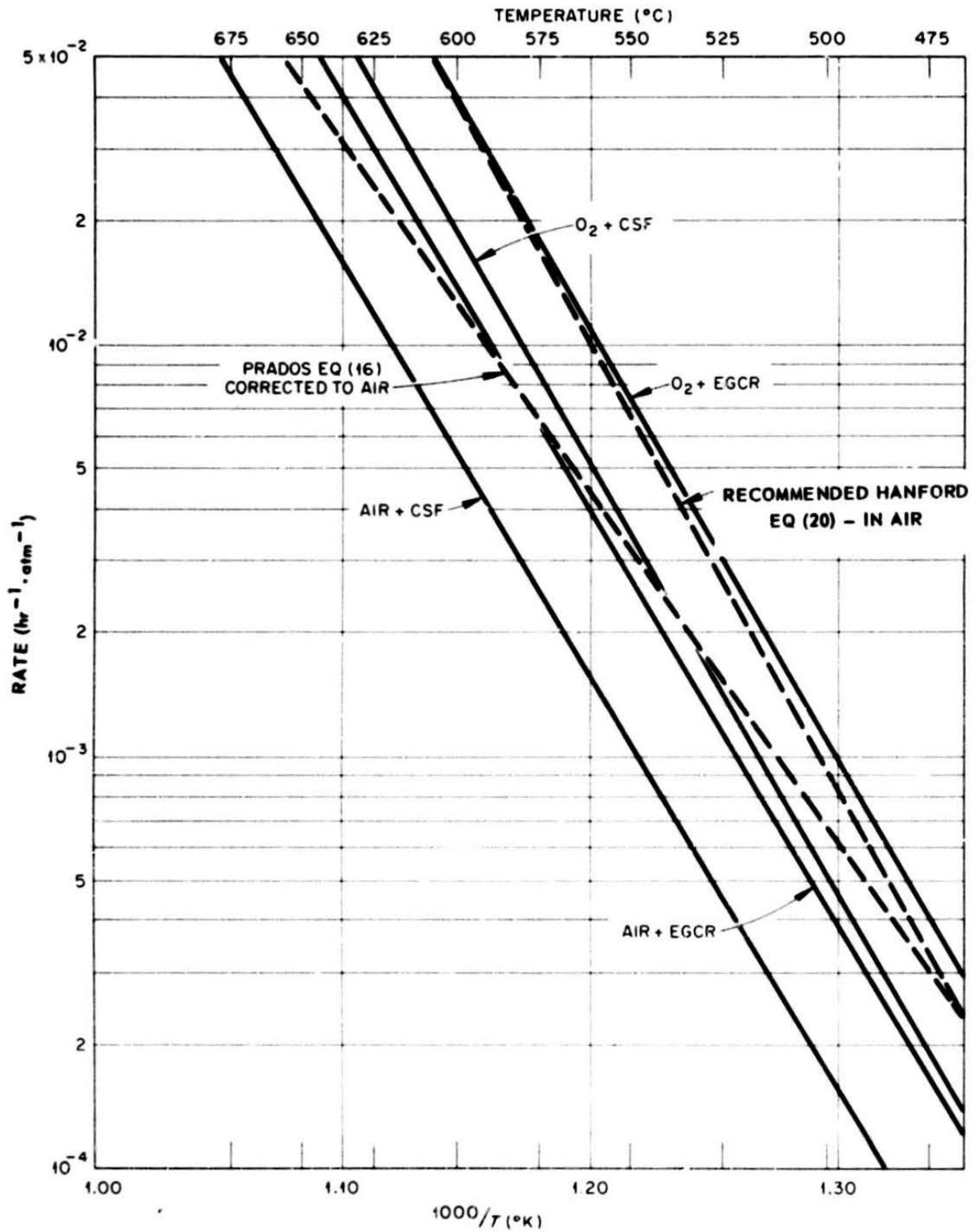


Fig. 19. Oxidation Rates of EGCR Graphite Compared to Gas Purified Control Samples.

TABLE II

EGCR Graphite Frequency Factor Determination

$$k = (a) \exp(-c/RT), \text{ hr}^{-1}$$

$$(c = 50,000 \text{ cal/mole})$$

<u>T °C</u>	<u>k (hr⁻¹ × 10⁻³)</u>	<u>a × 10¹⁰</u>
525	1.01	5.55
550	3.38	7.13
575	6.42	5.49
600	13.3	4.87
625	29.8	4.86
650	99.9	7.56

$$a = 5.91 \times 10^{10}$$

$$\text{standard deviation } \sigma = 1.16 \times 10^{10}$$

It should be noted that the gas constant, R, used to determine the values given in Table II was taken as 2.00 cal/mole-°K. Use of the actual value, R = 1.9872, yielded a frequency factor $a = 5.40 \times 10^{10}$. This would then require a gamma correction of 1.85X to give the same values as Eq. (20). Since the gamma effect cannot be accurately represented by such a simple factor, this difference is not considered to be important.

The reported rates were based on total weight of the sample. Samples used in these experiments were sleeves 2 in. long with an outside diameter of 0.426 in. and an inside diameter of 0.250 in. The wall thickness was 0.22 cm, or less than the predicted depth of diffusion at temperatures above 500°C. Cross-sectioning of a number

of samples revealed no apparent reaction gradient through the sample. However, for complete assurance that the experiments were not diffusion controlled, the surface-to-volume ratio was halved for several experiments. No effect on the oxidation rate was discernible.

Equation (16), given by Prados, and Eq. (20), recommended by Hanford, are shown in Fig. 19 along with the actual data on EGCR and CSF graphite. Prados' equation is quite close to the EGCR rate in air in the temperature range of interest (around 600°C) but yields lower rates at higher temperatures and is conservative at the lower temperatures. Also, no gamma effect is included. The Hanford equation yields higher rates throughout the temperature range, and because of the higher activation energy, becomes increasingly conservative with increases in temperature. Further use of these equations is made in section V.

V. Graphite Oxidation Analysis in the EGCR

A description of the principles of oxidation analysis was given in section II. This section will go into more detail on the applications of these principles specifically to the EGCR.

There are a great many considerations involved in the analysis of the EGCR. The geometry is complicated in that seven fuel rods are suspended within a graphite sleeve of 3-in.-i.d. and 5-in.-o.d. dimensions which are stacked, along with top and bottom dummies, in 5 1/4-in.-dia, 20-ft-long channels in the moderator graphite. Neither the axial nor radial power distributions is constant. The initial temperatures of the graphite components vary both along the channel and radially. The transient calculations must consider the radiant heat load on the inner surface of the sleeve due to the levelization of the temperature structure in the fuel elements, changes in flow rates and heat removal, heat transfer across the sleeve, heat

generation due to decay of fission products in the fuel, sleeve, and moderator, chemical heat release as a function of temperature and oxygen supply, and the heat capacity of the fuel and the graphite.

The original digital computer program was set up by Landoni at Allis-Chalmers (then ACF).² It has since been modified by Lampe of Allis-Chalmers and Edwards of the K-25 computer facility at Oak Ridge. The equations presented in Appendix B are according to Landoni and contain the following assumptions and features:

- 1) The radial temperature profile is treated by temperature nodes for the fuel element clad, sleeve, moderator, central channel coolant, and annulus coolant.
- 2) No axial heat transfer is assumed for the sleeve and moderator block.
- 3) Radiant and convective heat transfer are included.
- 4) A constant mass flow rate of air is assumed for the central channel and annular coolant.
- 5) Heat sources included are a) fuel element temperature levelization; b) gamma, beta, and neutron afterheat assumed all in the fuel element; c) graphite oxidation heat from reaction at sleeve and moderator block surfaces.
- 6) Oxygen consumption is calculated stepwise up through the core.

The program described in Appendix B was modified by Lampe¹⁹ in the following ways. The section on energy contributed by the delayed neutrons after shutdown was deleted because the effect is small. Landoni used the Way-Wigner relation ($t^{-0.2}$) for energy due to fission-product decay. This is somewhat low at times before 10^5 sec after shutdown and somewhat high thereafter. Lampe substituted the Untermeyer relation which is thought to be higher than actually expected. These curves along with preferred curve developed by ORNL²⁰ are shown in Fig. 20.

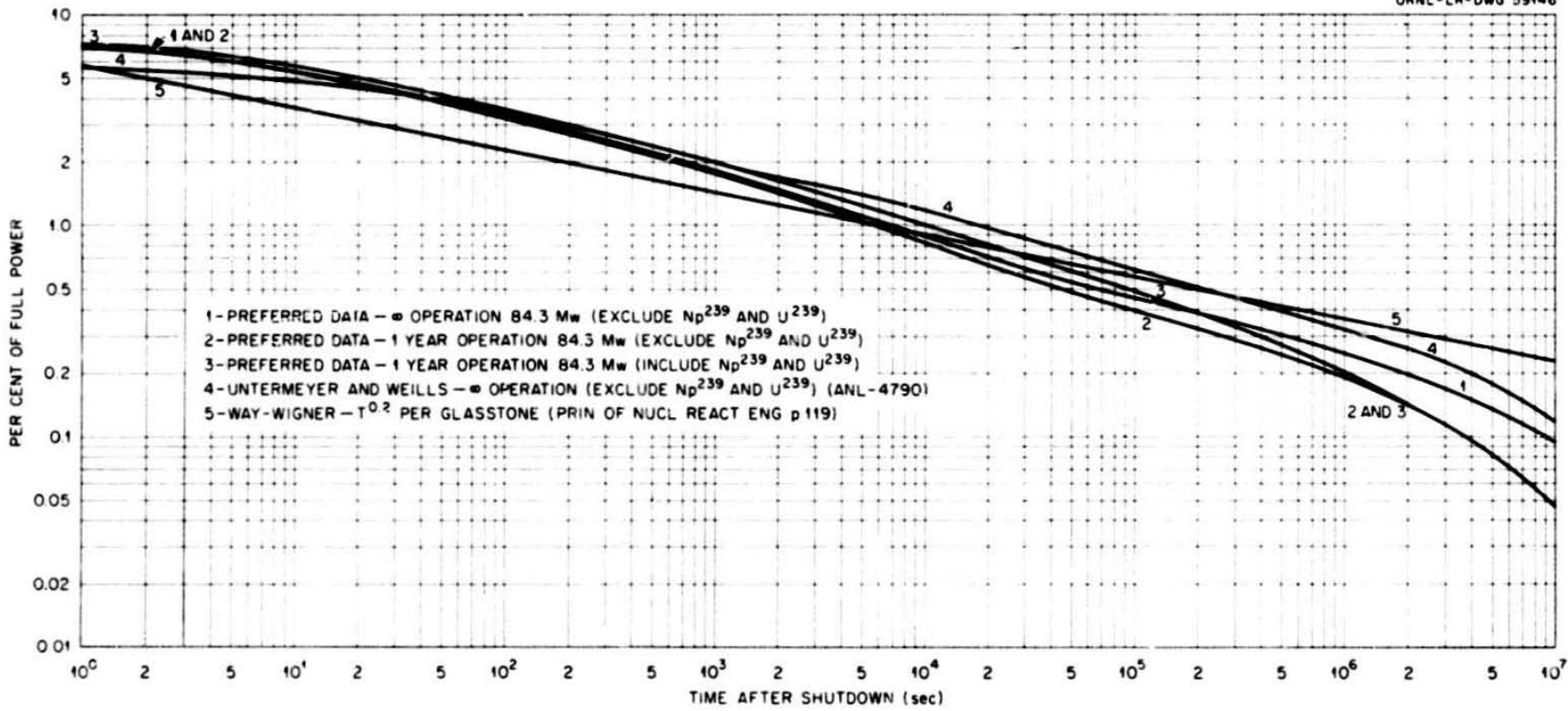


Fig. 20. Afterheat in the EGCR.

Lampe treated the effects of the radial temperature structure across the sleeves by varying the heat capacity of the graphite as an input to the computer in such a manner that rise of temperature is similar to that in the case under an imposed surface heat load. A six-node model of the sleeve at one axial position was calculated, and the transient radial temperature distributions were found. The average temperature of the inside node was then taken to represent the surface temperature. This temperature was then plotted, and from this a pseudoheat capacity was found for use in the calculations. The results of the fine-structure model at one axial position are shown in Fig. 21, and comparison of results using various pseudoheat capacities is shown in Fig. 22. In this calculation, 25% of the actual heat capacity of the sleeve was used for the first 10 sec and 90% thereafter. This procedure is somewhat conservative in terms of the heat stored in the graphite. In order to obtain the temperature match, it can be seen from Fig. 22 that the pseudoheat capacity must be low on the initial transient, and then increases at longer times. This would show a greater heat content in the core when the temperatures reach their peaks and begin to decline than would actually be the case. The full value of the heat capacity of the moderator was used because it is not subjected to a sudden large radiant heat load and the temperature gradient through the column is expected to be small. An extra measure of conservatism is present in this procedure in that the outer surfaces of the sleeves, according to the computer, will rise at the same rate as the inner surface. This will reflect itself in a quicker rise in the surface of the moderator which is uncoated. This is an area in which further work could be done.

The fuel element temperature levelization is treated by assuming that the heat transferred from the fuel region of the fuel element during a thermal transient can be expressed as:

$$q = Q_0 \exp(-\lambda\tau) \quad (21)$$

UNCLASSIFIED
ORNL-R-DWG 59447

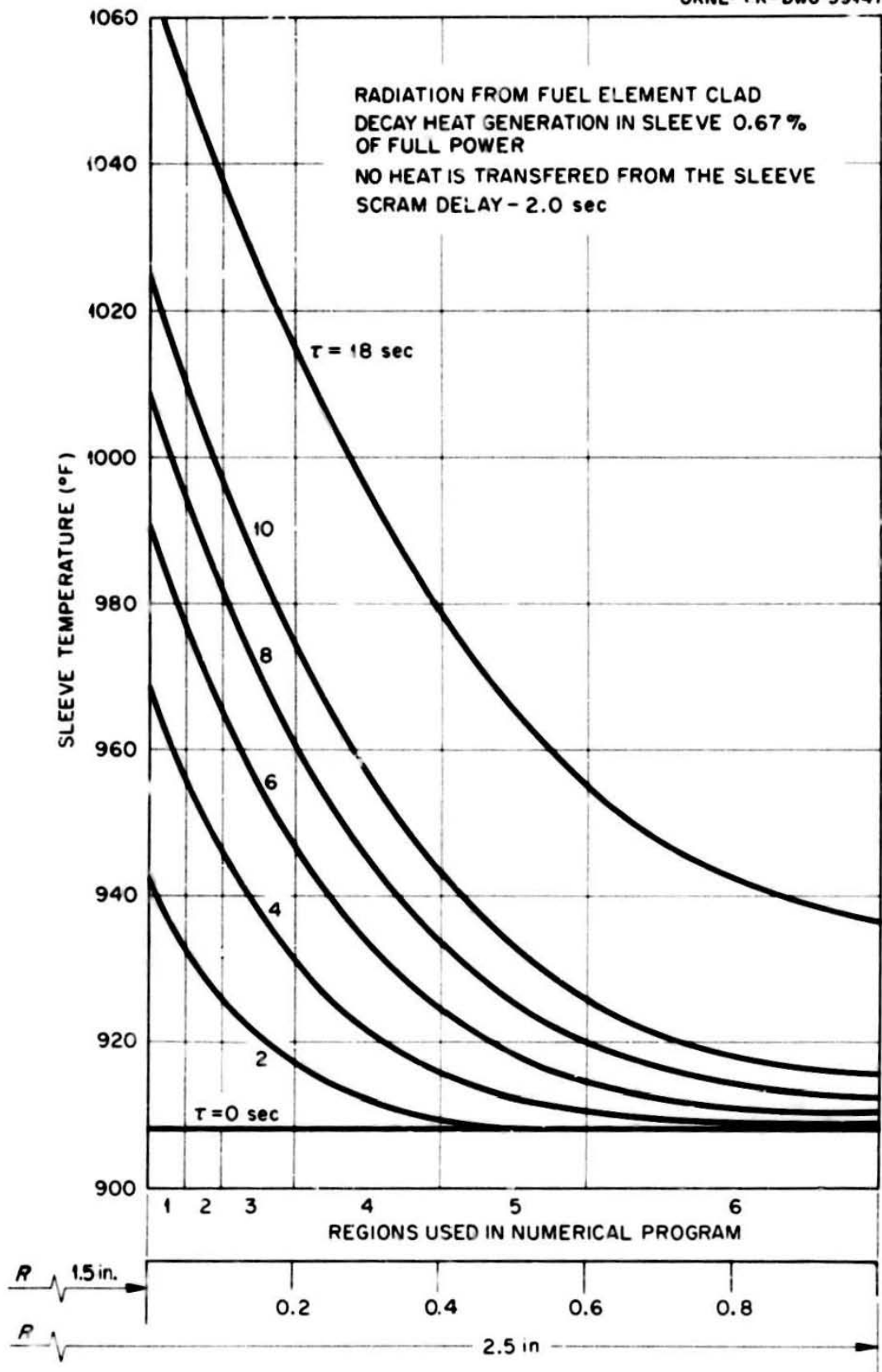


Fig. 21. Graphite Sleeve Temperature Distribution.

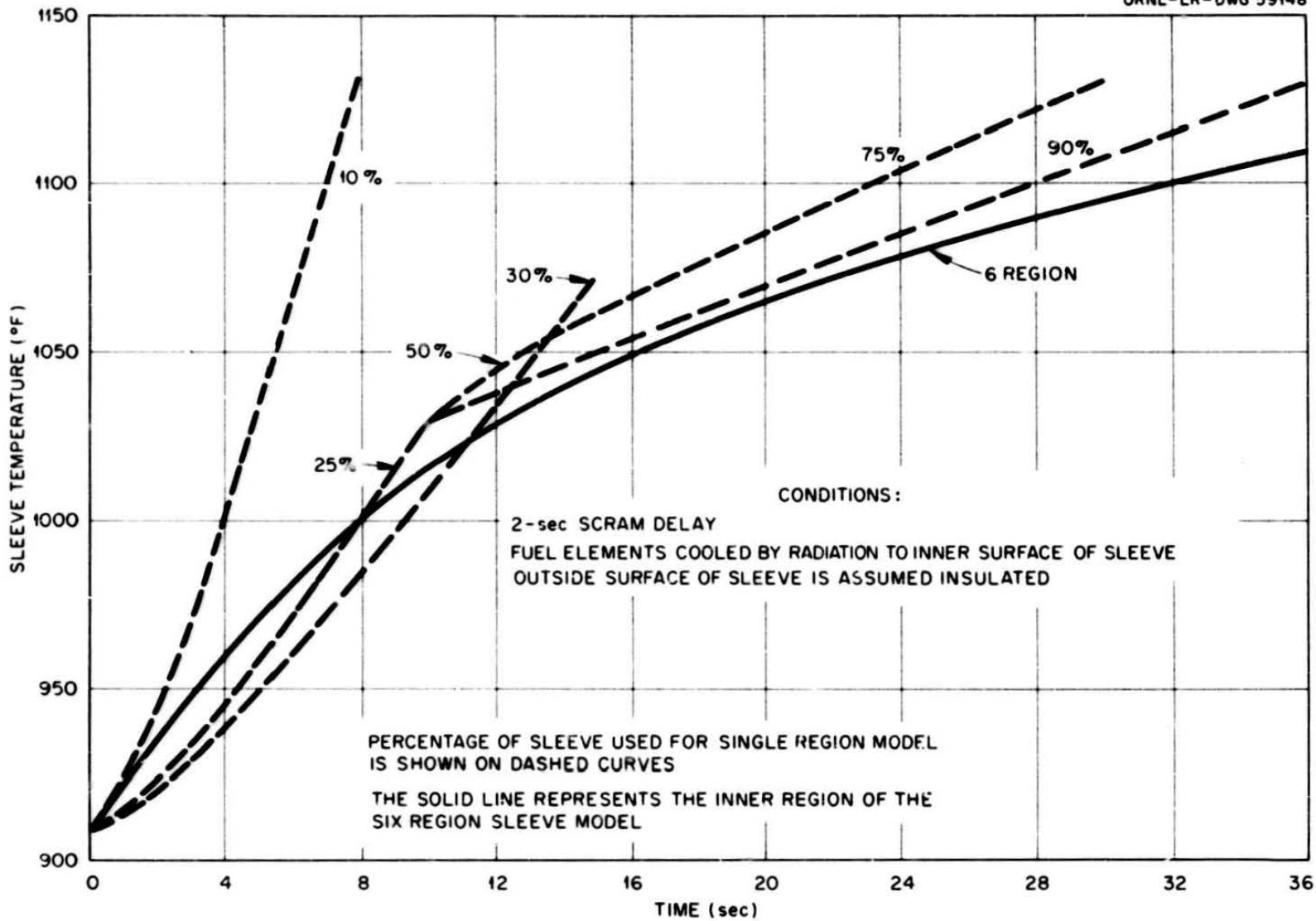


Fig. 22. Comparison of Graphite Sleeve Temperatures.

where

q = heat flux between fuel and clad

λ = time constant

Q_0 = heat stored on fuel element above clad steady-state temperature

τ = time

The above equation is an approximation of the actual analytical expression which is an infinite series of exponentials. Because the equation is an approximation it is valid only for short periods of time when used with a particular time constant. To calculate the transient temperatures of a fuel channel for a period of time greater than a few seconds, it is necessary to use different values of the time constant for each time increment. The time constant is determined by use of a numerical solution to the transient problem at a single axial location.

For a time 40 sec after the accident the fuel temperature profile has leveled out, and the temperatures of the fuel clad and fuel are within 200°F of each other. At this time the fuel element is treated as a single node combining the oxide and clad heat capacities; the decay of the fuel temperature profile is eliminated from the calculation.

The results of the Allis-Chalmers calculation are reported in ref. 19; only the results directly pertinent to graphite oxidation will be reported here.

The assumptions of the depressurization accident with air as a coolant are:

- 1) The reactor was operating in a steady-state condition at 100% power with fuel element temperatures as given in ref. 21 and power distributions as obtained from ref. 22 for bank insertions of all control rods 62 in. into the active core except for the central control rod which is fully inserted.

2) The rupture is located in the cold leg of the reactor coolant system.

3) The reactor coolant system pressure decreases to 18 psia within 5 sec.

4) The flow in the reactor core is instantaneously reversed. All the helium in the upper plenum and in the annulus between the moderator and temperature barrier is assumed to flow downward through the core during the 5-sec depressurization time. The flow is assumed to be zero when the depressurization is complete and is assumed to vary linearly with time during the depressurization.

5) The reactor is scrammed 2.0 sec after the start of the accident. Immediately following the scram the power generation in the fuel follows Untermeyer's curves of decay heat. The heat generation in the sleeve and column is assumed to be 2% of full-power heat generation and decays according to the Untermeyer curves. Thirty per cent of the heat generated in the graphite is in the fuel assembly sleeves with the remainder in the graphite column.

6) The blower in the ruptured loop deblades.

7) No steam tube ruptures occur during the accident.

8) The air entering the bottom of the reactor core from the bottom plenum is at 500°F.

9) The flow of air from this one operable blower is 85,000 lb/hr. Approximately 43% of this flow bypasses the reactor core through the ruptured loop.

10) Flow resistance through the failed blower is negligible.

11) The moderator is uncoated, and the coating on the sleeve is 95% effective.

12) The reaction is first order.

The rate equations used are those derived using Hanford's recommendation equation (20). As discussed in section IV, when the depth of diffusion exceeds the half-thickness of the sleeves and the cell diameter of the moderator, the reaction is no longer considered to be

diffusion controlled, and the dimensions of the piece are used in lieu of the depth-of-diffusion term. This procedure yields the following equations that were used in the A-C analysis:

1) For inside or outside surfaces of the coated graphite sleeves:

a) below 1411°R:

$$q = 2.99 \times 10^{14} \exp(-45,000/T) \quad (21)$$

b) above 1411°R:

$$q = 3.66 \times 10^7 \exp(-22,500/T) \quad (22)$$

2) For the annulus surface of the moderator:

a) below 1300°R:

$$q = 2.30 \times 10^{16} \exp(-45,000/T) \quad (23)$$

b) above 1300°R:

$$q = 7.16 \times 10^8 \exp(-22,500/T) \quad (24)$$

where

q = heat flux, Btu/hr-ft²

T = absolute temperature of graphite being oxidized, °R

The calculation was performed for 10 axial positions as shown in Fig. 23. The fuel channel clad, sleeve, and block temperatures are shown as functions of time for positions 4, 5, 6, and 7 on Figs. 24-27. Figure 28 shows the oxygen concentration in the main coolant channel and annulus as a function of time. Figure 29 shows the channel and annulus outlet temperature as a function of time.

It can be seen from Figs. 24-27 that the maximum temperatures reached are approximately 1200°F. Figure 29 shows that the air outlet temperature from the annulus reaches a peak of approximately 1160°F around 2.5 to 3.0 hr after the accident. Figure 28 shows that the bulk of the burning occurred in the annulus. The results of this study show that burning can be controlled if the sleeves are coated

UNCLASSIFIED
ORNL-LR-DWG 59149

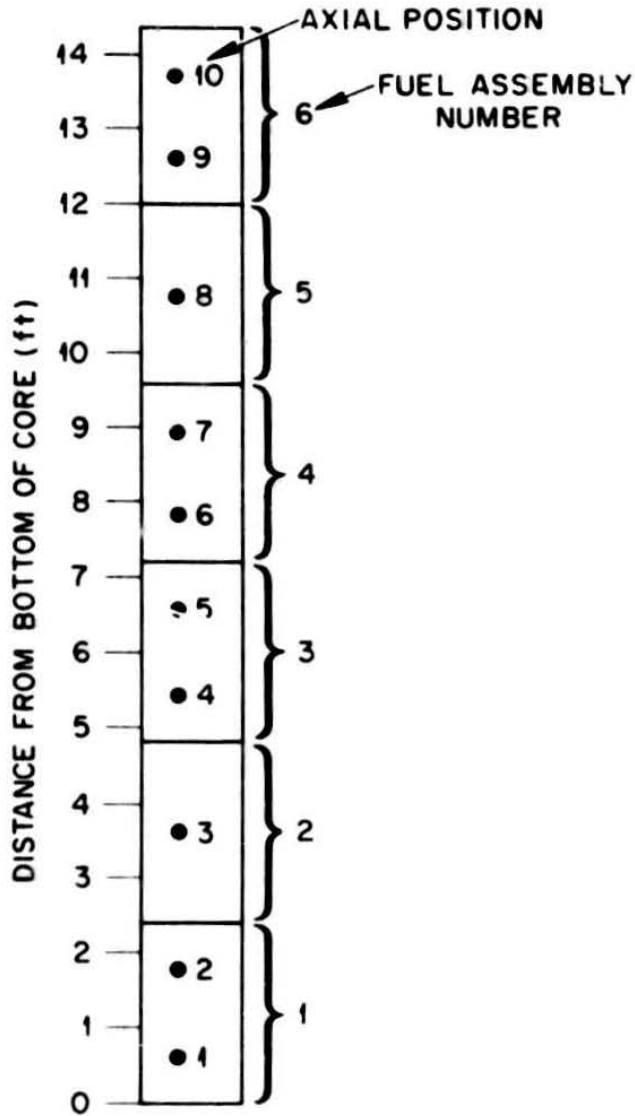


Fig. 23. Identification of Axial Positions in A-C Calculations.

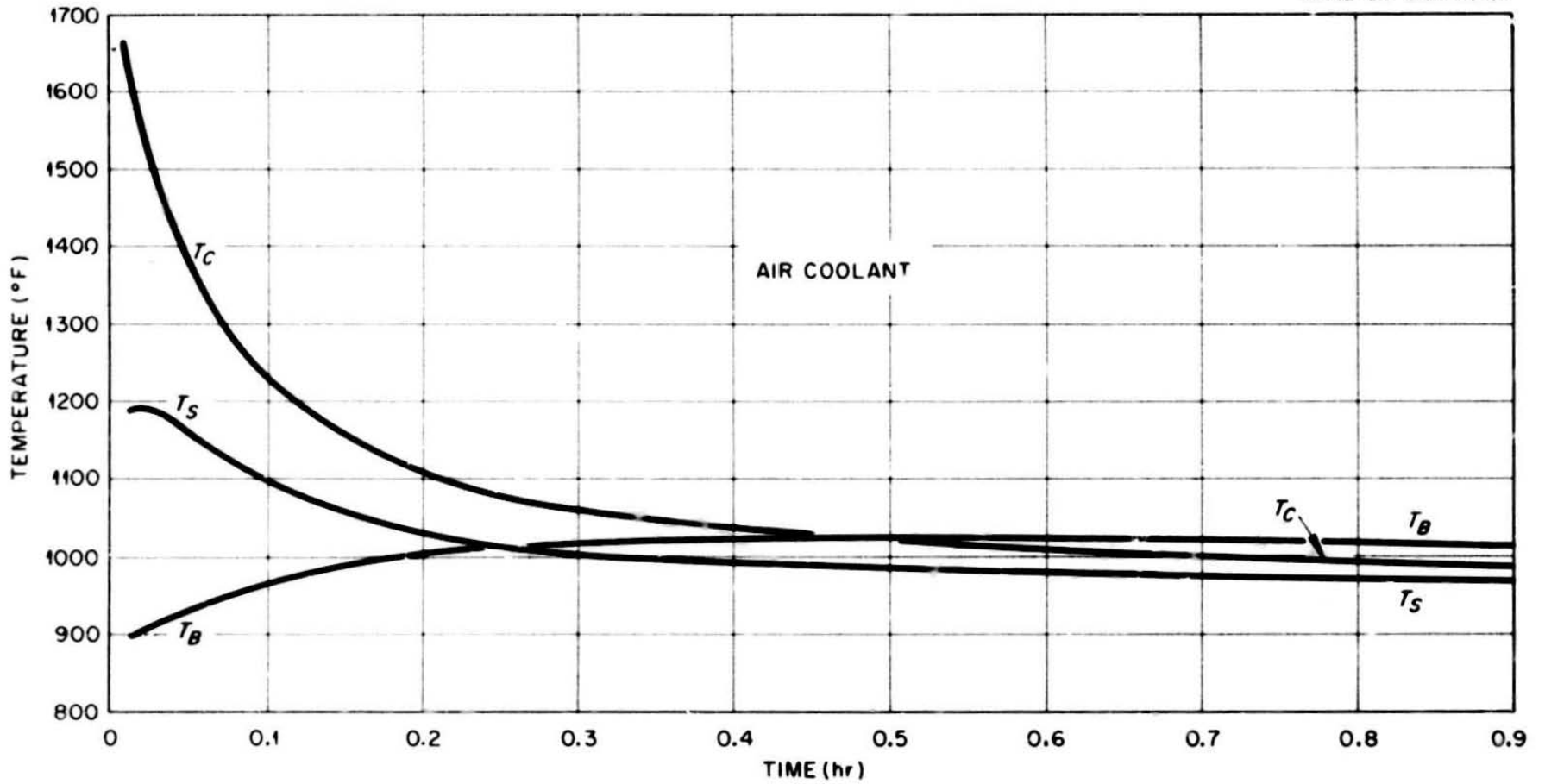


Fig. 24. Fuel Channel Temperatures, 4th Axial Position vs Time.

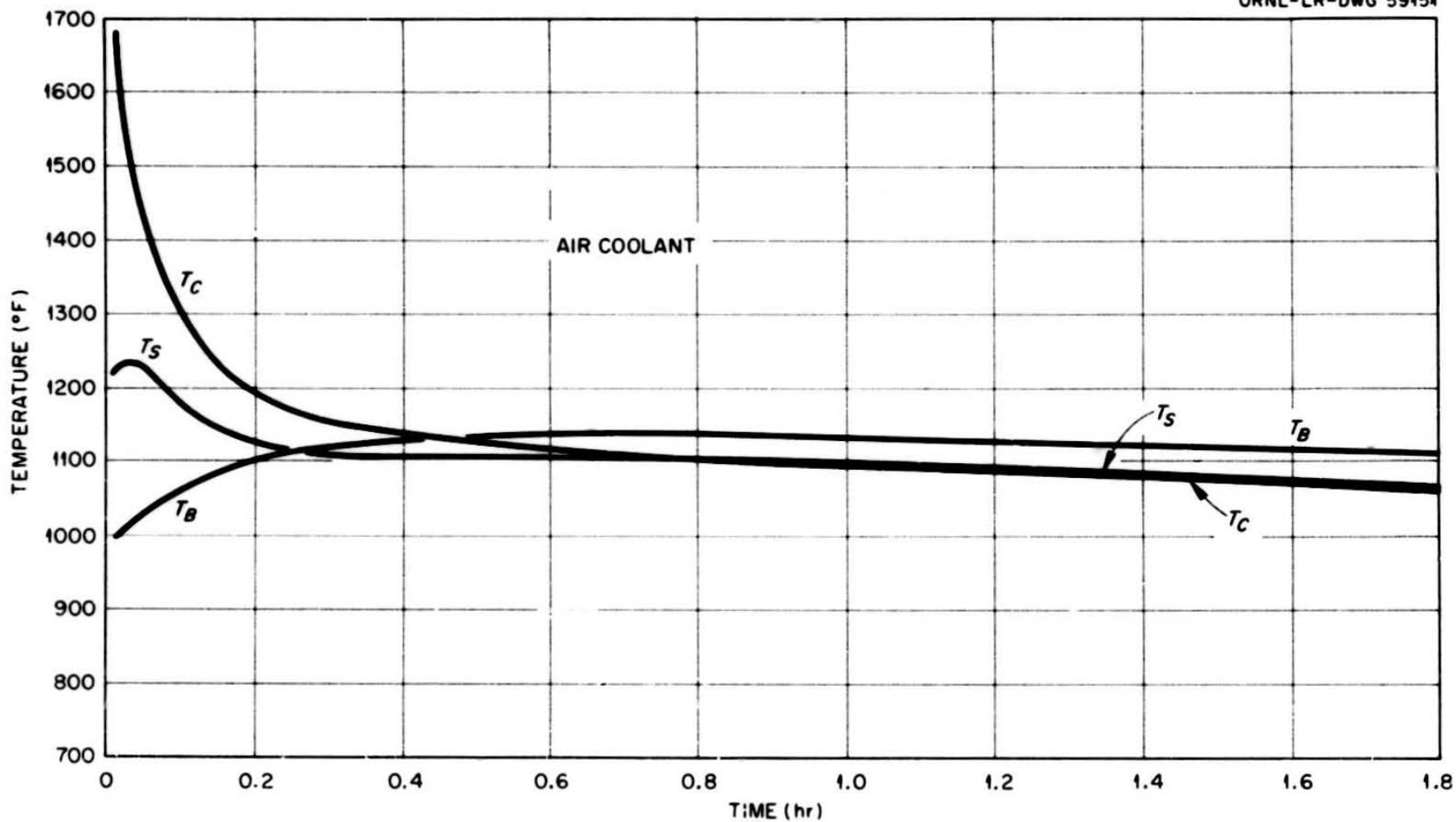


Fig. 25. Fuel Channel Temperatures, 5th Axial Position vs Time.

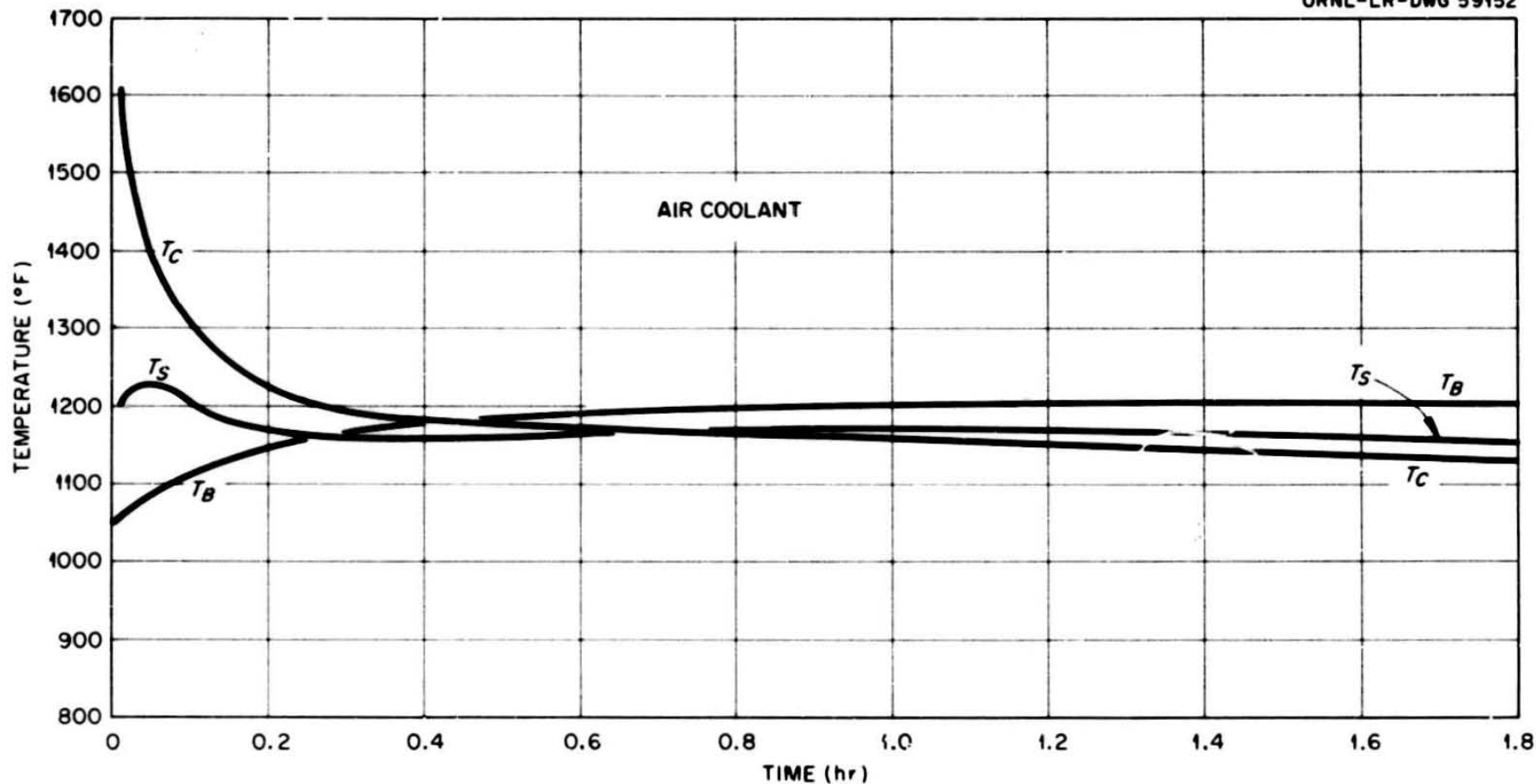


Fig. 26. Fuel Channel Temperatures, 6th Axial Position vs Time.

UNCLASSIFIED
ORNL-LR-DWG 59153

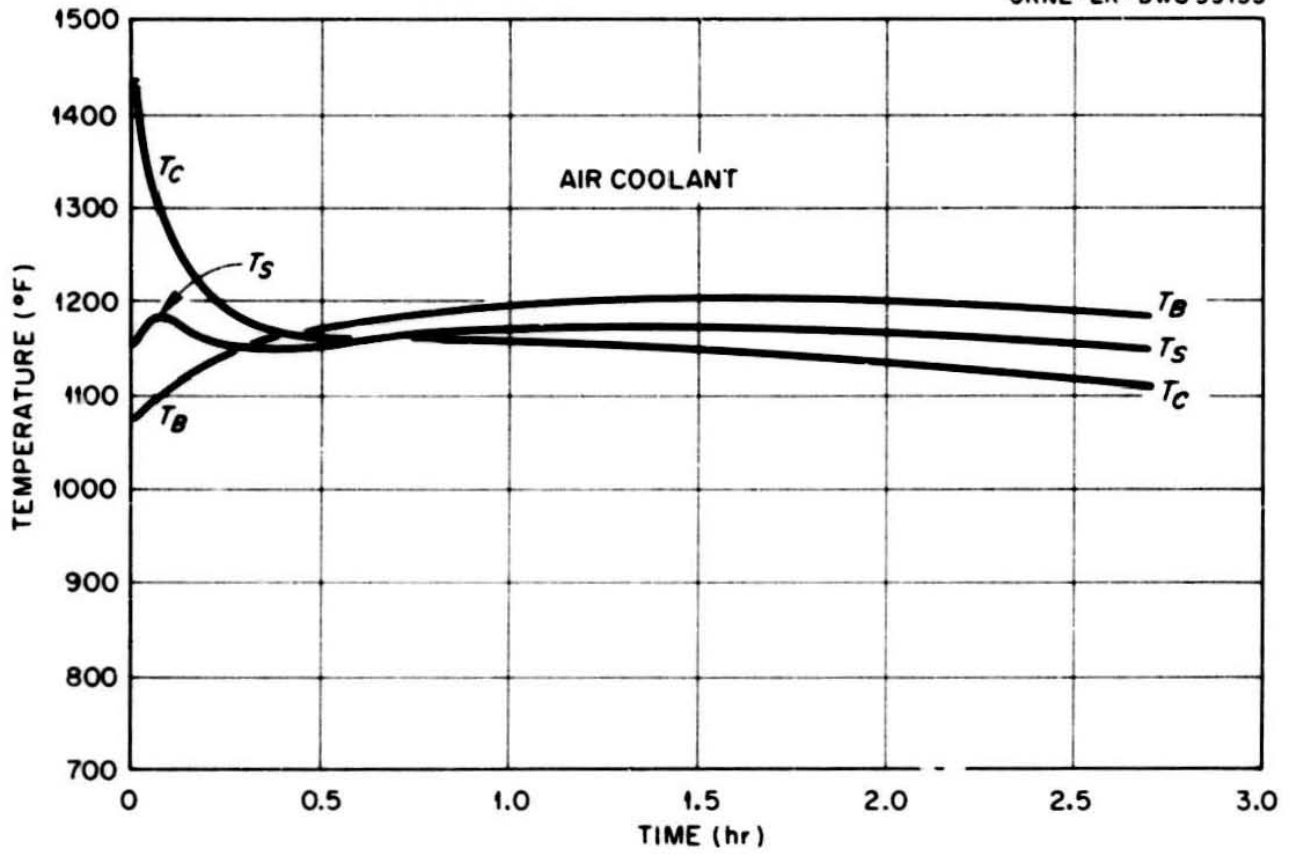


Fig. 27. Fuel Channel Temperatures, 7th Axial Position vs Time.

UNCLASSIFIED
ORNL-LR-DWG 59154

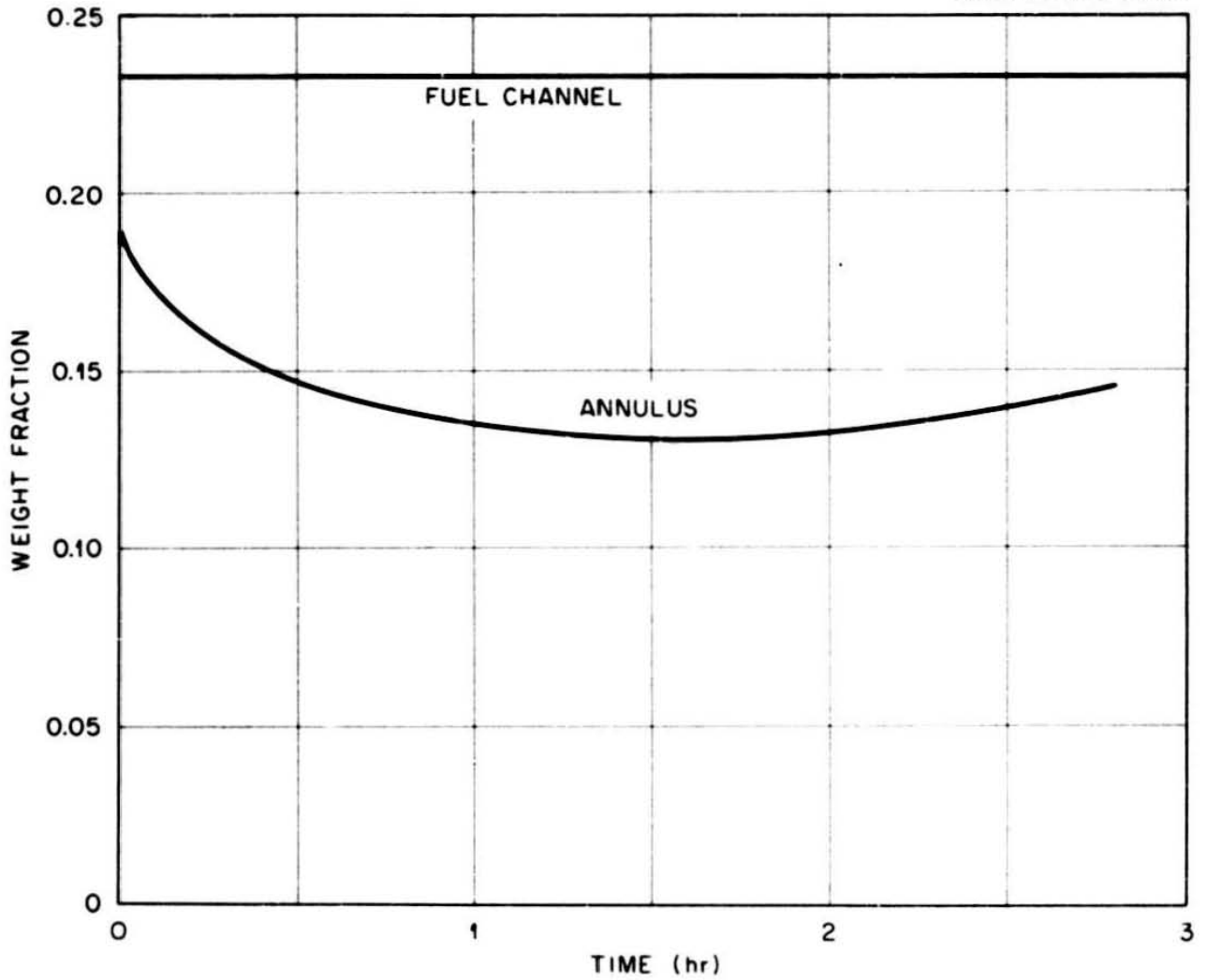


Fig. 28. Weight Fraction of Oxygen in Coolant vs Time.

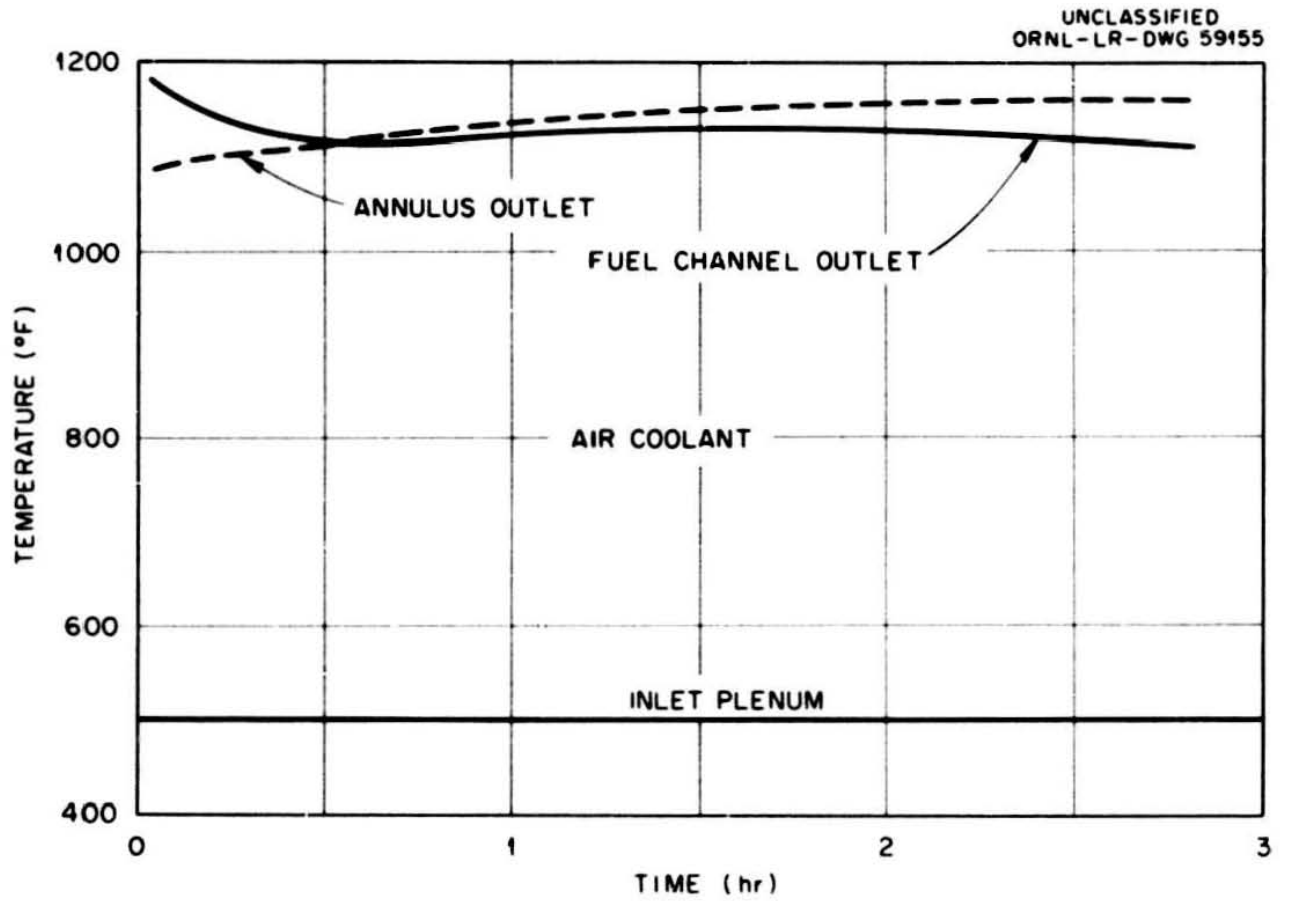


Fig. 29. Coolant Temperatures Following Depressurization vs Time.

to 95% effectiveness, and one blower can remain operative. In these calculations, 43% of the flow bypassed the core through the broken loop. Actually, if the blower in the broken loop did indeed deblade, it should be apparent to the operators through either the rpm reading or the power requirement to that blower. Thus the loop with the inoperative blower could be identified and the isolation valves closed. This would increase the flow through the core to approximately 85,000 lb/hr and result in an increased cooling effect.

The program described in this section was originally set up for the Bendix G-15. Essentially the same program is being set up for the IBM 7090 at Oak Ridge; the calculation assumptions and model are contained in Appendix C. The vastly greater speed of this machine should make it possible to test the effects of various sleeve coating effectivenesses, flow rates, inlet temperature as functions of steam generator behavior, blower failure for varying periods of time, changes in air concentrations, and other effects that one may wish to study as they come up. Also, the number of axial increments taken to represent the entire channel can be increased up to 50 on the IBM 7090, and thereby over-all channel heat balances can be made much more accurate. The cost of operating the IBM 7090 is quite modest compared to a comparable amount of work on the Bendix G-15.

The IBM 7090 formulation of the problem neglects the effects of the temperature levelization in the sleeve but includes it for the moderator. It should be noted also that in Landoni's differential equation for heat balance on the coolant, Eqs. (B-1) and (B-2) in Appendix B, the part of the total differential including the partial differential of temperature with respect to x , the axial distance, is not included. The effect of this differential, that is, the "carryover" from an upstream increment to the succeeding increment, is considered by adjusting the time increments in such a manner that the temperatures leaving the previous increment will be the entering temperatures in the succeeding increment. In the IBM 7090 formulation,

however, time increments of any size can be chosen (provided they are not sufficiently large to cause machine instability). The complete total differential of the temperature rise in the coolant stream is included as shown in Eqs. (C-1) and (C-2) in Appendix C.

Results of the IBM 7090 computations are now only of a preliminary nature and will be included in another report on the problem.

The above results are contingent on final validation of the analytical model which is currently being done by Lampe at Allis-Chalmers and will be reported in A-C Study IV-324. In this study, the computer will be used to analyze the burning in the Hanford burning rig. If the ignition temperatures and rates of change in the burning rig can be predicted with reasonable accuracy, this will serve as a check on the computations in the EGCR.

VI. Proposed Methods for Controlling Combustion in the EGCR

The following methods have been proposed for suppressing a graphite fire in the EGCR:

- 1) Valve off the broken loop and allow burning of air that has entered the system.
- 2) Valve off the broken loop and, in addition, provide a purge gas to reduce oxygen concentration in the core or to prevent entry of oxygen to the core. The gases that may be used are: a) helium, b) nitrogen, and c) carbon dioxide.
- 3) Valve off all coolant flow and remove decay heat externally through the pressure vessel walls to water tubes underneath the insulation.
- 4) Maintain the reactor blanketed with nitrogen.
- 5) Inject a chemical inhibitor such as: a) chlorine gas, b) freon, or c) carbon tetrachloride.
- 6) Use a solid-phase inhibitor in the graphite.

7) Cool the core by means of a water or fog spray.

8) Coat the sleeves and allow the moderator to burn. The low air supply in the annulus might produce heat from the combustion slowly enough so conduction of heat through the sleeve to the main gas stream could remove both the chemical heat and the decay heat. The main channel flow rate should be great enough to cool the core so that eventually the annulus would be below combustion temperature.

Method 1, valving off the broken loop, has merit and has been studied in a preliminary manner by Kaiser Engineers.²³ The results show, however, that the temperature of the gas passing through the blower will reach 1300°F about 3/4 min after the incidence of the accident. It is clear that the blower cannot withstand these conditions, and, if this temperature is credible, we would then be confronted with an accident in which both main blowers are lost in addition to loss of coolant. Also, serious instrumentation and control difficulties may be encountered in determining which loop has failed and which isolation valves to actuate.

The calculations in ref. 23 were performed with procedures yielding such extremely large factors of conservatism that the results are practically useless. A discussion of these calculations is given in ref. 24 and will not be repeated here. In short, to evaluate this procedure properly would require the use of the IBM 7090 program described in section V with the addition of subprograms for steam generator performance and inlet plenum gas composition, since the method depends on burning the available supply of oxygen entrained in the system previous to closure of the block valves.

If the break were to occur inboard of the isolation valves, closure of the other valve in the loop would prevent a positive driving force from being produced which could force air into the system. Any air entering the system under these conditions would do so by means of molecular and eddy diffusion through the broken ends of the pipe and the restricted annulus formed by the pipe and

surrounding concrete structure. It is not apparent of what magnitude this effect would be, but it probably would not be large.

Method 2, purging the system with a relatively inert gas such as helium, carbon dioxide, or nitrogen, is worthy of further study. KE²³ states that three volume changes of gas would reduce the oxygen concentration to 1% by volume if, after air were initially allowed to enter the system, no more air entry were allowed. It is important to analyze the problem further under these conditions to see how much damage will be wrought in the time required to dilute the oxygen in the system and the time period during which low oxygen concentrations must be maintained. Then it is necessary to see if the required pipe sizes are available or can be installed to provide the necessary flow rate of diluent gas. For example, if helium is used as the diluent and if it is deemed sufficient to provide three volume changes in 2 min, and assuming the helium will enter the system at sonic velocity at a temperature of 100°F, then about a 4-in.-dia pipe is required. If, on the other hand, 1 min is the maximum time allowed, then about a 6-in.-dia pipe is required. The helium supply would have to be at a sufficiently high pressure to provide the critical pressure ratio across the end of the pipe, that is, if the downstream pressure is about 22.2 psia (which would be the containment vessel pressure on loss of helium and the contents of one steam generator), then the critical pressure ratio for helium being 0.4875, the pressure at the pipe exit would need to be 45.5 psia. The available helium supply is only the amount of gas at pressures sufficiently greater than this to provide for pressure drop in the pipes and to allow for the increase in containment pressure due to inert gas injection. The purge would need to be coincident with closing of the isolation valves or the supply of gas may not be sufficient to maintain a positive pressure differential across the break long enough for the core to cool down to a temperature at which readmission of oxygen would not cause uncontrolled combustion. Also, the allowable containment vessel pressure

could limit the amount of helium blanket gas injected. This method suffers in that nothing can be done for breaks that cannot be valved off, that is, nozzle ruptures, and also suffers from the fact that identification of the ruptured loop may be impossible. In either of these cases, it is not expected that the core can be cooled down to a safe temperature in the time available, which would be limited by the supply of inert gas or the containment vessel pressure.

Method 3, valving off all coolant flow and removing decay heat externally through the pressure vessel walls to water tubes underneath the insulation, is an extreme procedure which should only be considered as a backup to other systems. It will be discussed more fully in section VII.

Method 4, maintaining the reactor blanketed with nitrogen or other relatively inert gas, would be effective in that operation of a mechanism on demand is not required. However, it would be extremely inconvenient to equip all workers entering the containment shell with aqualungs or air hoses. It must be remembered that the probability of the maximum credible accident is small, and, although it must be provided for, the means of combating it should not be an intolerable nuisance to the everyday operation of the reactor. At this late stage, it would be extremely expensive and inconvenient to attempt to construct a concentric envelope around the primary system to provide an inert gas blanket. Also, it would not be certain that rupture of the main system would not rupture the blanketing system.

Method 5, introduction of an inhibitor into the gas stream upon rupture of the main system envelope, would be a very effective way of preventing runaway oxidation. Preliminary results of Hanford's tests show that a small burst of chlorine gas giving a 2% concentration in the air stream will effectively poison the active sites in the graphite and will prevent combustion if the graphite can be cooled below the unstable temperature during the time period in which it remains chemisorbed on the graphite (about 3 min). If the graphite cannot be

cooled quickly enough, the chlorine concentration must be maintained until the critical temperature is passed. The chlorine injection equipment must be extremely reliable, for an accidental injection of chlorine into the system could be disastrous to the metal components of the reactor. Also, this kind of system could not be periodically tested for the same reasons. If, during the accident, the chlorine concentration in the atmosphere surrounding the electrical components becomes excessive, insulation breakdown will prevent operation of these items. Thus, if blower operation is required to remove combustion heat and decay heat, as is now the case, the use of chlorine is self-defeating. The use of other gaseous inhibitors has not been studied in much detail.

Method 6, use of a solid-phase inhibitor in the graphite, is an approach worthy of further study. Phosphorous pentoxide impregnated in graphite was found to be effective in inhibiting oxidation, but it is not stable under neutron irradiation. Perhaps other compounds containing atoms in the V and VI outer shell electron groups could be studied. Although this cannot be used in the EGCR, it might be worthwhile to expend some research effort in development compounds that can be impregnated in graphite for oxidation resistance.

Method 7, cooling the core by means of a water and fog spray, is another possibility. Although the graphite will react with water in the familiar "water-gas" reaction, the process is endothermic and would cool the core by removal of heat not only by the temperature rise and vaporization of water, but also by the heat required for the reaction, although the latter is probably small compared to the latent heat of vaporization. This scheme should be analyzed to determine the amounts of graphite consumed and the resultant containment vessel pressure from the addition of steam, carbon monoxide, and hydrogen from this reaction. Also, the concentrations of hydrogen and carbon monoxide should be determined to evaluate the explosion hazard.

Method 8, use of siliconized silicon-carbide coatings on the sleeves, is the method chosen for control of the oxidation in the EGCR. Coating of the sleeves can eliminate the oxidation of almost two-thirds of the geometrical surface available for combustion, but it is impractical to coat the moderator because of the tight temperature control required in the process, the cost of which could be prohibitive in large pieces such as the moderator blocks. The moderator will oxidize, but the heat of combustion is transferred through the sleeve to the large coolant flow in the center portion of the sleeve. As an upper limit, the rate of heat evolution from the moderator is limited by the oxygen supply in the annulus whose flow is approximately 6.5% of the total channel flow. As shown in the results of the analysis given in section V, Fig. 28, the partial pressure of oxygen in the annulus outlet is decreased to 0.14 atm. Thus oxygen starvation would not be the dominating influence; the main effect would be that the heat can be removed at a rate equal to or greater than that being generated. The results of Allis-Chalmers' study IV-312⁽¹⁹⁾ show that initial temperatures begin to rise. Without the coated sleeves, the temperatures would continue to rise to a runaway condition, but coating the sleeves allows the high heat removal of the higher central channel flow rates without the attendant large oxygen supply to the burning surfaces, which would occur if the sleeves were not coated.

Further problems that must be resolved with coated sleeves are enumerated in section VII.

VII. Discussion of the Coated Sleeves and Attendant Problems

As discussed in section VI, control of graphite oxidation by silicon-carbide coatings on the sleeves depends on conducting the heat generated in the moderator through the sleeve to the gas flowing in the channel inside the sleeves. Thus the heat removal of the large flow through the channel is used without allowing large amounts of air to reach the exposed moderator surfaces. The results shown in section V show that this method will be effective in controlling the core temperatures if a flow of 40,000 lb/hr is maintained through the core. This is a reasonable number in that it is the core flow with one blower operative and the blower in the broken loop debladed and the isolation valves open. However, there are several problems requiring solution before complete confidence is justified in this method.

Forced cooling of the core is necessary for long periods of time after the accident. For instance, natural convection using one loop with a stalled blower and with outlet temperatures of 2000°F and inlet temperatures of 150°F cannot remove the decay heat (as expressed by the Way-Wigner relation) until 70 days after shutdown.²⁵ Of course this is a rough calculation in that the heat capacity of the graphite is not considered; it is only the rate of heat removal available with air at atmospheric pressure at those conditions. A transient calculation was performed in which the core was taken as a solid piece at uniform temperature and the natural convection flow rates varied as a function of outlet temperature. It was found that maximum core temperatures of approximately 2600°F were attained at 21.9 days after shutdown. If the blower resistance were bypassed, the core temperature reached a maximum of 2000°F in 17.8 days. In these calculations perfectly coated sleeves were assumed, and the flow in the annuli was assumed to burn completely. The heat generated by the oxidation at these low flow rates was found to be

negligible compared to the decay heat. These results were obtained on an extremely simplified model by means of the OR-SFT code on the IBM 7090. It is evident, however, that some form of forced cooling is necessary.

This leads to problems in maintaining a heat sink. That is, at least one of the steam generators must remain available for long times after the accident, and blower operation must be maintained. In case of power supply failure it is expected that the rate of temperature rise will be slow enough so that at least one or two days are available to restore power. Under these conditions it seems that the weakest links in the chain required to remove the heat are the blower and the steam generator. Feedwater failure within months after the accident could be serious. Also, at the present time it has not been shown that the steam generators will be sufficiently effective at low flow rates. A bearing seizure in the rotating equipment could be serious if it happened within a month or so after the accident. The vessel cooling system could be used to cool the core if the block valves are shut, but it is not known at the present time at what time after shutdown it would be feasible to use them.

The above considerations may require that an alternate heat sink be provided which is completely independent of the operating equipment, and that does not require a long chain of events to effect its use. This heat sink may be obtained rather inexpensively by means of water tubes underneath the insulation exterior to the pressure vessel. These tubes would normally be dry, and water would be supplied to them only upon failure of the other modes of heat removal. Their position external to the pressure vessel makes the consequences of inadvertent operation unimportant since they would not be metallurgical bonded to the pressure vessel wall. Preliminary calculations have shown that central core temperatures between 2500°F and 2800°F can be expected if this mode of heat removal is used alone. Concurrent use with natural convection would probably reduce the peak temperatures

to approximately 2000°F if the sleeves remain coated. Of course, natural convection would require an operative steam generator along with water in the tubes. Use of this system would need to be studied further, especially the effects on the bottom grid structure. This structure can reach a temperature sufficiently high to cause failure, in which case the whole core would fall to the bottom of the pressure vessel. It is expected that before this happens the fuel cladding would have melted and allowed the UO_2 pellets to fall to the bottom of the core, the control rod cladding would have melted and allowed the B_4C rings to fall to the bottom of the core. Thus, even if the bottom grid plate did fail, it is not expected that a critical condition would result. If natural convection were available, however, the bottom grid should be maintained at a temperature below critical.

Fundamental to the use of the coated sleeve for controlling the graphite oxidation is the integrity of the coating. Preliminary tests on silicon-carbide coatings on Speer 901S graphite show good radiation stability and adherence under thermal cycling.²⁶ It is necessary to apply the coatings to an isotropic grade of graphite possessing the same coefficient of thermal expansion as the coating. Speer 901S graphite has been specified for the sleeves because of this property. Coatings applied to other grades of graphite have shown relatively poor oxidation protection because of cracks, porosity, or complete lack of coating in places.²⁷ Further details on coating work will be reported by F. L. Carlsen of the ORNL Metallurgy Division ceramics group, whose responsibility is to show that coating integrity can be maintained for three years in the EGCR.

The above discussion points out some of the problems remaining in the loss-of-pressure accident. It is felt that if a heat sink can be maintained, coating of the sleeves can be depended on to control the fire. The effects of loss of cooling for certain periods of time, alternate forms of coolant, decreased inlet temperature due to steam generator blowdown on loss of power, reductions in sleeve coating

effectiveness with time, are some areas that can be studied with the computer code described in section V to allow final decisions on the means taken to accommodate them.

Pertinent to the EGCR is the concentration of carbon monoxide formed when burning the moderator surfaces. Prados has calculated that if all the oxygen available in the annulus were to be burned to CO, the following would occur:²⁸

1) It is apparently impossible to initiate a detonation wave by combustion of the carbon monoxide. Since all carbon monoxide in the system would result ultimately from the oxidation of carbon by air, it would be diluted sufficiently with nitrogen to hold its maximum composition below the minimum value for detonation (38% by volume).²⁹

2) Rapid combustion can occur in a premixed carbon monoxide-air system (flash fire) if the carbon monoxide concentration is above 12.5% by volume.^{29,30} There is sufficient oxygen in the containment shell to permit the development of such a concentration throughout the containment shell and still leave a stoichiometric excess of oxygen to react with the carbon monoxide.

3) If the inflammable mixture of (2) existed throughout the containment shell and were ignited, the adiabatic temperature rise, calculated under conservative assumptions, would lead to an internal overpressure of 34 psig, about three times the design rating of the containment shell.³¹

4) A flash fire within the reactor coolant system alone would produce negligible overpressure in the containment shell.

5) If the carbon monoxide should burn at the outlet of the reactor coolant channels, no explosion hazard would exist. However, the minimum ignition temperature of about 1150°F is so close to the expected conditions at the reactor outlet that this cannot be claimed as a dependable safety factor.

6) The maximum production rate of carbon monoxide in the reactor core, based on a core flow rate of 90,000 lb/hr and a recirculation

rate between 0.1 and 10 times the fresh air intake to the system is sufficient to produce an inflammable concentration of carbon monoxide within the containment shell after about 10 hr of operation. The calculation involves the highly conservative assumptions: a) all oxygen fed to the annuli reacts instantaneously to form carbon monoxide, and no credit is taken for the decreasing reaction rate as the core temperature drops; b) the oxygen concentration in the fresh air fed to the system does not decrease as carbon monoxide is supplied to the containment volume.

Prados continues to say that based on the above results it can be concluded that there is a chance, although a remote one, that a carbon monoxide explosion of sufficient strength to rupture the containment shell could occur several hours after a rupture of the EGCR primary coolant loop. This would require the production of sufficient carbon monoxide to produce an inflammable concentration throughout the containment shell and the subsequent ignition of the mixture by a spark or heat from the reactor core. The probability of obtaining such a concentration can be better assessed after the analysis of results of the computer calculations on the graphite oxidation behavior in the reactor core.

VIII. Conclusions and Recommendations

Coated sleeves are to be used to control catastrophic oxidation in the EGCR in case of the loss-of-pressure accident. This method requires that the heat of oxidation and decay heat be removed by forced cooling in the first month or so after the accident. Thus, further study should find ways to provide the EGCR with cooling for this length of time. This could be done by means of pony motors on the main blower motor shafts, the vessel cooling compressors, bypassing the blowers for natural convection, water tubes underneath the pressure vessel insulation, or other means not apparent at this time.

To determine more accurately the level of urgency for standby cooling of the MCA, after the analytical model is validated by Allis-Chalmers study IV-324, the IBM 7090 program should be used to find the minimum flow rates required for various coating effectivenesses. Also, the effects of blower power failure occurring at various times after the onset of the accident and for varying duration should be studied. It may be advantageous to consider the effects of normal steam generator blowdown on loss of feedwater power which would tend to reduce the inlet air temperatures to approximately 380°F.

The alternate methods enumerated in section VI ought to be examined in more detail for possible further use in the EGCR if found to be less expensive and as reliable as the coated sleeves, and for future application on other graphite-moderated reactors. The IBM 7090 program should be made generally available because many classes of problem dealing with flow in channels can be studied with it using changes in the input data.

Nomenclature

a	= frequency factor in Arrhenius equation, time ⁻¹
A	= area perpendicular to the flow of heat, ft ²
b	= half-thickness of a slab or radius of a long cylinder, length
c	= activation energy in Arrhenius equation, kcal/gm-mole
C	= O ₂ concentration in graphite pores, moles/vol of gas
C _g	= oxygen concentration in gas phase
C _p	= specific heat at constant pressure, Btu/lbm-°R
D _{eq}	= equivalent diameter, ft
D _p	= effective diffusivity of oxygen in pores of sample, (length) ² /time
h	= heat transfer coefficient, Btu/hr-ft-°F
k	= thermal conductivity, Btu/hr-ft-°F
K	= observed rate constant, mass/(mass)(time)(O ₂ partial pressure)

k _v	= volume rate constant, moles of O ₂ reacting/(active vol of sample)(time)(moles of O ₂ /vol of gas)
L	= depth of diffusion, length
m	= mass of sample, gm
M	= molecular weight of carbon = 12.01, gm/gm-mole
P	= absolute pressure, atm
P _O	= partial pressure of oxygen, atm
q	= heat transfer rate, Btu/hr
Q	= reaction rate, (moles of oxygen reacting)/time
Q*	= diffusion-free reaction rate, moles O ₂ /time
R	= gas constant, kcal/gm-mole-°R
S _f	= area perpendicular to the flow of fluid, ft ²
S	= external surface area of sample, ft ²
T	= temperature, °K or °R
V	= volume of sample, length ³
W	= flow rate, lb/hr

Nomenclature (continued)

- ϵ = porosity, pore vol/total sample vol
- η = ratio of reaction rate to diffusion-free reaction rate
- k = chemical rate constant, mass/(mass)(time)(O₂ partial pressure)
- μ = viscosity, lbm/hr-ft
- ρ = graphite sample density, mass/vol
- ΔH = heat of oxidation reaction, BTU/lb. mole of graphite or O₂

APPENDIX A

Determination of Reaction Rates from Experimental Data⁷

The experimental reaction rates are usually reported as mass of carbon reacting per unit 1) sample mass, 2) sample external (geometrical) surface, or 3) internal surface as measured by gas adsorption. These can be all reduced to an observed rate constant, K , by multiplying sample surface-to-mass ratios and dividing by the experimental oxygen partial pressure (in atmosphere) where necessary.

In cases where the rate of oxygen mass transfers to the external surface may limit the rate of reaction (above 800°C), one must compute the "chemical rate constant", \mathcal{N} , as follows. From a material balance, the rate at which oxygen is transported to the surface must equal the rate at which it reacts with the graphite.

$$Q = \mathcal{N} (m/M) P_O = k_G S (P_G - P_O) \quad (\text{A-1})$$

where

- \mathcal{N} = chemical rate constant, mass/(mass)(time) (O_2 partial pressure)
- P_O = partial pressure of oxygen at the external sample surface
- P_G = partial pressure of oxygen in the bulk gas stream
- k_G = mass transfer coefficient, (moles of O_2)/[(area)(time) (atm of O_2)]

The coefficient k_G can be estimated from standard correlations.³² One can see that:

$$P_O = P_G - \frac{Q}{k_G S} \quad (\text{A-2})$$

Hence,

$$K = \frac{Q}{(m/N)(P_G - Q/k_G S)}$$

Note that if $k_G \gg Q/S$, $P_O = P_G$, and gas-phase mass transfer is unimportant.

The relation between K and \mathcal{R} is given by:

$$\mathcal{R} = K/\eta$$

η is computed from Eq. (15).

$$\eta = 1/\phi \tanh \phi \quad (A-3)$$

ϕ is given by:

$$\phi = \frac{V}{SL} = \frac{V}{S} \sqrt{k_v/D_p}$$

The relation between k_v and \mathcal{R} is (if one assumes that 1 mole of oxygen is equivalent to 1 mole of carbon, that is, complete oxidation):

$$k_v = \frac{\rho RT}{M} \mathcal{R}$$

This can be compared with the definition, $\phi = V/SL$, to yield:

$$\mathcal{R} = \gamma \phi^2 \quad (A-4)$$

where

$$\gamma = (S/V)^2 \frac{MD_p}{\rho RT} \quad (A-5)$$

If Eqs. (15) and (A-4) are combined with the relation between K and \mathcal{R} , one obtains:

$$\phi \tanh \phi = \frac{K}{\gamma} \quad (A-6)$$

These relations are sufficient to permit calculations of \mathcal{R} and η from observed over-all reaction rates. The procedure is as follows:

- 1) Calculate K from experimental results.
- 2) Estimate D_p from the relation:

$$D_p = \frac{0.223 \epsilon^2}{P} (T/273)^{1.5} \text{ ft}^2/\text{hr} \quad (A-7)$$

where

- T = absolute temperature, °K
P = absolute pressure, atm
ε = porosity, pore vol/total sample vol

3) Calculate γ from Eq. (A-5).

4) Calculate K/γ ; solve Eq. (A-6) for ϕ . This is a trial and error solution.

5) Find \mathcal{M} from Eq. (A-4).

6) Find η , if desired, from ratio of K to \mathcal{M} .

For limiting cases, steps 4 and 5 may be simplified as follows.

For $K/\gamma < 10^{-2}$:

$$\mathcal{M} = K$$

and

$$\eta = 1$$

For $K/\gamma > 10$:

$$\mathcal{M} = K^2/\gamma$$

and

$$\eta = SL/V$$

The results of this procedure on data reported by several investigators are presented in section III.

The above discussion of the depth-of-diffusion concept has gone into considerable detail because it is fundamental to the heat release equations used in the analysis. deHalas and Dahl³³ at Hanford have applied this concept in a simplified analysis of tests performed by Brookhaven, Hanford, and the French.³⁴

Originally, the analysis of the EGCR burning assumed a surface reaction in which the data of Kosiba¹⁵ were converted to the EGCR geometry by scaling the surface-to-volume ratio. deHalas and Dahl have shown that the original EGCR approach yielded ignition temperatures in the French experiment of 720°C, whereas in a typical experiment the graphite ignited between 540 and 600°C. Modification of the

approach to include the depth-of-diffusion concept yields a predicted ignition temperature of 520°C, considerably closer to the experimental results than that given by the initial analysis.

The Brookhaven tests show the validity of this approach when considering the variations in reaction rates of various graphites. The test was performed in a single channel that was held at constant temperature at the beginning of the run, and air was introduced into the bottom to initiate the test. This test can be described analytically by the following equations.

At the upper unstable point on Fig. 1, the heat generated by oxidation in the graphite equals the heat transferred to the gas stream. Thus:

$$hPx (T_g - T_a) = \Delta H_{ap} P L R_{400} e^{-c/RT_g} dx \quad (A-8)$$

where

P = perimeter of the channel

x = axial distance along the channel

a = frequency factor in Arrhenius equation

ρ = density

L = depth of diffusion

R_{400} = an arbitrary ratio to convert from data from one grade of graphite to another

c = activation energy

T_g = temperature of the graphite

T_a = temperature of the air

ΔH = heat of oxidation/lb (14,100 Btu/lb)

Solving Eq. (A-8) for $(T_g - T_a)$:

$$(T_g - T_a) = \frac{a\rho\Delta H L R_{400}}{h} e^{-c/RT_g} \quad (A-9)$$

The temperature rise of the air as it progresses along the channel is found from a heat balance with the heat transferred.

$$hP \, dx \, (T_g - T_a) = W C_p \, dT_a \quad (A-10)$$

Rearranging,

$$W C_p \, (dT_a/dx) = hP T_h - hP T_a$$

Rearranging,

$$\frac{dT_a}{dx} + \frac{hP}{WC_p} T_a = \frac{hP}{WC_p} T_g \quad (A-11)$$

Using an integrating factor, e^{hPx/WC_p} , the solution of Eq. (A-11) becomes:

$$e^{hPx/WC_p} T_a = T_g e^{hPx/WC_p} + C_1 \quad (A-12)$$

When

$$x = 0 \quad T_a = T_i$$

where

$$T_i = \text{inlet temperature of air}$$

Thus:

$$C_1 = T_i - T_g$$

Equation (A-12) becomes:

$$T_g - T_a = (T_g - T_i) e^{-hPx/WC_p} \quad (A-13)$$

Substituting Eq. (A-13) into Eq. (A-9):

$$(T_g - T_i) e^{-hPx/WC_p} = \frac{a\rho\Delta HLR_{400}}{h} e^{-c/RT_g} \quad (A-14)$$

This can be rearranged to yield:

$$\frac{c}{RT_g} = - \ln \left[\frac{(T_g - T_i) h}{a\rho\Delta HLR_{400}} e^{-hPx/WC_p} \right] \quad (A-15)$$

In the Brookhaven test, as analyzed by deHalan and Dahl, a was found to be equal to $3.3 \times 10^{11} \text{ hr}^{-1}$. Grouping the constants as follows:

$$\underline{a} = a_p PL \Delta HR_{400} = 4.8 \times 10^{17} PLR_{400} \text{ (Btu/hr/ft)}$$

$$A = \frac{hP}{WC_p}$$

$$\frac{C}{R} = B$$

Equation (A-15) becomes:

$$\frac{B}{T} = - \ln \frac{Ph}{\underline{a}} (T_g - T_i) e^{-AX} \quad (\text{A-16})$$

The conditions for the BNL experiment were as shown in Table A. Then $PL = 0.164 \text{ L}$.

From ref. 6 the depth of diffusion, L , can be determined by:

$$L \approx \frac{0.033}{2.54 \times 10^{12}} (T/273)^{0.38} M^{-1/2*} \quad (\text{A-17})$$

TABLE A

<u>Experiment No. 1</u>	<u>Experiment No. 2</u>
$A = 0.372 \text{ ft}^{-1}$	$A = 0.303 \text{ ft}^{-1}$
$X = 1.92 \text{ ft}$	$X = 1.92 \text{ ft}$
$h = 5.2 \text{ Btu/hr-ft}^2\text{-}^\circ\text{F}$	$h = 12.7 \text{ Btu/hr-ft}^2\text{-}^\circ\text{F}$
$P = 0.164 \text{ ft}$	$P = 0.164 \text{ ft}$
$T_i = 573^\circ\text{K}$	$T_i = 573^\circ\text{K}$

* Notice that the solid-phase diffusion control has the effect of reducing the activation energy by a factor of 2.

The term $(T/283)^{0.38}$ varies only from 1.48 to 1.80 in going from $T = 500$ to $T = 1000^\circ\text{C}$; therefore, assume an average value at 800°C .

From Kosiba's data, the reaction rate from Eq. (1) is:

$$\begin{aligned} M &= a e^{-c/RT} \\ M &= 3.3 \times 10^{11} e^{-(5.0 \times 10^4)/1.99 T} \\ &= 3.3 \times 10^{11} e^{-(2.5 \times 10^4)/T} \end{aligned}$$

From Eq. (A-17):

$$\begin{aligned} L &= 0.0018 M^{-1/2} \text{ (ft)} \\ &= 3.14 \times 10^{-9} e^{(1.24 \times 10^4)/T} \end{aligned}$$

Thus,

$$\begin{aligned} \underline{a} &= (4.8 \times 10^{17})(0.164)(3.14 \times 10^{-9}) e^{1.25 \times 10^4/T} R_{400} \\ &= 2.48 \times 10^8 e^{1.25 \times 10^4/T} R_{400} \end{aligned}$$

For experiment 1:

$$\begin{aligned} \frac{Ph}{\underline{a}} &= \frac{(0.164)(5.2)}{(2.48)(10^8) R_{400}} e^{-1.25 \times 10^4/T} \\ &= \frac{3.5 \times 10^{-9}}{R_{400}} e^{-1.25 \times 10^4/T} \end{aligned}$$

$$\begin{aligned} - \ln \left[(1.8) \frac{Ph}{\underline{a}} (T_g - T_i) e^{-AX} \right] &= 18.8 + \frac{1.25 \times 10^4}{T} - \ln (T_g - T_i) \\ &\quad + 0.71 \ln R_{400} \end{aligned}$$

Substituting into Eq. (A-16):

$$\frac{(2.5 - 1.25) \times 10^4}{T} = 19.5 - \ln (T_g - T_i) + \ln R_{400}$$

Let $R_{400} = 1$ for now:

$$\frac{1.25 \times 10^4}{T} = 19.5 - \ln(T - 573)$$

$$T = 630^\circ\text{C}$$

The reported temperature for experiment 1 is 830°C . To obtain this answer, R_{400} would have to equal 0.19. According to deHalas and Dahl, this is a reasonable value.

Using $R_{400} = 0.19$, the validity of this equation can be checked against experiment 2 which used the same graphite.

$$\frac{\text{Ph}}{\underline{a}} = \frac{(0.164)(12.7)}{(2.48)(10^8)(0.19)} e^{-1.25 \times 10^4/T}$$

$$= 4.4 \times 10^{-8} e^{-1.25 \times 10^4/T}$$

$$- \ln(1.8) \frac{\text{Ph}}{\underline{a}} (T_g - T_i) e^{-AX} = 16.9 + \frac{1.25 \times 10^4}{T} - \ln(T_g - T_i) + 0.58$$

$$\frac{1.25 \times 10^4}{T} = 17.7 - \ln(T - 573)$$

$$T = 930^\circ\text{C}$$

This checks with the experimental value, i.e., combustion is observed to start at 930°C in experiment 2.

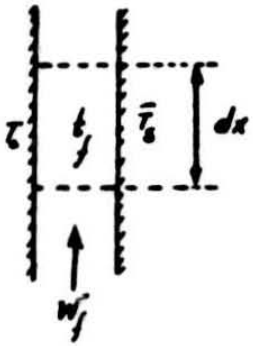
APPENDIX B

Original Allis-Chalmers Graphite Oxidation Calculation Model²

The original Allis-Chalmers graphite oxidation calculation model was developed in PEGCPR project job study 3-380 by J. Landoni. Only the transient-state calculations are shown because the initial steady-state conditions depend on the axial power distribution under actual conditions which are considerably different from the curve distribution originally assumed by Landoni. All terms are defined in the nomenclature on page 105.

TRANSIENT STATE

Differential Eq^s governing the transient state.

1. Fuel Coolant Eq.

Considering the heat balance

Heat transferred to the coolant

$$h_c P_c dx (T_c - t_f) d\theta + h_f P_f dx (\bar{T}_s - t_f) d\theta$$

Heat received by the coolant

$$W_f c_p d\theta dt_f = A_f P_f c_p dt_f dx$$

where the total differential dt_f is

$$dt_f = \frac{\partial t_f}{\partial \theta} d\theta + \frac{\partial t_f}{\partial x} dx$$

Equating heats:

$$A_f P_f c_p \frac{dt_f}{d\theta} = h_c P_c (T_c - t_f) + h_f P_f (\bar{T}_s - t_f)$$

2. Annulus Coolant Eq.

Similarly:

$$A_a P_a c_p \frac{dt_a}{d\theta} = h_c P_a (\bar{T}_s - t_a) + h_b P_b (T_b - t_a)$$

3. Fuel Elements Eq.

Considering the heat balance for the length dx , at x , during $d\theta$

Heat removed by the coolant

$$h_c P_c dx (T_c - t_f) d\theta$$

Heat radiated to the sleeve

$$h_r P_c dx F_c (T_c - \bar{T}_s) d\theta$$

Heat generated

$$A_f dx q_f d\theta \cos \frac{\pi}{L_0} x$$

Heat from the levelization of the temperature profile

$$\psi FE dx q_f \left(\cos \frac{\pi}{L_0} x \right) \lambda_f d\theta \cdot e^{-\lambda_f \theta}$$

Heat stored in the fuel elements by the clad outer surface increase in temperature

$$FE dx dT_c$$

Equating heats:

$$FE dT_c = \psi FE \left(\cos \frac{\pi}{L_0} x \right) q_f \lambda_f e^{-\lambda_f \theta} d\theta + A_f q_f d\theta \cdot \cos \frac{\pi}{L_0} x - h_c P_c (T_c - T_f) d\theta - h_{rc} P_c F_c (T_c - \bar{T}_c) d\theta$$

4. Graphite Blocks Eq.

The heat balance for the length dx at x , during $d\theta$

Heat removed by the coolant

$$h_b P_b dx (T_b - t_a) \cdot d\theta$$

Heat radiated to the sleeve

$$h_{rb} P_b F_b (T_b - \bar{T}_s) dx d\theta$$

Heat generated: Decay heat

$$A_b q_b \cos \frac{\pi}{L_0} x dx d\theta$$

: Chemical reaction with coolant

$$k_b \frac{P_a}{h} e^{-\frac{c}{T_b}} d\theta dx$$

Heat from the levelization of the temperature profile

$$\chi B q_{b0} \cos \frac{\pi}{L_0} x dx \cdot \lambda_b d\theta \cdot e^{-\lambda_b \theta}$$

Heat stored in the graphite blocks by the surface increase in temperature

$$B dx dT_b$$

Equating heats:

$$B dT_b = k_b \frac{P_a}{h_0} e^{-\frac{c}{T_b}} d\theta + \chi B q_{b0} \cos \frac{\pi}{L_0} x \lambda_b e^{-\lambda_b \theta} d\theta + A_b q_b \cos \frac{\pi}{L_0} x d\theta - h_b P_b (T_b - t_a) d\theta - h_{r,b} P_b F_b (T_b - \bar{T}_s) d\theta$$

4

5. Graphite Sleeve Eq.

The heat balance for the length dx , at x , during $d\theta$

Heat removed by coolants

$$h_f P_f (\bar{T}_s - t_f) dx d\theta + h_a P_a (\bar{T}_s - t_a) dx d\theta$$

Heat radiated to the sleeve

$$h_{r,c} P_c F_c (T_c - \bar{T}_s) dx d\theta + h_{r,b} P_b F_b (T_b - \bar{T}_s) dx d\theta$$

Heat generated : Decay heat

$$A_s q_s d\theta \cos \frac{\pi}{L_0} x dx$$

: Chemical reaction with coolant

$$k_s \frac{P_s}{h_0} e^{-\frac{c}{T_s}} \frac{P_f}{P_a + P_f} d\theta + k_s \frac{h_a}{h_0} e^{-\frac{c}{T_s}} \frac{P_a}{P_a + P_f} d\theta$$

Heat stored in the graphite sleeve

$$S dx d\bar{T}_s$$

(The temperature profile was disregarded)

Equating heats:

$$S d\bar{T}_s = k_s \frac{A}{L_0} \frac{P_f}{P_f + P_a} e^{-\frac{c}{\bar{T}_s}} d\theta + k_s \frac{A}{L_0} \frac{P_a}{P_f + P_a} e^{-\frac{c}{\bar{T}_s}} d\theta + A_s q_s d\theta \cos \frac{\pi}{L_0} x$$

$$+ h_{r_c} P_c F_c (T_c - \bar{T}_s) d\theta + h_{r_b} P_b F_b (T_b - \bar{T}_s) d\theta - h_f P_f (\bar{T}_s - t_f) d\theta - h_a P_a (\bar{T}_s - t_a) d\theta$$

6. Oxygen Consumption Eq. for the Fuel Coolant.

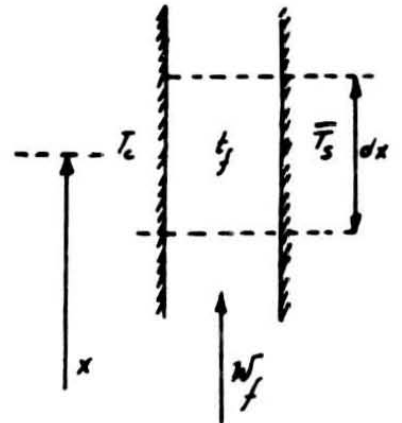
Considering the material balance

Oxygen entering at x , during $d\theta$

$$P_f w_f d\theta$$

Oxygen burnt along dx , during $d\theta$

$$\frac{k_s}{\Delta H} \frac{P_c}{L_0} \frac{P_f}{P_f + P_a} e^{-\frac{c}{\bar{T}_s}} dx d\theta$$



The percentage change in the concentration by weight, disregarding the mass flow increase by the carbon dioxide replacement of oxygen, is

$$dP_f = - \frac{k_s}{\Delta H} \frac{P_c}{L_0} \frac{P_f}{P_f + P_a} \frac{e^{-\frac{c}{\bar{T}_s}}}{w_f} dx$$

7. Oxygen Consumption Eq. for the Annulus Coolant.

Similarly:

$$dp_a = - \frac{h_s}{\Delta H} \frac{P_a}{P_0} \frac{P_a}{P_f + P_a} \frac{e^{-\frac{x}{L}}}{W_a} dx - \frac{h_b}{\Delta H} \frac{P_a}{P_0} \frac{e^{-\frac{x}{L}}}{W_a} dx \quad 7$$

Factors involved in the differential equations.

h The heat transfer coefficients are close to those for natural convection, when streamline flow prevails. $h = h_0 F_p F_T$

$h_0 = 0.210 (T-t)^{1/3}$: basic value for the heat transfer coefficient for air.

F_p : pressure factor, equal to 1 at 1 atm.

$F_T = 1.28 - 2.5 \times 10^{-4} (T+t)$: temperature factor for air.

When turbulent flow prevails, h comes out from the Dittus - Boelter correlation

$$Nu = 0.0225 Re^{0.8} Pr^{0.4}$$

h_r Coefficient of radiation

$$h_r = \sigma \frac{T^4 - T'^4}{T - T'}$$

F_r Hottel's factor

$F_c = \epsilon_c F_{w,c}$ for the clad-sleeve radiant heat

$F_b = F_{w,b} = \frac{P_a}{P_b}$ for the blocks-sleeve radiant heat

Heat Capacities per Foot:

Fuel Elements

$$FE = (A \rho c_p)_F + (A \rho c_p)_{cl}$$

Sleeve

$$S = (A \rho c_p)_s$$

Moderator Blocks

$$B = (A \rho c_p)_b$$

Fuel Coolant

$$(A \rho c_p)_f$$

Annulus Coolant

$$(A \rho c_p)_a$$

Heat Generated

Decay Heat (From S. Glasstone, "Nuclear Engineering", p. 118)

Heat release by β decay in the length dx at x , during $d\theta$ (This heat is assumed entirely released in the fuel elements)

$$0.0074 A_f q_{f\beta} \cos \frac{\pi}{L_0} x d\theta^{0.8} dx$$

Heat release by γ rays, in the length dx at x , during $d\theta$

$$0.0065 A_f q_{f\gamma} \cos \frac{\pi}{L_0} x d\theta^{0.8} dx$$

Heat release by neutrons, in the length dx at x during $d\theta$ (This heat is assumed entirely released in the fuel elements). From S. Glasstone, "Nuclear Engineering",

p. 231.

$$\left[\frac{f\ell}{(\beta-f)^2} d e^{-\frac{\beta-f}{\ell}\theta} + \frac{\beta}{f\lambda} d e^{-\frac{f\lambda}{\beta-f}\theta} \right] A_f q_{fn} \cos \frac{\pi}{L_0} x dx$$

Chemical Heat

From the experimental results on carbon samples oxidized by air after pile irradiation, the percent loss in weight per hour as a function of the carbon temperature is given by

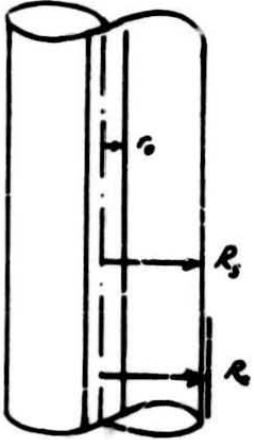
$$y = K e^{-\frac{C}{T}}$$

Taking into account the heat release in the reaction $C + O_2 \rightarrow CO_2 (\Delta H)$, the surface to volume (S/V) ratios for both sample and blocks or sleeve and the cross-sectional area of graphite in consideration

$$h dx = K A \frac{S/V}{(S/V)_{sample}} dx f \Delta H \quad \left(k \text{ in } \frac{BTU}{ft \cdot hr} \right)$$

Heat from the levelization of the temperature profile

Considering the average drop in temperature ΔT for a hollow cylinder (inside surface insulated):



$$\overline{\Delta T} = \frac{1}{\pi(R_2^2 - r_0^2)} \int_{r_0}^{R_2} \Delta T \cdot 2\pi r \, dr$$

where: $\Delta T = \frac{q_f}{4k_p} (R_2^2 - r^2 - 2r_0^2 \ln \frac{R_2}{r})$

$$\begin{aligned} \overline{\Delta T} &= \frac{q_f/2k_p}{R_2^2 - r_0^2} \int_{r_0}^{R_2} (R_2 r - r^2 - 2r_0^2 \ln \frac{R_2}{r}) \, dr \\ &= \frac{q_f/2k_p}{R_2^2 - r_0^2} \left[\frac{R_2^2}{2} - \frac{R_2^2 r_0^2}{2} - \frac{R_2^4}{4} + \frac{r_0^4}{4} - 2r_0^2 \frac{R_2^2}{2} \ln R_2 + 2 \frac{r_0^4}{2} \ln R_2 \right. \\ &\quad \left. + 2r_0^2 \int_{r_0}^{R_2} r \ln r \, dr \right] \end{aligned}$$

$$\begin{aligned} &= \frac{q_f/2k_p}{R_2^2 - r_0^2} \left[\frac{R_2^4}{4} + \frac{r_0^4}{4} - \frac{R_2^2 r_0^2}{2} - r_0^2 R_2^2 \ln R_2 + r_0^4 \ln R_2 + \right. \\ &\quad \left. + r_0^2 R_2^2 (\ln R_2 - \frac{1}{2}) - r_0^4 (\ln r_0 - \frac{1}{2}) \right] \end{aligned}$$

$$= \frac{q_f/2k_p}{R_2^2 - r_0^2} \left[\frac{R_2^4}{4} + \frac{3}{4} r_0^4 - R_2^2 r_0^2 + r_0^4 \ln \frac{R_2}{r_0} \right]$$

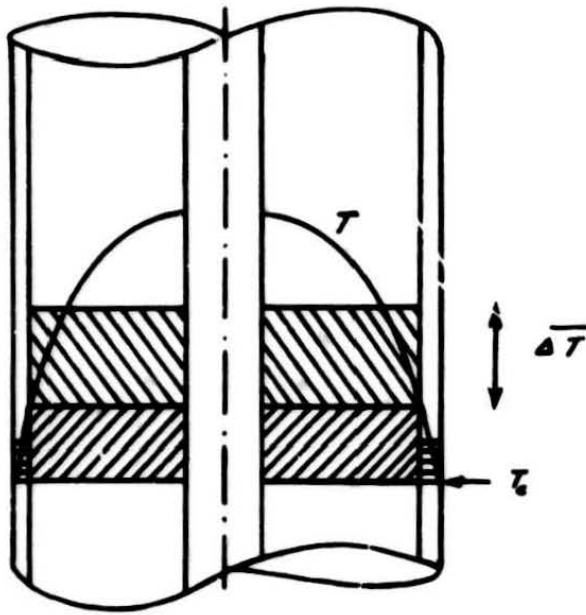
$$\overline{\Delta T} = \frac{q_f}{4k_p} \left[\frac{R_2^2}{2} - \frac{3}{2} r_0^2 + \frac{2r_0^4}{R_2^2 - r_0^2} \ln \frac{R_2}{r_0} \right] = \mu q_f$$

$$\mu = \frac{1}{4k_p} \left(\frac{R_2^2}{2} - \frac{3}{2} r_0^2 + \frac{2r_0^4}{R_2^2 - r_0^2} \ln \frac{R_2}{r_0} \right)$$

If the temperatures are referred to the clad outer surface temperature; thus

$$\psi_{FE} = \gamma + (\eta A_r + \mu) F$$

where $\eta = \frac{\ln \frac{R_2}{r_0}}{2\pi n k_c}$; $\gamma = A_r CL \frac{q}{2}$; $CL = (A_{fc})_{cl}$
 $F = (A_{fc})_c$



$$\begin{aligned} \text{///} & \mu q_f F \\ \text{///} & \eta A_F q_f F \\ \text{≡} & \delta q_f \end{aligned}$$

$$\psi q_f FE = \delta q_f + (\eta A_F + \mu) F q_f$$

When the levelization of the temperature profile is primordially determined by the heat diffusion process, q_f is replaced by $q_{f_0} (1 - e^{-\lambda_f \theta})$ and its contribution to the heat release is given by

$$\psi FE dx \cdot q_{f_0} (\cos \frac{\pi}{L_0} x) e^{-\lambda_f \theta} \lambda_f d\theta$$

The moderator blocks cell is considered to be equivalent to a cylindrical shell with the same cross-sectional area. The outer surface corresponds to the center of the blocks, which is essentially adiabatic. Hence, the moderator is assumed to be a cylindrical shell with its outer boundary thermically insulated.

Similarly, for a hollow cylinder with its outer surface insulated

$$\mu = \frac{1}{4k_g} \left(\frac{R_0^2}{2} - \frac{3}{2} R_0^2 + \frac{2R_0^4}{R_0^2 - R_i^2} \cdot \ln \frac{R_0}{R_i} \right) = \chi$$

being R_0 the radius of the equivalent cell.

Therefore, the heat release from the levelization of the temperature profile in the moderator blocks, comes out to be:

$$\chi B dx q_{b0} \left(\cos \frac{\pi}{L_0} x \right) e^{-\lambda_b x} \lambda_b dx$$

$$(2C_f + H_f + H_c) \Delta t_f - H_c \Delta T_c - H_f \Delta \bar{T}_s = 2H_f (\bar{T}_s - t_f) + 2H_c (T_c - t_f)$$

or

$$a_{11} \Delta t_f + a_{12} \Delta T_c + a_{13} \Delta \bar{T}_s = K_1$$

where

$$a_{11} = 2C_f + H_f + H_c$$

$$a_{14} = 0$$

$$a_{12} = -H_c$$

$$a_{15} = 0$$

$$a_{13} = -H_f$$

$$K_1 = 2H_f (\bar{T}_s - t_f) + 2H_c (T_c - t_f)$$

2. Fuel Elements

$$FE \Delta T_c = \psi FE q_{f0} \cos \frac{\pi}{L_0} x_0 \left(e^{-\lambda_f \theta_0} - e^{-\lambda_f (\theta_0 + \Delta \theta)} \right) + A_r q_f \Delta \theta \cos \frac{\pi}{L_0} x_0$$

$$-h_c P_c \left\{ T_c(x_0, \theta_0) + \frac{\Delta T_c}{2} - t_f(x_0, \theta_0) - \frac{\Delta t_f}{2} \right\} \Delta \theta - h_{rc} P_c F_c \left\{ T_c(x_0, \theta_0) + \frac{\Delta T_c}{2} - \bar{T}_s(x_0, \theta_0) - \frac{\Delta \bar{T}_s}{2} \right\} \Delta \theta$$

$$\Delta T_c \left\{ 2FE + (h_c P_c + h_{rc} P_c F_c) \Delta \theta \right\} = 2 \psi FE q_{f0} \cos \frac{\pi}{L_0} x_0 \left(e^{-\lambda_f \theta_0} - e^{-\lambda_f (\theta_0 + \Delta \theta)} \right) + A_r q_f \Delta \theta \cos \frac{\pi}{L_0} x_0$$

$$-2h_c P_c (T_c - t_f) \Delta \theta - 2h_{rc} P_c F_c (T_c - \bar{T}_s) \Delta \theta$$

$$+ h_c P_c \Delta t_f \Delta \theta + h_{rc} P_c F_c \Delta \bar{T}_s \Delta \theta$$

Calling: $H_c = h_c P_c \Delta \theta$

$$R_c = h_{rc} P_c F_c \Delta \theta$$

$$-H_c \Delta t_f + (2FE + H_c + R_c) \Delta T_c - R_c \Delta \bar{T}_s = 2 \psi FE q_{f0} \cos \frac{\pi}{L_0} x_0 \left(e^{-\lambda_f \theta_0} - e^{-\lambda_f (\theta_0 + \Delta \theta)} \right)$$

$$+ 2A_r q_f \Delta \theta \cos \frac{\pi}{L_0} x_0 - 2H_c (T_c - t_f) - 2R_c (T_c - \bar{T}_s)$$

or

$$a_{21} \Delta t_f + a_{22} \Delta T_c + a_{23} \Delta \bar{T}_s = K_2$$

where

$$a_{21} = -H_c$$

$$a_{24} = 0$$

$$a_{22} = 2FE + H_c + R_c$$

$$a_{25} = 0$$

$$a_{23} = -R_c$$

$$K_2 = 2\psi FE q_{f_0} \cos \frac{\pi}{L_0} x_0 \left(e^{-\lambda_j \theta} - e^{-\lambda_j (l_0 + \theta)} \right) + 2A_f q_j \Delta \theta \cos \frac{\pi}{L_0} x_0 - 2H_c (T_c - t_j) - 2R_c (T_c - \bar{T}_s)$$

3. Graphite Sleeve.

$$\begin{aligned} S \Delta \bar{T}_s &= k_s \frac{P_f}{h} \frac{P_f}{P_f + P_a} e^{-\frac{c}{\bar{T}_s(x_0, \theta_0)}} \Delta \theta + \frac{k_s C}{\bar{T}_s^2(x_0, \theta_0)} \frac{H_c}{h} \frac{P_f}{P_f + P_a} e^{-\frac{c}{\bar{T}_s(x_0, \theta_0)}} \Delta \theta \frac{\Delta \bar{T}_s}{2} \\ &+ k_s \frac{h_a}{h} \frac{P_a}{P_f + P_a} e^{-\frac{c}{\bar{T}_s(x_0, \theta_0)}} \Delta \theta + \frac{k_s C}{\bar{T}_s^2(x_0, \theta_0)} \frac{P_a}{P_0} \frac{P_a}{P_f + P_a} e^{-\frac{c}{\bar{T}_s(x_0, \theta_0)}} \Delta \theta \frac{\Delta \bar{T}_s}{2} \\ &+ h_{r_c} P_c F_c \left\{ T_c(x_0, \theta_0) + \frac{\Delta T_c}{2} - \bar{T}_s(x_0, \theta_0) - \frac{\Delta \bar{T}_s}{2} \right\} \Delta \theta \\ &+ h_{r_b} P_b F_b \left\{ T_b(x_0, \theta_0) + \frac{\Delta T_b}{2} - \bar{T}_s(x_0, \theta_0) - \frac{\Delta \bar{T}_s}{2} \right\} \Delta \theta \\ &- h_f P_f \left\{ \bar{T}_s(x_0, \theta_0) + \frac{\Delta \bar{T}_s}{2} - t_f(x_0', \theta_0) - \frac{\Delta t_f}{2} \right\} \Delta \theta \\ &- h_a P_a \left\{ \bar{T}_s(x_0, \theta_0) + \frac{\Delta \bar{T}_s}{2} - t_a(x_0', \theta_0) - \frac{\Delta t_a}{2} \right\} \Delta \theta \\ &+ A_s q_s \Delta \theta \cos \frac{\pi}{L_0} x_0 \end{aligned}$$

Calling $Q_s = \frac{k_s C}{\bar{T}_s^2} e^{-\frac{c}{\bar{T}_s}} \Delta \theta \left(\frac{h_f P_f + P_a P_a}{P_0 (P_f + P_a)} \right)$ $R_c = h_{r_c} P_c F_c \Delta \theta$

$$H_a = h_a P_a \Delta \theta$$

$$R_b = h_{r_b} P_b F_b \Delta \theta$$

$$H_f = h_f P_f \Delta \theta$$

$$\begin{aligned} -H_f \Delta t_f - R_c \Delta T_c + (2S + H_f + H_a + R_c + R_b - Q_s) \Delta \bar{T}_s - R_b \Delta T_b - H_a \Delta t_a \cdot \frac{2k_s}{P_0 (P_f + P_a)} (P_f P_f + P_a P_a) e^{-\frac{c}{\bar{T}_s}} \Delta \theta + \\ + 2R_c (T_c - \bar{T}_s) + 2R_b (T_b - \bar{T}_s) - 2H_f (\bar{T}_s - t_f) - 2H_a (\bar{T}_s - t_a) + 2A_s q_s \Delta \theta \cos \frac{\pi}{L_0} x_0 \end{aligned}$$

or

$$a_{31} \Delta t_f + a_{32} \Delta T_c + a_{33} \Delta \bar{T}_s + a_{34} \Delta T_b + a_{35} \Delta t_a = K_3$$

where: $a_{31} = -H_f$

$$a_{32} = -R_c$$

$$a_{33} = 2S + H_f + H_a + R_c + R_b - Q_s$$

$$a_{34} = -R_b$$

$$a_{35} = -H_a$$

$$K_3 = \frac{2k_b}{\rho_o (P_f + P_a)} (P_f P_f + P_a P_a) e^{-\frac{c}{T_b}} \Delta \theta + 2R_c (T_c - \bar{T}_s) + 2R_b (T_b - \bar{T}_s) - 2H_f (\bar{t} - t_f) - 2H_a (\bar{T}_s - t_a) + 2A_b q_b \Delta \theta \cos \frac{\pi}{L_o} x_o$$

4. Graphite Blocks.

$$B \Delta T_b = k_b \frac{A}{\rho_o} e^{-\frac{c}{T_b(x_o, \theta_o)}} \Delta \theta + \frac{k_b c}{T_b^2(x_o, \theta_o)} \frac{A}{\rho_o} e^{-\frac{c}{T_b(x_o, \theta_o)}} \Delta \theta \frac{\Delta T_b}{2} + X B q_b \cos \frac{\pi}{L_o} x_o (e^{-\lambda_b x_o} - e^{-\lambda_b (\theta_o + \Delta \theta)}) + A_b q_b \Delta \theta \cos \frac{\pi}{L_o} x_o$$

$$-h_b P_b \left\{ T_b(x_o, \theta_o) + \frac{\Delta T_b}{2} - t_a(x_o, \theta_o) - \frac{\Delta t_a}{2} \right\} \Delta \theta$$

$$-h_r P_b F_b \left\{ T_b(x_o, \theta_o) + \frac{\Delta T_b}{2} - \bar{T}_s(x_o, \theta_o) - \frac{\Delta \bar{T}_s}{2} \right\} \Delta \theta$$

Calling: $Q_b = \frac{k_b c}{T_b^2} \frac{A}{\rho_o} e^{-\frac{c}{T_b}} \Delta \theta$

$$H_b = h_b P_b \Delta \theta$$

$$R_b = h_r P_b F_b \Delta \theta$$

- 101 -

$$\begin{aligned}
 -R_b \Delta \bar{T}_s + (2B + H_b + R_b - Q_b) \Delta T_b - H_b \Delta t_a &= 2k_b \frac{A_b}{P_b} e^{-\frac{c}{T_b}} \Delta \theta + 2A_b q_b \Delta \theta \cos \frac{\pi}{L_0} x_0 \\
 &+ 2\chi B q_{b0} \cos \frac{\pi}{L_0} x_0 (e^{-\lambda_b \theta_0} - e^{-\lambda_b (\theta_0 + \Delta \theta)}) \\
 &- 2H_b (T_b - t_a) - 2R_b (T_b - \bar{T}_s)
 \end{aligned}$$

or

$$a_{43} \Delta \bar{T}_s + a_{44} \Delta T_b + a_{45} \Delta t_a = K_4$$

4

where

$$a_{43} = -R_b$$

$$a_{41} = 0$$

$$a_{44} = 2B + H_b + R_b - Q_b$$

$$a_{42} = 0$$

$$a_{45} = -H_b$$

$$K_4 = 2k_b \frac{A_b}{P_b} e^{-\frac{c}{T_b}} \Delta \theta + 2A_b q_b \Delta \theta \cos \frac{\pi}{L_0} x_0 + 2\chi B q_{b0} \cos \frac{\pi}{L_0} x_0 (e^{-\lambda_b \theta_0} - e^{-\lambda_b (\theta_0 + \Delta \theta)})$$

$$-2H_b (T_b - t_a) - 2R_b (T_b - \bar{T}_s)$$

5. Annulus Coolant

Similarly to the fuel coolant

$$\begin{aligned}
 \Delta t_a \left\{ 2A_a \rho_a c_p \frac{\Delta \theta}{\Delta \theta_{a,in}} + (h_a P_a + h_b P_b) \Delta \theta \right\} &= 2h_a P_a \bar{T}_s \Delta \theta + 2h_b P_b T_b \Delta \theta - 2(h_a P_a + h_b P_b) \frac{t}{f} \Delta \theta \\
 &+ h_a P_a \Delta \bar{T}_s \Delta \theta + h_b P_b \Delta T_b \Delta \theta
 \end{aligned}$$

Calling: $C_a = A_a \rho_a c_p \frac{\Delta \theta}{\Delta \theta_{a,in}}$

$$H_a = h_a P_a \Delta \theta$$

$$H_b = h_b P_b \Delta \theta$$

$$-H_a \Delta \bar{T}_s - H_b \Delta T_b + (2C_a + H_a + H_b) \Delta t_a = 2H_a (\bar{T}_s - t_a) + 2H_b (T_b - t_a)$$

or

$$a_{s3} \Delta \bar{T}_s + a_{s4} \Delta T_b + a_{s5} \Delta t_a = K_S \quad 5$$

where

$$a_{s3} = -H_a$$

$$a_{s1} = 0$$

$$a_{s4} = -H_b$$

$$a_{s2} = 0$$

$$a_{s5} = 2C_a + H_a + H_b$$

$$K_S = 2H_a(\bar{T}_s - t_a) + 2H_b(T_b - t_a)$$

Oxygen Consumption.

Assuming no significant changes in the oxygen concentration and mass flow through Δx , Eq.^s 6 and 7 can be expressed as follows:

Fuel Channel:

$$\Delta p_f(x_0' + \Delta x, \theta_0 + \Delta \theta) = - \frac{k_s}{\Delta H} \frac{p_f(x_0', \theta)}{p_0} \frac{P_f}{P_f + P_a} \frac{e^{-\frac{c}{5T}}}{W_f} \Delta x \quad 6$$

Annulus Channel:

$$\begin{aligned} \Delta p_a(x_0' + \Delta x, \theta_0 + \Delta \theta) &= - \frac{k_s}{\Delta H} \frac{p_a(x_0', \theta)}{p_0} \frac{P_a}{P_f + P_a} \frac{e^{-\frac{c}{5T}}}{W_a} \Delta x \\ &\quad - \frac{k_b}{\Delta H} \frac{p_a(x_0', \theta)}{p_0} \frac{e^{-\frac{c}{T_b}}}{W_a} \Delta x \\ &= - \frac{p_a(x_0', \theta)}{p_0 W_a \Delta H} \left\{ \frac{P_a}{P_f + P_a} e^{-\frac{c}{5T}} + e^{-\frac{c}{T_b}} \right\} \Delta x \quad 7 \end{aligned}$$

Equations 1 to 5 are five linear equations for the five unknown increments in temperature Δt_f , ΔT_b , $\Delta \bar{T}_s$, ΔT_b , Δt_a .

These five equations can be written in the matrixial form

$$\begin{vmatrix} x & x & x & 0 & 0 \\ x & x & x & 0 & 0 \\ x & x & x & x & x \\ 0 & 0 & x & x & x \\ 0 & 0 & x & x & x \end{vmatrix} = \begin{vmatrix} x \\ x \\ x \\ x \\ x \end{vmatrix}$$

where the x 's indicate the non-zero coefficients.

This system can be solved by elimination of unknowns; as follows

$$\begin{vmatrix} 1 & x & x & 0 & 0 \\ 1 & x & x & 0 & 0 \\ 1 & x & x & x & x \\ 0 & 0 & x & x & x \\ 0 & 0 & x & x & x \end{vmatrix} = \begin{vmatrix} x \\ y \\ x \\ x \\ x \end{vmatrix}$$

$$\begin{vmatrix} x & x & 0 & 0 \\ x & x & x & x \\ 0 & x & x & x \\ 0 & x & x & x \end{vmatrix} = \begin{vmatrix} x \\ x \\ x \\ x \end{vmatrix}$$

$$\begin{vmatrix} 1 & x & 0 & 0 \\ 1 & x & x & x \\ 0 & x & x & x \\ 0 & x & x & x \end{vmatrix} = \begin{vmatrix} x \\ x \\ x \\ x \end{vmatrix}$$

$$\begin{vmatrix} x & x & x \\ x & x & x \\ x & x & x \end{vmatrix} = \begin{vmatrix} x \\ x \\ x \end{vmatrix}$$

$$\begin{vmatrix} / & x & x \\ / & x & x \\ / & x & x \end{vmatrix} = \begin{vmatrix} x \\ x \\ x \end{vmatrix}$$

$$\begin{vmatrix} x & x \\ x & x \end{vmatrix} = \begin{vmatrix} x \\ x \end{vmatrix}$$

Finally a system of two equations with two unknowns ΔT_b and Δt_a is solved and replacing their values in the previous equations, the other unknowns are obtained: $\Delta \bar{T}_s$, ΔT_c and Δt_f .

Nomenclature

- A cross-sectional area, ft^2
- B graphite blocks heat capacitance per foot, $\frac{\text{BTU}}{^\circ\text{F hr}}$
- C constant, $^\circ\text{R}$
- c_p coolant specific heat at constant pressure, $\frac{\text{BTU}}{\text{lb } ^\circ\text{F}}$
- CL clad heat capacitance per foot, $\frac{\text{BTU}}{^\circ\text{F ft}}$
- F fuel heat capacitance per foot, $\frac{\text{BTU}}{^\circ\text{F ft}}$
- FE fuel elements heat capacitance per foot, $\frac{\text{BTU}}{^\circ\text{F ft}}$
- F_v view factor
- F_r Hottel's factor for radiant heat
- h heat transfer coefficient, $\frac{\text{BTU}}{\text{ft}^2 \text{ hr } ^\circ\text{F}}$
- h_r coefficient of radiation, $\frac{\text{BTU}}{\text{ft}^2 \text{ hr } ^\circ\text{F}}$
- k conductivity, $\frac{\text{BTU}}{\text{ft hr } ^\circ\text{F}}$
- k constant for chemical reaction, $\frac{\text{BTU}}{\text{ft hr}}$
- L_0 extrapolated height of the reactor core, ft
- l thermal neutrons life-time, hr
- P perimeter correspondent to the cross-sectional area, ft
- p oxygen concentration in coolant by weight
- q heat density source at the mid-plane of the reactor core, $\frac{\text{BTU}}{\text{ft}^2 \text{ hr}}$
- r, R radius, ft
- S sleeve heat capacitance per foot, $\frac{\text{BTU}}{^\circ\text{F ft}}$

- T surface temperature, $^{\circ}R$
 t coolant temperature, $^{\circ}R$
 v coolant velocity, $\frac{ft}{hr}$
 W mass flow, $\frac{lb}{hr}$
 x distance from the mid-plane of the reactor core, ft.

β fraction of delayed fission neutrons

ΔH reaction heat, $\frac{BTU}{lb \text{ of } O_2}$

ϵ emissivity

λ decay time constant for heat diffusion, hr^{-1}

λ precursor decay constant, hr^{-1}

ρ density, $\frac{lb}{ft^3}$

ρ reactivity

σ Boltzmann constant, $\frac{BTU}{^{\circ}R^2 ft^2 hr}$

θ time

Δ differences

Super- and Sub-scripts.

- refers to average value

A	{	a	annulus channel
		b	graphite blocks
		F	fuel (total area of n elements)
		f	fuel channel
		s	sleeve
F_s	{	b	graphite block emitting surface
		c	clad emitting surface
P	{	a	sleeve outer surface
		b	graphite blocks surface
		c	clad surface
		f	sleeve inner surface
h_r	{	b	graphite blocks emitting surface
		c	clad emitting surface
k cond.	{	f	fuel
		g	graphite
k const.	{	b	graphite blocks
		s	sleeve
p	{	a	annulus coolant
		f	fuel coolant
		o	normal air

g	{	b	refers to graphite blocks
		f	fuel
		s	sleeve
		o	steady state
R	{	b	graphite blocks surface
		c	clad outer surface
		s	clad inner surface
		o	equivalent cell
r	:	o	fuel interior hole.
T	{	b	graphite blocks
		c	clad outer surface
		s	sleeve
W, t	{	a	annulus coolant
		f	fuel coolant
v	:	o	inlet
x	:	o	arbitrary location
ε	{	b	graphite blocks emitting surface
		c	clad emitting surface
λ diff.	{	b	graphite blocks
		f	fuel

ρ density { a refers to annular coolant
f fuel coolant
o inlet coolant

θ { a annular coolant
f fuel coolant
in inlet coolant through Δx
o arbitrary time.

APPENDIX C

IBM 7090 Graphite Oxidation Calculation Model

The EGCR graphite oxidation problem has been coded for the IBM 7090 computer by R. Edwards of the ORGDP problem setup group. The calculation is based on the following assumptions:

1) The clad temperature is determined only by a) heat flux due to the levelization of temperature in the fuel elements and gamma heating, b) heat flux due to radiation to the sleeve, and c) heat flux due to Newtonian heat transfer to the central coolant.

2) The afterheat in the fuel element, sleeve, and moderator block is assumed to be proportional to θ^{z_i} , where z_i is a constant given three values to fit curve 3 of Fig. 20 in three time intervals.

3) The heat balance across the sleeve is assumed to depend only upon the following heat fluxes, based on a mean sleeve temperature: a) radiative flux from the fuel clad, b) Newtonian flux to the central coolant, c) radiative flux from the moderator (based on mean moderator temperature), d) Newtonian flux to the annulus coolant, e) heat generation due to gamma heating, f) heat generation due to graphite oxidation, and g) increase in the enthalpy of the sleeve.

4) The heat balance on the moderator is assumed dependent on the following, based on a mean moderator temperature: a) radiative flux from the sleeve (based on mean sleeve temperature), b) Newtonian flux to the annulus coolant, c) heat generation due to gamma heating, d) heat generation due to graphite oxidation, and e) increase in the enthalpy of the moderator.

5) Graphite oxidation is assumed to be governed by:

$$q = \bar{K}_p (T/1660)^{0.25} e^{-c/T}$$

where

- q = heat generation rate per unit of surface
 \bar{K} = constant
 p = partial pressure of oxygen
 T = surface temperature
 c = constant

With the aid of the above assumptions, the following equations govern the temperatures defined in the nomenclature:

$$W_f c_p \frac{\partial t_f}{\partial x} + \frac{A_f \pi c_p}{R t_f} \frac{\partial t_f}{\partial \theta} = h_f P_c (T_c - t_f) + h_f P_f (T_s - t_f) \quad (C-1)$$

$$W_a c_p \frac{\partial t_a}{\partial x} + \frac{A_a \pi c_p}{R t_a} \frac{\partial t_a}{\partial \theta} = h_a P_a (T_s - t_a) + h_a P_b (T_b - t_a) \quad (C-2)$$

$$Q_{FE} = h_f P_c (T_c - t_f) + \bar{r}_c P_c (T_c^4 - T_s^4) \quad (C-3)$$

$$Q_s - A_s G \frac{\partial T_s}{\partial \theta} = h_f P_f (T_s - t_f) + h_a P_a (T_s - t_a) + \bar{r}_c P_c (T_s^4 - T_c^4) + \bar{r}_a P_a (T_s^4 - T_b^4) \quad (C-4)$$

$$Q_b - A_b \delta_b G \frac{\partial T_b}{\partial \theta} = h_a P_b (T_b - t_a) + \bar{r}_a P_a (T_b^4 - T_s^4) \quad (C-5)$$

$$W_f \frac{\partial p_f}{\partial x} + \frac{A_f \pi}{R t_f} \frac{\partial p_f}{\partial \theta} = - \frac{q_f}{\Delta H} \quad (C-6)$$

$$W_a \frac{\partial p_a}{\partial x} + \frac{A_a \pi}{R t_a} \frac{\partial p_a}{\partial \theta} = - \frac{q_a}{\Delta H} \quad (C-7)$$

The heat generation terms are:

$$Q_{FE} = q_{F0} A_F (\psi e^{-y_f \theta} + D_F y_i \theta^{2i}) \cos \frac{\pi x}{L_0} \quad (C-8)$$

$$Q_b = q_{bo} A_b (D_b y_1 \theta^{z_1}) \cos \frac{\pi x}{L_o} + \bar{K} P_b \frac{P_a}{P_o} (T_b/1660)^{0.25} e^{-c/T_b} \quad (C-9)$$

$$Q_s = q_{so} A_s (D_s y_1 \theta^{z_1}) \cos \frac{\pi x}{L_o} + \bar{K} \xi_s \left(\frac{P_a}{P_o} P_a + \frac{P_f}{P_o} P_f \right) (T_s/1660)^{0.25} e^{-c/T_s} \quad (C-10)$$

$$q_f = \bar{K} \xi_s \frac{P_f}{P_o} P_f (T_s/1660)^{0.25} e^{-c/T_s} \quad (C-11)$$

$$q_a = \bar{K} \frac{P_a}{P_o} [\xi_s P_a (T_s/1660)^{0.25} e^{-c/T_s} + P_b (T_b/1660)^{0.25} e^{-c/T_b}] \quad (C-12)$$

The parameter ξ_s is the measure of coating on the sleeve. The notation used above is defined in the nomenclature on page 115.

In terms of finite differences:

$$t_f (x + \frac{1}{2} \Delta x, \theta + \Delta \theta) =$$

$$\frac{\frac{W_f c_p t_f (x - 1/2 \Delta x, \theta + \Delta \theta)}{\Delta x} + \frac{A_f \pi c_p}{R \Delta \theta} + h_f [P_c T_c (\theta) + P_f \bar{T}_s (\theta)]}{\frac{W_f c_p}{\Delta x} + \frac{A_f \pi c_p}{R t_f (x + 1/2 \Delta x, \theta) \Delta \theta} + h_f (P_c + P_f)}$$

$$t_a (x + 1/2 \Delta x, \theta + \Delta \theta) =$$

$$\frac{\frac{W_a c_p t_a (x - 1/2 \Delta x, \theta + \Delta \theta)}{\Delta x} + \frac{A_a \pi c_p}{R \Delta \theta} + h_a [P_a \bar{T}_s (\theta) + P_b T_b (\theta)]}{\frac{W_a c_p}{\Delta x} + \frac{A_a P_o c_p}{R t_a (x + 1/2 \Delta x, \theta) \Delta \theta} + h_a (P_a + P_b)}$$

$$P_f (x + 1/2 \Delta x, \theta + \Delta \theta) =$$

$$\frac{W_f P_f (x - 1/2 \Delta x, \theta + \Delta\theta)}{\Delta x} + \frac{A_f \pi p_f (x + 1/2 \Delta x, \theta)}{R t_f (x + 1/2 \Delta x, \theta) \Delta\theta} - \frac{q_f}{\Delta H}$$

$$\frac{W_f}{\Delta x} + \frac{A_f \pi}{R t_f (x + 1/2 \Delta x, \theta) \Delta\theta}$$

$$P_a (x + 1/2 \Delta x, \theta + \Delta\theta) =$$

$$\frac{W_a P_a (x - 1/2 \Delta x, \theta + \Delta\theta)}{\Delta x} + \frac{A_a \pi P_a (x + 1/2 \Delta x, \theta)}{R t_a (x + 1/2 \Delta x, \theta) \Delta\theta} - \frac{q_a}{\Delta H}$$

$$\frac{W_a}{\Delta x} + \frac{A_a \pi}{R t_a (x + 1/2 \Delta x, \theta) \Delta\theta}$$

$$Q_{FE} = (q_{FO} A_F \psi e^{-\lambda_f \theta} + q_{FO} A_F D_F y_1 \theta^{z_1}) \cos(\pi x / L_0)$$

$$Q_b = q_{bo} A_b D_b y_1 \theta^{z_1} \cos \frac{\pi x}{L_0} + \bar{K} P_b \left(\frac{P_a (x + 1/2 \Delta x, \theta) + P_a (x - 1/2 \Delta x, \theta)}{2 P_0} \right)$$

$$(\bar{T}_b / 1660)^{0.25} e^{-c / \bar{T}_b}$$

$$Q_s = (q_{so} A_s D_s y_1 \theta^{z_1}) \cos \frac{\pi x}{L_0} + \bar{K} \xi_s \left[\frac{P_a (x + 1/2 \Delta x, \theta) + P_a (x - 1/2 \Delta x, \theta)}{2 P_0} \right. \\ \left. P_a + P_f \frac{P_f (x + 1/2 \Delta x, \theta) + P_f (x - 1/2 \Delta x, \theta)}{2 P_0} \right] (\bar{T}_s / 1660)^{0.25} e^{-c / \bar{T}_s}$$

$$q_f = \bar{K} \xi_s \frac{P_f (x + 1/2 \Delta x, \theta) + P_f (x - 1/2 \Delta x, \theta)}{2 P_0} I_f (\bar{T}_s / 1660)^{0.25} e^{-c / \bar{T}_s}$$

$$q_a = \bar{K} \frac{P_a (x + 1/2 \Delta x, \theta) + P_a (x - 1/2 \Delta x, \theta)}{2 P_0} \left[\xi_s P_a (\bar{T}_s / 1660)^{0.25} \right. \\ \left. e^{-c / \bar{T}_s} + P_b (\bar{T}_b / 1660)^{0.25} e^{-c / \bar{T}_b} \right]$$

Writing the equations as difference equations:

$$T_c(\theta + \Delta\theta) = \frac{h_f P_c \frac{t_f(x + 1/2 \Delta x, \theta) + t_f(x - 1/2 \Delta x, \theta)}{2} + \dots}{h_f P_c + \sigma \mathcal{F}_c P_c \frac{\bar{T}_s^4(\theta) - T_c^4(\theta)}{\bar{T}_s(\theta) - T_c(\theta)}} + \dots$$

$$\dots \frac{\sigma \mathcal{F}_c P_c \frac{\bar{T}_s^4(\theta) - T_c^4(\theta)}{\bar{T}_s(\theta) - T_c(\theta)} \bar{T}_s(\theta) + Q_{FE}}{\dots}$$

$$T_b(\theta + \Delta\theta) = T_b(\theta) + \frac{\Delta\theta}{B A_b \delta_b} \left[h_a P_a \left(\frac{t_a(x + 1/2 \Delta x, \theta) + t_a(x - 1/2 \Delta x, \theta)}{2} - T_b(x, \theta) \right) + \sigma \mathcal{F}_b P_b (\bar{T}_s^4(\theta) - T_b^4(\theta)) + Q_b \right]$$

$$\bar{T}_s(\theta + \Delta\theta) = \bar{T}_s(\theta) + \frac{\Delta\theta}{S A_s} \left[h_f P_f \left(\frac{t_f(x + 1/2 \Delta x, \theta) + t_f(x - 1/2 \Delta x, \theta)}{2} - \bar{T}_s(\theta) \right) + \sigma \mathcal{F}_c P_c (T_c^4(\theta) - \bar{T}_s^4(\theta)) + h_a P_a \left(\frac{t_o(x + 1/2 \Delta x, \theta) + t_a(x - 1/2 \Delta x, \theta)}{2} - \bar{T}_s(\theta) \right) + \sigma \mathcal{F}_b P_b (T_b^4(\theta) - \bar{T}_s^4(\theta)) + Q_s \right]$$

Nomenclature for IBM 7090 Graphite Oxidation Code

I. Independent Variables:

x = axial distance from the midplane of the core, ft

θ = time, hr

II. Dependent Variables:

t_f = central channel coolant temperature, °R

t_a = annulus coolant temperature, °R

T_c = clad temperature, °R

T_s = sleeve temperature, °R

T_b = moderator block temperature, °R

p_f = weight fraction of O_2 in central channel, lb O_2 /lb air

p_a = weight fraction of O_2 in annulus, lb O_2 /lb air

III. Constants:

T_{in} = inlet temperature to reactor, °R

q_{FO} = steady-state volumetric heat generation rate in the fuel at the core midplane, Btu/hr-ft³

q_{bo} = steady-state volumetric heat generation rate in the moderator block at the core midplane, Btu/hr-ft³

q_{so} = steady-state volumetric heat generation rate in the sleeve at the core midplane, Btu/hr-ft³

Q_{FE}, Q_b, Q_s = heat generation rate per unit length of fuel, moderator block, and sleeve, Btu/hr-ft

A_f, A_b, A_s, A_c, A_a = area of fuel, moderator block, sleeve, channel coolant and annulus coolant, ft²

q_f, q_a = oxidation heat rate per unit length to central channel and annulus coolant, Btu/hr-ft

\bar{K} = oxidation heat flux constant for normal air, Btu/hr-ft²

ξ_s = measure of sleeve coating, perfect coating = 0.0, no coating = 1.0

- P_a, P_b, P_f, P_c = perimeter of annulus (sleeve o.d.), moderator block, central channel (sleeve i.d.), and fuel clad, ft.
- p_o = weight fraction of oxygen in normal air, lb O_2 /lb air
- Ψ = temperature levelization constant, dimensionless
- λ_F = relaxation constant for temperature levelization, hr^{-1}
- D_F, D_b, D_s = fuel, moderator block, and sleeve afterheat constants, dimensionless
- y_i = afterheat constant for different time regions, dimensionless
- z_i = afterheat time dependence constant for different time regions, dimensionless
- L_o = extrapolated core half-length, ft
- c = oxidation rate temperature constant, $^{\circ}R$
- ΔH = heat of oxidation, Btu/lb O_2
- W_f, W_a = central channel and annuli coolant main flow rate, lb air/hr
- c_p = specific heat of air, Btu/lb air- $^{\circ}R$
- \bar{r}_c, \bar{r}_a = radiant heat transfer coefficients, Btu/hr-ft 2 - $^{\circ}R$
- \bar{P} = ambient pressure of system/mole wt of air, psi-lb air/mole air
- R = gas constant, psi-ft 3 /mole- $^{\circ}R = 10.73$
- G = volumetric heat capacity for sleeve and moderator block (ρc_p), Btu/ $^{\circ}R$ -ft 2
- δ_b = fraction of moderator block assumed present, during temperature rise
- σ = Boltzman constant, Btu/ $^{\circ}R^4$ -ft 2 -hr
- $\mathcal{F}_c, \mathcal{F}_b$ = Hottel's factor for radiant heat for clad and moderator block, dimensionless
- S, B = sleeve and moderator block heat capacity per foot, Btu/hr-ft- $^{\circ}R$

References

- 1) E. C. Miller, et al., Identification of Maximum Credible Loss-of-Pressure Accident for the EGCR, November 18, 1960.
- 2) J. Landoni, P. Perry, Energy Release, Hazards, ACF Job Study 3-380-4, December 9, 1959.
- 3) J. W. Prados, Graphite Combustion Hazard in the EGCR, CF-59-11-134, November 11, 1959.
- 4) W. H. McAdams, Heat Transmission, 3rd ed., McGraw-Hill, New York, 1954.
- 5) P. L. Walker, et al., Gas Reactions of Carbon, Advance in Catalysis, Vol. XI, pp 133-221, Academic Press, New York, 1959.
- 6) P. J. Robinson, The Effects of Diffusional Control of Oxidation of Graphite on the Highest Safe Temperature in Air, GCM-UK-9, Research and Development Branch, Windscale, 1959.
- 7) J. W. Prados, Estimation of Reaction and Heat Release Rates for Graphite Oxidations, CF-60-10-131, October 19, 1960.
- 8) Letter from R. E. Dahl, Hanford Atomic Products Operation, to M. H. Fontana, December 2, 1960.
- 9) M. H. Fontana and F. L. Carlsen, Jr., Report on Trip to Hanford, June 28-29, 1960, Concerning the Graphite Research Program Pertinent to the EGCR, CF-60-7-78, July 20, 1960.
- 10) Letter from R. E. Dahl, Hanford Atomic Products Operation, to R. A. Charpie, Oak Ridge National Laboratory, Preliminary Results of EGCR Oxidation Prototype Experimentation, September 23, 1960.
- 11) G. Henning, Surface Reactions of Single Crystals of Graphite, US/UK Graphite Conference Held at Oak Ridge National Laboratory, 1960, to be issued.
- 12) Letter from R. E. Dahl, Hanford Atomic Products Operation, to M. H. Fontana, Oak Ridge National Laboratory, February 14, 1961.
- 13) Letter from R. E. Dahl, Hanford Atomic Products Operation, to F. L. Carlsen, Oak Ridge National Laboratory, Preliminary Results of EGCR Combustion Experiment 12, March 1, 1961.

- 14) Intra-Laboratory Correspondence, Wm. B. Cottrell from M. H. Fontana, Summary of Telephone Conversation of February 23, 1961, with Ray Dahl, of Hanford, Concerning Catastrophic Oxidation of the EGCR Coated Sleeves and Comments Thereon, February 24, 1961.
- 15) W. L. Kosiba, G. J. Dienes, The Effect of Radiation on the Rate of Oxidation of Graphite, US/UK Graphite Conference, London, TID-7565, pp 121-32, 1957.
- 16) Letter from R. E. Dahl, Hanford Atomic Products Operation, to R. A. Charpie, Oak Ridge National Laboratory, October 31, 1960.
- 17) Letter from R. E. Dahl, Hanford Atomic Products Operation, to R. A. Charpie, Oak Ridge National Laboratory, November 10, 1960.
- 18) Letter from R. E. Dahl, Hanford Atomic Products Operation, to M. H. Fontana, Oak Ridge National Laboratory, December 2, 1960.
- 19) D. A. Lampe, Study IV-312, Hazards Analysis, Depressurization Accident, Allis-Chalmers Manufacturing Company, Washington, D. C., November 18, 1960.
- 20) Personal communication, J. Delene to M. H. Fontana, April 10, 1961.
- 21) Letter from G. Samuels, Status of EGCR Fuel Element Design, Analysis, and Failure Criteria, September 14, 1960.
- 22) Letter from L. H. Jackson to P. D. Bush, August 15, 1960, attachment, Suggested Operating Programs for EGCR Control Rods, by C. A. Preskitt.
- 23) G. Humphreys, Kaiser Engineers, Graphite Oxidation Calculations, Job No. 5927, August 9, 1960.
- 24) Intra-Laboratory Correspondence, M. H. Fontana to Wm. B. Cottrell, Comments on the Following KE Material Pertinent to Graphite Oxidation in the EGCR, September 29, 1960.
- 25) Intra-Laboratory Correspondence, M. H. Fontana to Wm. B. Cottrell, Long Term Cooling Requirements in the EGCR Subsequent to the Loss of Pressure Accident, May 3, 1961.
- 26) J. L. Jackson, HW-68494.

- 27) F. L. Carlsen, et al., Coating for EGCR Graphite Support Sleeves, Gas-Cooled Reactor Project Quarterly Progress Report for Period Ending December 31, 1960, ORNL-3049, March 2, 1961, pp 208-212.
- 28) Intra-Laboratory Correspondence, J. W. Prados to W. B. Cottrell, Consideration of the Possibility of Carbon Monoxide Explosion Following Coolant System Rupture in the EGCR, February 8, 1961.
- 29) B. Lewis, G. von Elbe, Combustion, Flames, and Explosions of Gases, Academic Press, 1951, pp 75-93, 579-86.
- 30) J. H. Perry, ed., Chemical Engineers Handbook, 3rd. ed., McGraw-Hill, 1950, pp 1582-88.
- 31) Experimental Gas-Cooled Reactor - Preliminary Summary Hazards Report, ORO-196, May 1959.
- 32) O. A. Haugen, K. M. Watson, Chemical Process Principles, John Wiley & Sons, New York, 1947, Part III.
- 33) D. R. deHalas and R. Dahl, Comments on Graphite Oxidation Study for Experimental Gas-Cooled Reactor, HAPO-2065, June 1960.
- 34) Aubeau, et al., Experimental Determination of the Conditions of Sustained Combustion in a Channel for the G-1 Reactor, CP-58-533-BM-MLL, September 19, 1958.